On Enabling Virtualization and Millimeter Wave Technologies in Cellular Networks

Shubhajeet Chatterjee

Dissertation submitted to the Faculty of the
Virginia Polytechnic Institute and State University
in partial fulfillment of the requirements for the degree of

Doctor of Philosophy
in
Electrical Engineering

Allen B. MacKenzie, Co-chair
Mohammad J. Abdel-Rahman, Co-chair
Harpreet S. Dhillon
Yaling Yang
Mazen H. Farhood

September 18, 2020
Blacksburg, Virginia

Keywords: Wireless network virtualization, millimeter wave communications, resource allocation, base station deployment, rate coverage probability, coverage probability, stochastic optimization.

On Enabling Virtualization and Millimeter Wave Technologies in Cellular Networks

Shubhajeet Chatterjee

(ABSTRACT)

Wireless network virtualization (WNV) and millimeter wave (mmW) communications are emerging as two key technologies for cellular networks. Virtualization in cellular networks enables wireless services to be decoupled from network resources (e.g., infrastructure and spectrum) so that multiple virtual networks can be built using a shared pool of network resources. At the same time, utilization of the large bandwidth available in mmW frequency band would help to overcome ongoing spectrum scarcity issues. In this context, this dissertation presents efficient frameworks for building virtual networks in sub-6 GHz and mmW bands. Towards developing the frameworks, first, we derive a closed-form expression for the downlink rate coverage probability of a typical sub-6 GHz cellular network with known base station (BS) locations and stochastic user equipment (UE) locations and channel conditions. Then, using the closed-form expression, we develop a sub-6 GHz virtual resource allocation framework that aggregates, slices, and allocates the sub-6 Ghz network resources to the virtual networks in such a way that the virtual networks' sub-6 GHz downlink coverage and rate demands are probabilistically satisfied while resource over-provisioning is minimized in the presence of uncertainty in UE locations and channel conditions. Furthermore, considering the possibility of lack of sufficient sub-6 GHz resources to satisfy the rate coverage demands of all virtual networks, we design a prioritized sub-6 GHz virtual resource allocation scheme where virtual networks are built sequentially based on their given priorities. To this end, we develop static frameworks that allocate sub-6 GHz resources in the presence of uncertainty in UE locations and channel conditions, i.e., before the UE locations and channel conditions are revealed. As a result, when a slice of a BS serves its associated UEs, it can be over-satisfied

(i.e., resources left after satisfying the rate demands of all UEs) or under-satisfied (i.e., lack of resources to satisfy the rate demands of all UEs). On the other hand, it is extremely challenging to execute the entire virtual resource allocation process in real time due to the small transmission time intervals (TTIs) of cellular technologies. Taking this into consideration, we develop an efficient scheme that performs the virtual resource allocation in two phases, i.e., virtual network deployment phase (static) and statistical multiplexing phase (adaptive). In the virtual network deployment phase, sub-6 GHz resources are aggregated, sliced, and allocated to the virtual networks considering the presence of uncertainty in UE locations and channel conditions, without knowing which realization of UE locations and channel conditions will occur. Once the virtual networks are deployed, each of the aggregated BSs performs statistical multiplexing, i.e., allocates excess resources from the over-satisfied slices to the under-satisfied slices, according to the realized channel conditions of associated UEs. In this way, we further improve the sub-6 GHz resource utilization. Next, we steer our focus on the mmW virtual resource allocation process. MmW systems typically use beamforming techniques to compensate for the high pathloss. The directional communication in the presence of uncertainty in UE locations and channel conditions, make maintaining connectivity and performing initial access and cell discovery challenging. To address these challenges, we develop an efficient framework for mmW virtual network deployment and UE assignment. The deployment decisions (i.e., the required set of mmW BSs and their optimal beam directions) are taken in the presence of uncertainty in UE locations and channel conditions, i.e., before the UE locations and channel conditions are revealed. Once the virtual networks are deployed, an optimal mmW link (or a fallback sub-6 GHz link) is assigned to each UE according to the realized UE locations and channel conditions. Our numerical results demonstrate the gains brought by our proposed scheme in terms of minimizing resource over-provisioning while probabilistically satisfying virtual networks' sub-6 GHz and mmW demands in the presence of uncertainty in UE locations and channel conditions.

On Enabling Virtualization and Millimeter Wave Technologies in Cellular Networks

Shubhajeet Chatterjee

(GENERAL AUDIENCE ABSTRACT)

In cellular networks, mobile network operators (MNOs) have been sharing resources (e.g., infrastructure and spectrum) as a solution to extend coverage, increase capacity, and decrease expenditures. Recently, due to the advent of 5G wireless services with enormous coverage and capacity demands and potential revenue losses due to over-provisioning to serve peak demands, the motivation for sharing and virtualization has significantly increased in cellular networks. Through wireless network virtualization (WNV), wireless services can be decoupled from the network resources so that various services can efficiently share the resources. At the same time, utilization of the large bandwidth available in millimeter wave (mmW) frequency band would help to overcome ongoing spectrum scarcity issues. However, due to the inherent features of cellular networks, i.e., the uncertainty in user equipment (UE) locations and channel conditions, enabling WNV and mmW communications in cellular networks is a challenging task. Specifically, we need to build the virtual networks in such a way that UE demands are satisfied, isolation among the virtual networks are maintained, and resource over-provisioning is minimized in the presence of uncertainty in UE locations and channel conditions. In addition, the mmW channels experience higher attenuation and blockage due to their small wavelengths compared to conventional sub-6 GHz channels. To compensate for the high pathloss, mmW systems typically use beamforming techniques. The directional communication in the presence of uncertainty in UE locations and channel conditions, make maintaining connectivity and performing initial access and cell discovery challenging. Our goal is to address these challenges and develop optimization frameworks to efficiently enable virtualization and mmW technologies in cellular networks.

Acknowledgments

First, I would like to express my sincere gratitude to my advisor Dr. Allen B. MacKenzie and co-advisor Dr. Mohammad J. Abdel-Rahman for their esteemed guidance, motivations, and patience during my work on this dissertation. Words can not express how grateful I am to have advisors like you. Your styles of identifying and analyzing research problems, and developing solution approaches are the most valuable things a student can learn during the PhD. I am thankful for all the time and efforts that you have dedicated to guide me.

Dr. Abdel-Rahman, I would like to specially thank you for introducing me with this excellent field called stochastic optimization which helps me to build the foundation of this dissertation. Thank you for believing in me and guiding my research step by step.

Besides my advisors, I would like to thank my PhD. committee members Dr. Harpreet Dhillon, Dr. Yaling Yang, and Dr. Mazen Farhood for their valuable suggestions and comments. I would also like to thank Dr. Carl B. Dietrich for his esteemed guidance at the earlier stage of my PhD.

Above all, I would like to thank my mother, Jolly Chatterjee and father, Monotosh Chatterjee. Any word of gratitude will fall short to describe your contributions in my success. I am here because of you. Also, I would like to specially thank my cousin (who has been more than an elder brother to me) Avishek Mukherjee for his motivations, guidance, and unwavering supports since my schooldays. Last, but not least, I would like to thank my folks at Blacksburg, especially my friends, Shibaji, Shuvodeep, Rubayet, Holt, Emad, Kory, and Biplav and my friends from undergrad, Spandan, Surid, and Sourav for helping me survive all the stress in past years. Thank you all.

Contents

List of Figures

List of Tables

Chapter 1

Introduction

With network densification leading towards saturation, it becomes extremely challenging to meet the coverage and capacity demands of next-generation (e.g., 5G) cellular networks [1]. In this context, virtualization of the network resources (e.g., infrastructure, bandwidth) and utilization of the large bandwidth available in millimeter wave (mmW) frequency bands are two potential solutions. This dissertation will investigate these two key enabling technologies for next-generation cellular networks. In the following sections, first, we briefly discuss backgrounds and motivations in enabling virtualization and mmW communications in cellular networks. Then, we provide an overview of our proposed deployment architecture followed by the related challenges and a summary of our contributions.

1.1 Motivation and Background on Virtualizing Cellular Networks

In current wireless network standards, mobile network operators (MNO) need to have network resources (e.g. infrastructure, electromagnetic spectrum) in order to independently host and manage wireless services (e.g., data, video) for their subscribed user equipments (UEs). To decrease operational expenditures (OPEX) and to extend network coverage, MNOs often share their resources based on mutual agreements [2, 3]. Recently, due to the advent of next-generation wireless services with enormous coverage and capacity demands, scarcity of the overall spectrum, and potential revenue losses due to over-provisioning to

serve peak demands, the motivation for resource sharing has significantly increased in cellular networks [4, 5, 6, 7, 8, 9, 10, 11]. However, various Quality-of-Service (QoS) requirements of 5G services and inflexibility of network resources impose unprecedented challenges on managing resource sharing in the existing model of cellular networks. In this context, wireless network virtualization (WNV) emerges as a promising solution. Through virtualization, wireless services can be decoupled from the network resources so that a pool of network resources can be logically sliced among various services. Thus, virtualization enables robust sharing of the network resources among various services. Apart from the robust resource sharing, another interesting outcome of WNV is that the service providers can manage and host their services without owning the network resources. Let us explain it with an example. Consider you are watching an Youtube video. In the existing cellular network model, the quality of the video depends on the network connection (e.g., AT&T, Verizon etc.) you are using. In other words, the service providers do not have any control over their users' experience. Now, the advantage of WNV is that the service providers (e.g., Youtube) can build a virtual network over the city, and thus manage their users' experience without actually owning or managing the network resources (the network resources will be managed by the conventional MNOs or other entities). Following such motivations, in this dissertation, we aim to design an efficient virtualization framework that enables network-wide large-scale resource sharing in cellular networks.

We consider a three-layer architecture for WNV as proposed in [12], shown in Figure 1.1. Service providers (SPs) are in charge of providing regular data, voice, and messaging services, as well as specialized services that apply to specific applications such as the Internet of Things (IoTs) or other over-the-top (OTT) services. Resource providers (RPs) own the network resources. Virtual network builders (VNBs) aggregate (*pool*) the resources from various RPs, create logical partitions (*slices*) among these aggregated resources and allocate

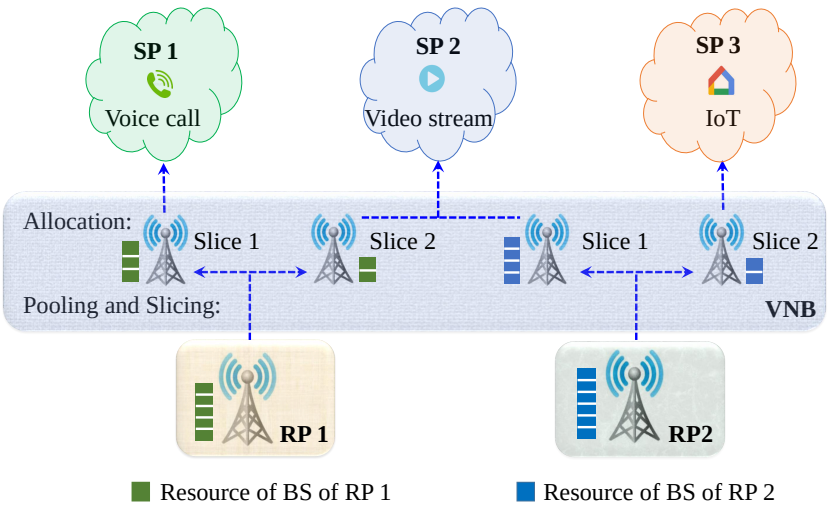

Figure 1.1: Wireless network virtualization architecture.

them to SPs. A network resource allocated to an SP is known as the *virtual resource* of the SP and a network built with the virtual resources is known as a *virtual network* of the SP.

1.2 Motivation and Background on Utilizing Millimeter Wave Frequencies in Cellular Networks

Current cellular networks use carrier frequency spectrum that is limited between 700 MHz and 6 GHz (as shown in Figure 1.2 [13]). Due to the large-scale dense deployments of Base Stations (BSs), these bands are almost saturated [1]. In this context, to support the enormous coverage and capacity requirements of the next-generation cellular networks, it becomes necessary to utilize the large bandwidth available in mmW frequency bands (30 GHz-300 GHz). MmW channels have distinctive propagation characteristics. Specifically, mmW channels experience high attenuation and blockage due to their small wavelengths compared to conventional sub-6 GHz channels. To compensate for the high pathloss, mmW systems typically use beamforming techniques, i.e., highly directional transmit antennas

Band	Technologies	Uplink (MHz)	Downlink (MHz)	Carrier Bandwidth (MHz)
700 MHz	4G	746-763	776-793	1.25, 5, 10
Cellular 850	2G, 3G, 4G	824-849	869-894	1.25, 5
GSM 900	2G	880-915	925-960	1.25, 5
AWS	3G, 4G	1710-1755	2110-2155	5, 10, 15
PCS	3G, 4G	1850-1910	1930-1990	1.25, 5
WCS	4G	2305-2320	2345-2360	5, 10, 15, 20
IMT Extension	4G	2500-2700	2620-2690	5, 10, 15, 20
Unlicensed	4G	5150-5925		5, 10, 15, 20

Figure 1.2: Current spectrum and bandwidth allocation.

focusing their power on receivers.

1.3 Deployment Architecture

We consider a deployment architecture for enabling virtualization and mmW communications in cellular networks as shown in Figure 1.3. As can be seen that RPs make a set of BSs available to VNB. Some of the BSs are operating in sub-6 GHz bands (e.g., LTE eNodeBs, NR low-frequency gNodeBs) and rest of the BSs are operating in mmW bands (e.g., NR high-frequency gNodeBs). The sub-6 GHz BSs have limited resources (e.g., LTE BSs typically operate over a carrier bandwidth of up to 20 MHz with a frequency reuse factor close to 1) with good channel propagation characteristics, whereas the mmW BSs have abundant resources (e.g., NR high-frequency BSs will typically operate over a carrier bandwidth

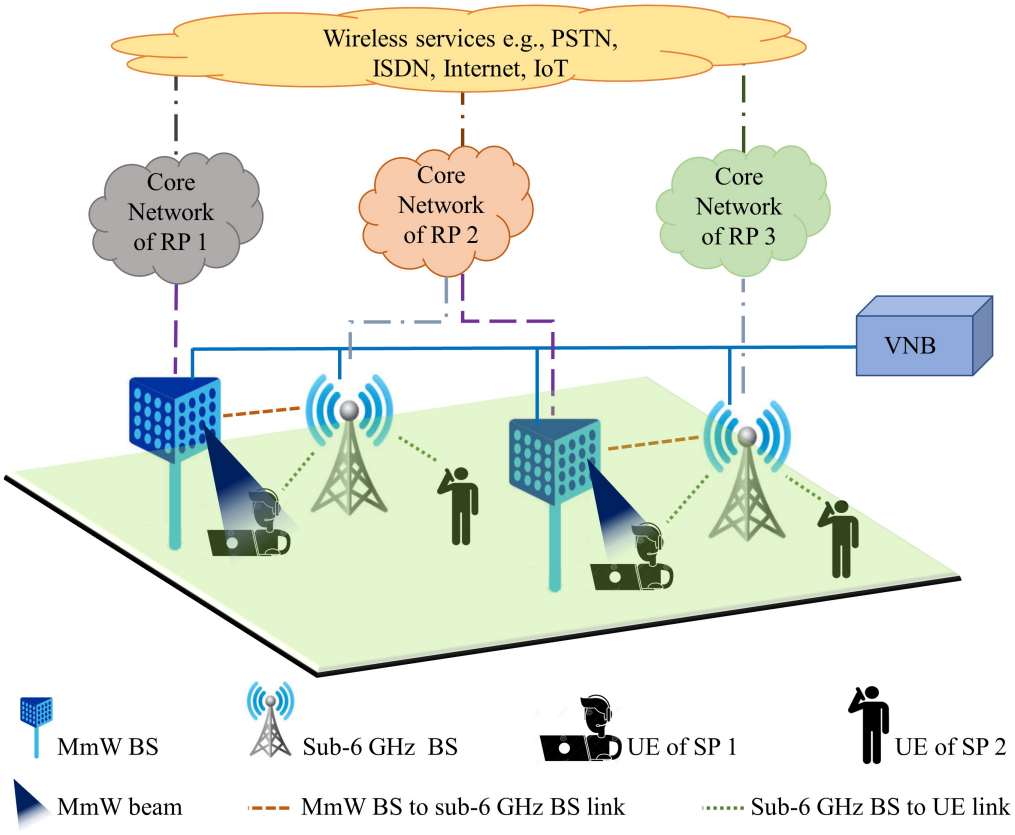

Figure 1.3: Deployment Framework.

of up to 400 MHz [14] with a small frequency reuse factor) with poor channel propagation characteristics. There is a set of SPs who wish to provide wireless services with on-demand mmW connectivity and fallback sub-6 GHz connectivity in the considered geographical area. SPs place their QoS demands for sub-6 GHz communications and mmW communications to VNB. Based on the SPs' QoS demands, VNB builds their virtual networks with the resources provided by the RPs. In a virtual network, each mmW BS is linked with a sub-6 GHz BS. The sub-6 GHz BSs act as central controllers for assigning mmW/sub-6 GHz links to UEs.

When a UE of an SP enters its virtual network, it camps over the nearest sub-6 GHz BS among the set of sub-6 GHz BSs assigned to the SP. When the UE wants to access the mmW BSs, it sends a request to the sub-6 GHz BS. Upon receiving the request, the sub-6

GHz BS informs all of its associated mmW BSs that are assigned to the SP to switch on their beams. The UE starts to scan the availability of the mmW beams. In each resource allocation cycle/time period, the UE sends its mmW beam availability information to the sub-6 GHz BS. If there is no mmW beam available for the UE, the sub-6 GHz BS is assigned to the UE. If more than one mmW beam is available for the UE, the sub-6 GHz BS assigns an optimal mmW beam to the UE.

Let us call a network resource operating in sub-6 GHz band allocated to an SP as the *sub-6 GHz virtual resource* of the SP and a network built with the sub-6 GHz virtual resources as a *sub-6 GHz virtual network* of the SP. Likewise, let us call a network resource operating in mmW band allocated to an SP as the *mmW virtual resource* of the SP and a network built with the mmW virtual resources as a *mmW virtual network* of the SP. To efficiently design this deployment architecture, the virtual resource allocation process is one of the key features that needs to be investigated thoroughly. There are various technical challenges associated with the virtual resource allocation process as described in the followings.

1.4 Challenges

The virtual resource allocation process has high computation complexity which makes it difficult for real time (i.e., instantaneous) execution. For example, if we want to allocate virtual resources in real time, VNB needs to know the channel state information (CSI) and demands of UEs of SPs, and then instantaneously aggregate, slice, and allocate network resources to the SPs. However, the time required to aggregate, slice, and allocate resources typically exceeds the conventional resource allocation time in cellular networks (e.g., the period of time in which packet scheduling is done in LTE, known as transmission time interval, is one millisecond). Besides, the frequent interactions among the virtualizing entities (i.e., SPs, VNB, and RPs) to identify instantaneous demands and CSI of individual UEs

would significantly increase network overhead and processor loads. Therefore, the virtual resource allocation process needs to be executed in offline in the presence of uncertainty in UE locations and channel conditions, i.e., before knowing which realization of UE locations and channel conditions will occur. This requires the SPs to efficiently express their QoS demands to the VNB. Furthermore, the VNB needs to allocate the network resources in such a way that the SP demands are satisfied, isolation among the virtual networks are maintained, and resource over-provisioning is minimized in the presence of uncertainty in UE locations and channel conditions with affordable computational complexity.

In addition, RPs have not yet deployed the mmW BSs. Therefore, we need to determine the optimal candidate locations for the BSs to facilitate VNB in the mmW virtual resource allocation process. There are distinctive challenges in mmW network deployment process. One key challenge arises from the fact that the mmW systems typically use beamforming techniques, i.e., rely on directional communication, in contrast to the sub-6 GHz systems that use omnidirectional communication. Specifically, directional communication requires aligning the transmit beam and the receive beam. Due to UE mobility and stochastic channel effects (e.g., blockages), it becomes challenging to align the beams of UEs and BSs with affordable delay, hardware complexity, and overhead. For example, during the initial access and cell discovery, if a BS needs to search through all possible spatial directions to align its beams with the individual UEs, then the delay and overhead would be high. Moreover, phase-shifters introduce calibration issues due to their limited adaptability (angle is quantized). Furthermore, even if the beams are aligned and the connection is established, mmW channel effects (e.g., blockages) frequently disrupt the communication.

1.5 Stochastic Optimization

The challenges on enabling virtualization and mmW communications in cellular networks arise primarily from the uncertainty in UE locations and channel conditions. To tackle this uncertainty issue, we borrow stochastic optimization techniques [15]. Stochastic optimization provides powerful mathematical tools to design efficient schemes under uncertainty. These tools have been widely applied in operations research (e.g., supply chain network design, unit commitment in electrical power production) [16]. In recent times, stochastic optimization has gained popularity for optimizing resource allocation in various types of wireless networks operating under uncertainty (examples include [17, 18, 19, 20, 21, 22, 23, 24, 25, 26, 27, 28, 29, 30, 31]). Taking these into consideration, in this dissertation we develop frameworks based on stochastic optimization to efficiently deploy sub-6 GHz and mmW virtual networks. We use two classes of stochastic optimization, i.e., single-stage chance-constrained optimization and two-stage chance-constrained optimization. In single-stage chance-constrained optimization, decisions are taken to minimize (or maximize) objective function value while ensuring the probability of meeting a certain constraint is above a certain threshold in the presence of uncertainty in system parameters. The decisions taken in a single-stage stochastic optimization are static, i.e., the decisions do not adapt with the realizations of uncertain system parameters. In two-stage chance-constrained optimization, decision variables are divided into two categories, i.e., first-stage (static) and second-stage (adaptive) decisions. First-stage decisions are static and are taken in the presence of uncertainty in system parameters. Second-stage decisions are taken adaptively according to the realizations of uncertain system parameters. The two stages are jointly optimized to minimize (or maximize) objective function value while ensuring the probability of meeting a certain constraint is above a certain threshold in the presence of uncertainty in system parameters.

1.6 Contributions

1.6.1 SP Demands Characterization

We propose new models for characterizing SP demands for sub-6 GHz and mmW communications. The requested sub-6 GHz virtual network of an SP is fully characterized using four parameters: UE distributions, minimum downlink data rate, minimum downlink rate coverage probability (defined as the probability of achieving the minimum downlink rate by an arbitrarily chosen UE of the SP), and the geographical area to be covered. In mmW virtual networks, mmW BSs have abundant bandwidth to satisfy data rate demands of UEs of SPs. However, the mmW channels have poor propagation characteristics. Therefore, the key challenge in mmW networks is to provide a minimum downlink signal-to-noise ratio (SNR) to UEs. Taking this into account, the requested mmW virtual network of an SP is fully characterized using four parameters: UE distributions, minimum downlink SNR, minimum downlink SNR coverage probability (defined as the probability of achieving the minimum SNR by an arbitrarily chosen UE of the SP), and the geographical area to be covered.

1.6.2 Rate Coverage Analysis of Sub-6 GHz Cellular Networks

One important performance metric for a sub-6 GHz cellular network is its downlink rate coverage probability. Due to UE mobility and stochastic channel effects (such as multipath fading, shadowing, interference), rate coverage probability analysis of a network is extremely challenging. Previous works derived the downlink rate coverage probability assuming certain stochastic models for the distribution of both UEs and BSs. Seeking further precision, we derive the downlink rate coverage probability of a cellular network with *deterministically known BS locations* and stochastic UE locations and channel conditions.

1.6.3 Sub-6 GHz Virtual Resource Allocation Framework

We develop a chance-constrained stochastic optimization framework to aggregate an optimal set of sub-6 GHz network resources and optimally slice them among SPs to meet their sub-6 GHz rate coverage demands. Specifically, we first formulate a chance-constrained optimization problem that aims at meeting sub-6 GHz rate coverage demands of SPs while minimizing resource over-provisioning in the presence of uncertainty in UE locations and channel conditions. In order to solve the optimization problem, we derive a closed form expression of the downlink rate coverage probability of a typical sub-6 GHz virtual network. With the closed-form expression, we design an efficient algorithm to solve the chance-constrained problem with affordable computation complexity. Furthermore, considering the possibility of the optimization model being infeasible due to lack of sufficient resources in the sub-6 GHz resource pool, we propose a prioritized sub-6 GHz virtual resource allocation mechanism where sub-6 GHz virtual networks are sequentially built for SPs based on given priorities. Our results demonstrate that the proposed stochastic framework outperforms existing deterministic frameworks in terms of probabilistically satisfying SPs' sub-6 GHz rate coverage demands.

1.6.4 Sub-6 GHz Virtual Resource Allocation with Adaptive Statistical Multiplexing Framework

We develop a joint optimization framework for orchestrating virtualized sub-6 GHz cellular networks while enabling and exploiting statistical multiplexing. Our proposed framework has two phases: virtual network deployment (static) and statistical multiplexing (adaptive). In the virtual network deployment phase, the VNB aggregates, slices, and allocates sub-6 GHz network resources to the SPs considering the presence of uncertainty in UE locations and channel conditions, without knowing which realization of UE locations and channel con-

ditions will occur. Once the virtual networks are deployed, each of the aggregated sub-6 GHz BSs performs statistical multiplexing, i.e., allocates excess resources from the over-satisfied slices to the under-satisfied slices, according to the realized channel conditions of associated UEs. Our numerical results demonstrate that the proposed framework outperforms existing sub-6 GHz virtualization frameworks in terms of probabilistically satisfying SPs' sub-6 GHz rate and coverage demands while minimizing the number of deployed sub-6 GHz BSs, in the presence of uncertainty in UE locations and channel conditions.

1.6.5 MmW Virtual Resource Allocation Framework

We propose a two-stage chance-constrained optimization framework to determine the optimal set of mmW BSs to deploy (or aggregate), their optimal beam directions, and their optimal assignments to individual UEs of SPs in order to satisfy the mmW SNR coverage demands of the SPs and maximize the stability of the mmW connections. The mmW virtual network deployment decisions (i.e., the required set of mmW BSs and their beam directions) are static and are taken before UE locations and channel conditions are revealed. The UE assignment decisions are taken under each realization of UE locations and channel conditions considering the availability and stability of the mmW beams. Our numerical results demonstrate the gains brought by our proposed scheme in terms of satisfying SPs mmW coverage demands while minimizing the number of deployed mmW BSs, in the presence of uncertainty in UE locations and channel conditions.

1.7 Dissertation Outline

The remainder of this Dissertation is organized as follows: In Chapter 2, we review the literature. In Chapter 3, we describe the system model. In Chapter 4, we derive the downlink rate coverage probability of a typical sub-6 GHz cellular network with deterministically known BS locations. Then, in Chapter 5, we describe the chance-constrained sub-6 GHz

virtual resource allocation framework. After that, in Chapter 6, we describe the joint sub-6 GHz virtual resource allocation and statistical multiplexing framework. In Chapter 7, we describe the mmW virtual network deployment and adaptive UE assignment framework. Finally, we conclude and discuss future works in Chapter 8.

Chapter 2

Literature Review

In this chapter, we review the existing works on enabling virtualization and mmW communications in cellular networks. To the best of our knowledge, all existing virtual resource allocation schemes are focused on sub-6 GHz cellular networks which we discuss in the first section of this chapter. The second covers the previous work on enabling mmW communications in cellular networks.

2.1 Enabling Virtualization in Sub-6 GHz Cellular Networks

In recent years, a number of frameworks have been proposed to enable virtualization in sub-6 GHz cellular networks. Some of the proposed frameworks are distributed schemes, in which autonomous SPs build their own sub-6 GHz virtual networks. Others are centralized schemes, in which a central controller (like the VNB) builds sub-6 GHz virtual networks for SPs.

2.1.1 Distributed Schemes

The distributed schemes are developed primarily based on game-theoretic auction models, such as [4, 5, 6, 7, 8, 9]. In [4], the authors designed a Vickrey-Clarke-Groves (VCG) auction model between SPs and RPs, where SPs bid for sub-6 GHz spectrum based on a stochastic game and RPs slice and allocate their sub-6 GHz spectrum to the SPs following a

conjectural pricing mechanism. In each resource allocation cycle, SPs set a conjectural price and announce the required sum-rate for their UEs. Based on the bids received from SPs, RPs determine the spectrum allocation and the corresponding prices for the SPs. The authors shown that there exists a Nash equilibrium in the conjectural pricing mechanism that maximizes average sum-rate of UEs. However, since the auction model is developed considering TDMA networks, its performance in real systems that assign UEs both time and frequency (e.g., physical resource blocks in LTE) remains unaddressed. In [6], the authors developed a similar VCG auction model for sub-6 GHz spectrum slicing in OFDMA networks. To reduce overall computation complexity, the authors approximated the original stochastic game as an abstract stochastic game. The abstract game is played considering local state information instead of global state information. As a result, it has low computation complexity with a certain performance regrets. Note that both works [4, 6] considered only one type of wireless resources, i.e., sub-6 GHz spectrum of RPs in their virtualization models. In [5], the authors overcame this limitation by considering sub-6 GHz spectrum and power of sub-6 GHz BSs as virtualized commodities. Specifically, the authors proposed an auction model where SPs bid for sub-6 GHz channels and power allocated over those channels by BSs of RPs. The auction model is designed based on a Bayesian game where each SP determines bidding strategy by estimating payoff resulted from the bidding strategies of the other SPs. However, the authors considered discrete sets of power and spectrum to design the auction model whereas, power and spectrum are typically treated as continuous parameters in real systems. To address this issue, in [7] the authors considered slices (i.e., fraction of capacity) of sub-6 GHz BSs as virtualized commodities. The authors designed a three-sided matching game among UEs, SPs, and RPs, where a low-level matching game is played between UEs and SPs for service selection and a high-level matching game is played between SPs and RPs for sub-6 GHz BS slicing. With similar motivations, a three-sided matching game is developed in [9] that considers sub-6 GHz wireless resources and servers as virtualized com-

modities. The authors designed a Firm-Buyer game between UEs and SPs for service and content selection and a Supplier-Firm game between SPs and RPs for slicing sub-6 GHz BSs and servers among SPs. However, these works do not optimize the pricing strategies of RPs. To design an efficient pricing strategy, in [8] the authors designed a Stackelberg game for RPs and SPs to determine the prices that SPs need to pay to the RPs to provide the required sum-rate of its UEs. Along with the stackelberg game, a matching game is played between SPs and RPs to slice sub-6 GHz BSs among SPs. Although these distributed approaches can improve resource utilizations, they suffer from high network overhead and computation complexity, due to the frequent interactions among the virtualizing entities (i.e., SPs and RPs) to identify instantaneous demands of individual UEs. Consequently, these schemes have poor scalability.

2.1.2 Centralized Schemes

An alternative approach for enabling virtualization in cellular networks is the centralized virtual resource allocation, in which a central node allocates virtual resources to SPs. Such an approach was advocated in several recent works. For example, in [32], the authors proposed that a central node (known as the hypervisor) optimally slices sub-6 GHz spectrum of RPs among SPs. To optimally slice spectrum among SPs, the authors designed a biconcave deterministic optimization framework for the hypervisor. The objective is to maximize the sum-rate obtained by the SPs. The problem is solved by using the alternative concave search algorithm. In [10] the authors designed a deterministic convex optimization framework for the hypervisor to optimally slice sub-6 GHz BSs among SPs. The objective of the optimization problem is to minimize the costs of SPs while satisfying their sum-rate demands in the presence of the capacity limitations of backhaul links. To solve the problem, the authors derived the Lagrangian dual of the true problem and solved it using Hungarian method. With a similar motivation, in [11] the authors designed a deterministic optimiza-

tion framework for the hypervisor to slice sub-6 GHz BSs among SPs. The objective of this work is to maximize energy efficiency of sub-6 GHz virtual networks while satisfying the sum-rate demands of SPs. The problem is solved using the nonlinear fractional programming method. However, in these works sub-6 GHz BS slicing is optimized under fixed UE assignment strategies, i.e., UEs are assigned to the sub-6 GHz BS that provides the highest received signal strength (RSS). To further enhance resource utilizations, in [33], the authors jointly optimized UE assignment and sub-6 GHz BS slicing. The authors designed a deterministic convex optimization framework for the hypervisor to jointly optimize UE assignment and sub-6 GHz BS slicing. The objective of the optimization problem is to maximize the sum-rate demand of SPs. The problem is solved by a two-step iterative algorithm where the first step optimizes the UE assignment for given slicing decisions and the second step optimizes the slicing decisions for given UE assignment. In each step, the true optimization problem is approximated by the successive convex approximation technique, and then solved by the complementary geometric programming method. The authors further extend their works in [34] where they designed a deterministic convex optimization framework for the hypervisor to jointly optimize UE assignment, sub-6 GHz antenna selection, and sub-6 GHz BS slicing. The objective of the optimization problem is to maximize the sum-rate demands of SPs. The problem is solved by using the similar approach as developed in [33]. All these optimization schemes assume that the hypervisor has perfect knowledge of sub-6 GHz channel conditions. However, due to the time-varying nature of the wireless channel, it is extremely challenging for the hypervisor to know exact channel conditions. As a result, in a real wireless network, these existing approaches would have difficulty ensuring SPs' rate and coverage demand satisfaction, maintain isolation among slices, and minimizing resource over-provisioning with affordable network overhead and reasonable computation complexity. To account for imperfect channel state information, in [35] the authors designed a discrete stochastic optimization framework for the hypervisor to jointly optimize UE assignment and

sub-6 GHz BS slicing. The objective of the optimization problem is to maximize the sum-rate obtained by the SPs in the presence of uncertainty in channel conditions. However, the authors did not study the optimality gap of the proposed discrete approximation technique. Furthermore, all these existing optimization works characterized SP demands as the sum-rate demands. Consequently, individual UEs' rate demand satisfaction remains unaddressed.

2.1.3 Discussions

To overcome the limitations of the existing schemes in the literature, in this dissertation, we propose centralized stochastic virtual resource allocation schemes that probabilistically satisfy SPs' sub-6 GHz rate and coverage demands and minimize resource over-provisioning in the presence of uncertainties in UE locations and channel conditions. Specifically, in Chapter 4, we derive the downlink rate coverage probability of a sub-6 GHz cellular network with deterministically known BS locations. Then, using this result, in Chapter 5, we develop a chance-constrained sub-6 GHz virtual resource allocation model that aims at probabilistically satisfying SPs' sub-6 GHz rate and coverage demands while minimizing sub-6 GHz resource over-provisioning in the presence of uncertainty in UE locations and channel conditions. Furthermore, in Chapter 6, we develop a joint stochastic optimization framework for sub-6 GHz virtual resource allocation and adaptive statistical multiplexing in the presence of uncertainty in UE locations and channel conditions. In our proposed frameworks, the SPs, the VNB, and the RPs do not need to interact to identify the instantaneous demands of individual UEs. As a result, network overhead and computational complexity of our approach are significantly less than the aforementioned schemes. In addition, the overall role of the VNB in our work is fairly different than the role of hypervisor proposed in previous works. Specifically, the VNB *aggregates* appropriate resources from different RPs and then slices and allocates them to SPs whereas a hypervisor typically operates on resources belonging to a single RP. This improves overall resource utilization. To the best of our knowledge, we

are presenting the first works that jointly optimize resource aggregation, slicing, allocation, and statistical multiplexing to satisfy sub-6 GHz virtual network rate coverage probability demands of SPs.

2.2 Enabling MmW Communications in Cellular Networks

In this section, we briefly review the existing literature on mmW BS deployment, beam alignment, and link assignment.

2.2.1 MmW BS Deployment

In cellular networks, optimal BS placement has been a topic of immense interest for decades. A number of heuristic and meta-heuristic schemes were developed to optimally place BSs in cellular networks [36, 37, 38]. However, these existing works consider omnidirectional communications. As a result, they are not feasible for mmW networks that use directional communications. Little research has been done so far for optimal BS placement in mmW networks [39, 40]. For example, in [39], the authors divided the considered geographical area into grids and designed a computational geometry-based BS placement algorithm to provide Line-of-Sight (LOS) communications to as many gird-points as possible. In [40], the authors proposed a deterministic optimization framework that aimed to optimally place the minimum number of BSs to provide LOS communications and a minimum RSS to all the grid points. However, ensuring LOS communications or minimum RSS cannot guarantee connectivity and coverage in mmW networks due to the dispersiveness of mmW channels. In addition, the distribution of UE locations need to be considered for optimal BS placement. Furthermore, these works do not consider the beam alignment problem.

2.2.2 MmW Beam Alignment

In search of efficient beam alignment techniques in mmW networks, a number of adaptive and static schemes have been developed in past years [41]. In the adaptive schemes, transmit and receive beams are aligned in real time based on the instantaneous locations of the transmitter and the receiver and the channel conditions [42, 43, 44, 45, 46, 47]. For example, in [42], the authors proposed to exhaustively sweep transmit and receive beams of the mmW BSs and UEs in all possible directions until they are aligned. Although the exhaustive sweeping scheme can ensure beam alignment, it causes high delay and network overhead. To reduce the delay of exhaustive sweeping, in [43], the authors used wide beams for the initial access and cell discovery, then refined to narrow beams during the data transmission. With a similar motivation, in [48], the authors proposed to use multi-armed beams (simultaneously sampling signals along multiple directions) for the cell discovery, and then refine to single-armed beams for data transmission. To avoid the high overhead of the beam sweeping procedure, in [44], the authors proposed to obtain a coarse estimation of the spatial direction, i.e., Angle-of-Arrival (AoA)/Angle-of-Departure (AoD) of individual UEs based on the sub-6 GHz communications and steer mmW beams towards the estimated directions. Furthermore, various learning algorithms have been developed recently to train the BSs and UEs to optimally align their beams (e.g., [45, 46, 47]).

Although the aforementioned adaptive beam alignment schemes are valuable in terms of providing adequate connectivity and coverage in mmW networks, they require significant modifications to existing hardware, such as analog phase shifters [49]. In addition, to align the downlink beams based on individual UE locations and channel conditions, we need to frequently change beam directions, i.e., adjust the transmit precoders and the receiver combiners of BSs. This adjustment procedure is challenging in general since it requires to solve a non-convex combinatorial optimization problem with NP-hard complexity [50].

Besides, the delay for realigning the beams can be high (several seconds) in the scenarios with high blockage density [51]. Furthermore, the out-of-band channel information based approach requires translating the AoA/AoD from the sub-6 GHz band to the mmW band. This translation procedure is challenging due to differences in the angle spreads, the size of the antenna array, and the channel gain between the two bands. In addition, the beam training approach often requires the knowledge of UE locations. Furthermore, to make good predictions, a large amount of training data is required.

On the other hand, fixed directional downlink beams (e.g., BSs with fixed directional antennas steering down from the ceiling in a theater, creating narrow spotlight of coverage) are easy to implement since they do not need frequent adjustments or the knowledge of the AoA/AoD of UEs. There are few prior works (e.g., [52, 53, 54]) that consider to use fixed directional beams to provide coverage in mmW networks. For example, in [52], the authors used passive reflectors to point fixed directional mmW beams towards the NLOS regions to to improve RSS at NLOS regions in mmW networks. With similar motivations, in [53, 54], the authors optimize the dimensions of reflectors and their directions to improve RSS in NLOS regions in mmW networks. However, these works did not consider the challenges for providing adequate coverage and connectivity with fixed directional downlink beams in the presence of uncertainty in UE locations and channel conditions. In addition, due to the uncertainty of mmW links, it is often required to make multiple beams available for each UE. In such cases, i.e., when more than one beam is available for a UE, it is important to optimally assign one of the available beams for the UE to improve the overall network performance. However, the aforementioned beam alignment schemes do not optimize the UE assignment in multi-beam enabled systems.

2.2.3 MmW UE Assignment

To design optimal mmW UE assignment strategy, a number of distributed and centralized schemes were proposed in past years. In the distributed schemes, individual UEs select one of the available mmW links without a centralized controller. For example, in [55], the authors formulated the optimal mmW UE assignment problem as a mixed integer nonlinear problem (MINLP) that aims to maximize the sum of logarithms of the instantaneous rates for all UEs in the network. To solve the optimization problem, the authors designed two suboptimal algorithms based on dual decomposition and auctions that are executed at individual UEs and BSs. The authors shown that the proposed scheme ensures on-average high throughput in a time-variant environment. However, in this work, the authors did not consider the small-scale fading of mmW channels and the interference experienced by UEs from the neighbor BSs. To account for interference, in [56], the authors formulated the optimal mmW UE assignment problem as a MINLP that aims to maximize the sum-rate of the individual UEs while balancing the interference caused by the BSs. The MINLP is solved at each UE by an iterative process where in each iteration, the link providing the lowest rate is swapped with an available link of a higher rate and if all the links are providing the same rate then, the link requiring the highest transmission power is swapped with a link requiring lower transmission power. The authors shown that their proposed algorithm produces good results with polynomial time complexity. With similar motivations, a non-cooperative game is designed in [57] where each UE aims to maximize its signal-to-noise-plus-interference-ratio (SINR) through interactions with neighbor UEs. However, the works in [55, 56, 57] primarily focus on improving spectral efficiency and ignore the energy efficiency of mmW networks. In [58], the authors overcame this limitation and jointly optimized spectral efficiency and energy efficiency of mmW networks. Specifically, the authors formulated an MINLP problem to maximize sum of the data rate per unit power consumption of the UEs while satisfying load

and power limitations of the mmW BSs, data rate requirements of the UEs, and limitations of the cross-tier interference. To solve the problem, the authors decomposed the original problem to a convex problem using Lagrangian duality and designed a gradient based algorithm that is executed by each UE. With a different perspective, in [59], the authors optimized the UE assignment to minimize power consumption in BSs and backhauls instead of UEs while ensuring each UE achieves a minimum data rate. Specifically, the authors designed a meta-heuristic algorithm that is executed by each UE to select the BS and corresponding backhaul that can serve its traffic with the lowest transmit power consumption. Although these distributed schemes improve the throughput and energy efficiency of mmW networks, they do not consider the delay and network overhead of the handover process. Furthermore the high computation complexity of the algorithms will impose significant challenges on hardware and system designs of UEs.

An alternative approach is centralized UE assignment schemes in which sub-6 GHz BSs act as central controllers for managing the connections between mmW BSs and UEs. For example, in [60], the authors proposed a three phase UE assignment strategy. In the first phase, the UEs transmit reference signals in all possible directions. In the second phase, the mmW BSs report their instantaneous received SNR to sub-6 GHz BS. Then, the sub-6 GHz BS assigns an optimal mmW link (i.e., the mmW link with highest SNR) to each UE. The authors shown that the proposed centralized scheme ensures a high throughput and low latency. In [61], three different centralized UE assignment strategies, i.e., assigning the nearest mmW BS, assigning the mmW BS that provides strongest RSS, and assigning the mmW BSs randomly are compared in terms of providing network-wide coverage. The authors concluded that assigning mmW links based on RSS outperforms the other two approaches in terms of providing network-wide coverage. However, in this work, the authors assumed uncertainty in the locations and beam directions of BSs to derive the coverage probability.

Furthermore, the authors modeled mmW channel fading as Nakagami fading that cannot truly capture the dispersiveness (e.g., high doppler spread) of mmW channels. Therefore, the applicability of this analysis in real systems remains unassesed.

Note that all of the aforementioned schemes assign mmW links based on instantaneous SNR or RSS. However, assigning the mmW links based on the instantaneous SNR or RSS cannot guarantee good performance due to the temporal dynamics of the mmW channels. In [62], the authors presented the impact of temporal dynamics of the mmW channels on the performance of the mmW UE assignment strategies. Therefore, consideration of the *stability* of the mmW links along with their instantaneous SNR is needed when assigning them to UEs to improve the overall network performance.

2.2.4 Discussions

In this dissertation, we aim to overcome the limitations of the existing schemes in the literature. Specifically, in Chapter 7, we develop an efficient mmW virtual resource allocation framework. The proposed framework jointly determines the optimal set of mmW BSs to deploy (or aggregate), their beam directions, and their assignment to individual UEs of SPs to provide adequate coverage and connectivity in the presence of uncertainty in UE locations and channel conditions. To make our framework cost-effective and readily implementable, we allow the mmW BSs to use existing low-complexity fixed directional beams. In addition, we allow a single downlink beam to cover more than one UE. Furthermore, our framework considers the temporal dynamics (e.g., stability) of the mmW beams while assigning them to UEs. To the best of our knowledge, we are presenting the first optimization framework that jointly optimizes placement (or aggregation) of mmW BSs, their beam directions, and their assignment to individual UEs of SPs considering the uncertainty in UE locations and channel conditions.

2.3 Summary

In this chapter, we reviewed existing work related to this dissertation. In the first section, we reviewed previous works and their limitations on enabling virtualization in sub-6 GHz cellular networks. The second section of the chapter presented related work and its limitations for enabling mmW communications in cellular networks.

Chapter 3

System Model

We consider a two-dimensional geographical area $\mathcal{A}$ that is covered by a set of RPs. Each RP has a set of BSs deployed in $\mathcal{A}$. The union of the sets of BSs operating in sub-6 GHz band is denoted by $\mathcal{B}$. The union of the sets of BSs operating in mmW band is denoted by $\mathcal{N}$. The location of sub-6 GHz BS $b,\ b \in \mathcal{B}$, is given by l_b and the location of mmW BS $n,\ n \in \mathcal{N}$, is l_n. The BS locations can also be viewed as potential candidate locations to place the respective BSs. There exists a set $\mathcal{S} = \{1, 2, ..., S\}$ of SPs. Each SP wants to cover the entire geographical area $\mathcal{A}$.

3.1 UE Distribution Model

The UEs of SP $s,\ s \in \mathcal{S}$, are assumed to be distributed in $\mathcal{A}$ according to a homogeneous Poisson Point Process (PPP) ϕ_s of intensity λ_s.

Now, in order to incorporate the beamforming, i.e., directional communication feature of mmW BSs, we divide the geographical area $\mathcal{A}$ into a finite set of equally spaced gird points. Let $\mathcal{K} = \{1, 2, \ldots, K\}$ denotes the set of grid points in $\mathcal{A}$. Let a denote the area of a grid. Since the UEs of SP $s,\ s \in \mathcal{S}$, are distributed in $\mathcal{A}$ according to a homogeneous PPP of intensity λ_s, the number of UEs of SP s that are located within a is a Poisson random variable of parameter $\lambda_s\ a$. Hence, we can express the distribution of the number of UEs of

SP s in the area of a grid as:

$$\Pr\left\{\tilde{N}_a = n\right\} = e^{-\lambda_s\, a}\, \frac{\lambda_s^n a^n}{n!}. \tag{3.1}$$

We assume that the grids are small enough such that $\Pr\left\{\tilde{N}_a \geq 2\right\} \approx 0$, i.e., each grid point in $\mathcal{K}$ can have at most one UE of SP $s,\ s \in \mathcal{S}$. Then, the probability that there is a UE of SP s in grid point $k,\ k \in \mathcal{K}$, that wishes to access the mmW connectivity can be expressed as:

$$m_{sk} = g_{sk}\ \Pr\left\{\tilde{N}_a = 1\right\} = g_{sk}\ \lambda_s\ a\ e^{-\lambda_s\, a} \tag{3.2}$$

where g_{sk} is the probability of the UE of SP s at grid k wishes to access the mmW connectivity.

To summarize, the UEs of SP $s,\ s \in \mathcal{S}$ that require sub-6 GHz connections are assumed to be distributed in $\mathcal{A}$ according to the homogeneous PPP ϕ_s of intensity λ_s. The UEs of SP s that require mmW connections are assumed to be distributed over the set of grid points $\mathcal{K}$ in $\mathcal{A}$. The probability of grid $k,\ k \in \mathcal{K}$, has a UE of SP $s,\ s \in \mathcal{S}$, is $m_{sk},\ k \in \mathcal{K}$.

3.2 Channel Models

3.2.1 Sub-6 GHz Channel Model

BS $b, b \in \mathcal{B}$, operates on bandwidth W_b and transmits omnidirectionally with a constant power $1/\mu_b$. A UE of an SP is served by its nearest sub-6 GHz BS among the set of sub-6 GHz BSs allocated to the SP. Hence, the tessellation formed by the collection of the association regions of BSs in $\mathcal{B}$ forms a Voronoi diagram, an example of which is shown in Figure 3.1. The channel gains experienced by UEs from their associated sub-6 GHz BS are assumed to follow a Rayleigh distribution with mean 1 (i.e., there is no shadowing). Hence, the SINR experienced by a typical UE at an arbitrarily distance $\tilde{d}$ from its associated sub-6 GHz BS

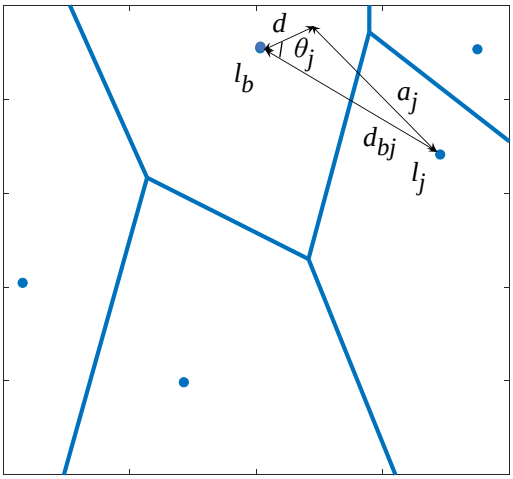

Figure 3.1: Voronoi tessellation of a set of sub-6 GHz BSs.

(say BS b) can be expressed as [63]:

$$\tilde{\text{SINR}}_b = \frac{\tilde{h}\,\tilde{d}^{-\alpha}}{\sigma^2 + \tilde{I}} \tag{3.3}$$

where $\tilde{h}$ is the stochastic channel gain, which is exponentially distributed with mean $1/\mu_b$, σ^2 is the variance of the additive noise, α is the pathloss exponent, and $\tilde{I}$ is the cumulative downlink interference from all other BSs[1]. $\tilde{I}$ can be expressed as:

$$\tilde{I} = \sum_{j \in \mathcal{B}/b} \tilde{I}_j = \sum_{j \in \mathcal{B}/b} \tilde{g}_j \tilde{a}_j^{-\alpha} \tag{3.4}$$

where $\tilde{a}_j$ is the distance between the typical UE and the interfering BS j and $\tilde{g}_j$ is the stochastic gain of the channel between them. We assume that the interference also experiences Rayleigh fading without shadowing. Therefore, $\tilde{g}_j$ is exponentially distributed with mean $1/\mu_j$.

[1]We put ˜ on top of a variable to indicate that this variable is a stochastic variable.

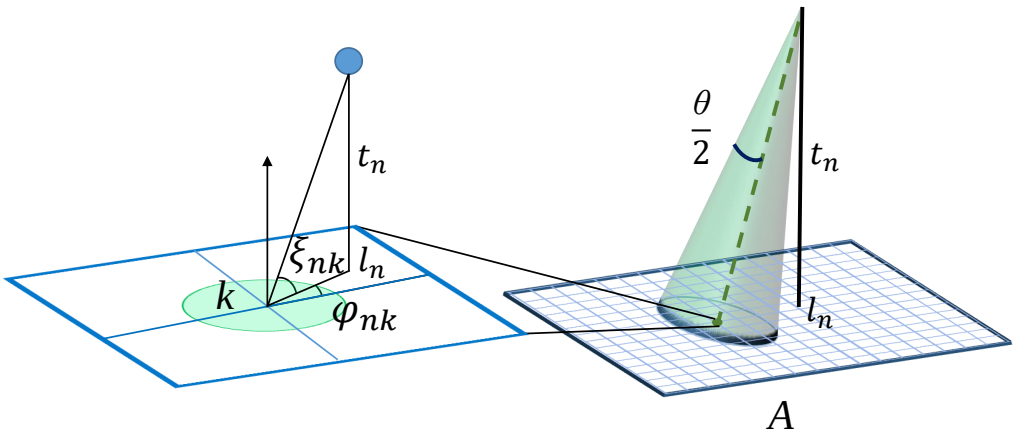

Figure 3.2: MmW network deployment architecture.

Let $\tilde{\theta}_j$ be the angle between the two lines: the line connecting sub-6 GHz BS b with the typical UE, and the line connecting sub-6 GHz BS b with its neighboring BS j as shown in Figure 3.1. Then, a_j can be expressed as $\tilde{a}_j = \sqrt{\tilde{d}^2 + d_{bj}^2 - 2\tilde{d}\, d_{bj}\, \cos\tilde{\theta}_j}$.

3.2.2 MmW Channel Model

To incorporate the beamforming, i.e., directional communication feature of mmW BSs, we include the third dimension, i.e., height of the mmW BSs in our system model as shown in Figure 3.2. The height of mmW BS n, $n \in \mathcal{N}$, is t_n. MmW BS n, $n \in \mathcal{N}$, can have at most B_n beams. BS n can aim its beam towards any grid point in $\mathcal{K}$. The beam directions are fixed, i.e., the beams cannot be steered in real time. A beam aimed towards a grid point may cover multiple surrounding grid points based on its beamwidth.

Directionality Gain:

We assume that the mmW BSs transmit with constant power in fixed beam directions. Let $\theta_n, n \in \mathcal{N}$, be the elevation and azimuth beamwidth of BS n. BS $n, n \in \mathcal{N}$, has a main-lobe

gain G_n and negligible side-lobe gains. Let $\phi_{nk}, n \in \mathcal{N}, k \in \mathcal{K}$, be the azimuth angle of BS n directed towards grid point k and $\xi_{nk}, n \in \mathcal{N}, k \in \mathcal{K}$, be the elevation angle of BS n directed towards grid point k, as shown in Figure 3.2. Then, the antenna gain experienced at grid j from the beam of BS n that is aimed towards grid point k is given by:

$$G_{nk}^{(j)} = \begin{cases} G_n, & \text{if } |\phi_{nk} - \phi_{nj}| \leq \frac{\theta_n}{2}, |\xi_{nk} - \xi_{nj}| \leq \frac{\theta_n}{2} \\ 0, & \text{otherwise.} \end{cases} \tag{3.5}$$

Blockage Model:

The blockages over the links between the mmW BSs and the grids are assumed to be independent and identically distributed (i.i.d.) Bernoulli random variables [64]. $P_{L_{nk}}, n \in \mathcal{N}, k \in \mathcal{K}$, denotes the probability that grid point k is in LOS of BS n, and $P_{NL_{nk}} = 1 - P_{L_{nk}}$ denotes the probability that there is a blockage on the link between BS n and grid k.

MmW SNR Distribution Model:

We assume that there is no downlink interference among the mmW beams (i.e., frequency reuse factor for the intersecting beams are assumed to be < 1). Furthermore, the multipath fading experienced by the channels between the grids (or UEs) and their associated mmW BSs are assumed to follow $\kappa - \mu$ distribution [65]. Then, the PDF of the SNR experienced at grid j from the beam of BS n that is steered towards grid k is given by:

$$f_{\gamma_{nk}}^{(j)}(x) = \frac{2\mu \left(\sigma^4 (\kappa+1)\right)^{\frac{\mu+1}{2}} x^{\mu}}{\kappa^{\left(\frac{\mu-1}{2}\right)} \exp(\mu\kappa)\ G_{nk}^{(j)}\ R_{nj}^{\frac{\mu+1}{2}}} \exp\left(\frac{-\mu(\kappa+1)(\sigma^2 x)^2}{G_{nk}^{(j)}\ R_{nj}}\right) I_{\mu-1} \frac{2\sigma^2 x \mu \sqrt{\kappa(\kappa+1)}}{\sqrt{G_{nk}^{(j)}\ R_{nj}}} \tag{3.6}$$

where $I_v(.)$ represents the modified Bessel function of the first kind with order v, κ is defined as the ratio between the total power in the dominant signal components and the total power

in the scattered signal components, μ is related to the number of multipath clusters, σ^2 is the noise variance, and R_{nj} is the power received from BS n at grid j.

We adopt the power-law pathloss model, in which the power received at grid j from BS n is given by:

$$R_{nj} = \begin{cases} R_0, & \text{for } d_{nj} \leq d_0 \\ R_0 \, d_{nj}^{-\alpha}, & \text{otherwise} \end{cases} \tag{3.7}$$

where α is the pathloss exponent, d_{nj} is the length of the link between BS n and grid j, and R_0 is the pathloss at reference distance d_0.

Note that κ and μ in (3.6) and R_0, α, and d_0 in (3.7) differ from the LOS case to the NLOS case.

Temporal Dynamics of MmW Beam:

We introduce a new parameter to measure the quality of a mmW beam, i.e., *beam stability*. The beam stability is measured by the expected duration of time that a currently available beam remains available. On the other hand, beam availability is measured by the long term fraction of time that a beam is available. (e.g. A beam that was up an average of 1 second then down an average of 1 second would be much more stable than a beam that was up an average of 50 ms then down an average of 50 ms, though both beams would have an availability of 50%.)

We assume that the sojourn time of a mmW beam availability follows the exponential distribution [66]. Specifically, if a beam of BS $n, n \in \mathcal{N}$, is available at grid $k, k \in \mathcal{K}$, at time instant t, then the probability that this beam remains available for the next T seconds

is given by:

$$l_{nk} = \exp(-\nu_{nk}\, T) \tag{3.8}$$

where ν_{nk} is the rate of failure of the beam of BS n at grid k. (Note that $\frac{1}{\nu_{nk}}$ is the mean up time of the beam, a measure of the beam stability.)

3.3 UE Association Model

When a UE of an SP enters its virtual network, it camps over the nearest sub-6 GHz BS among the set of sub-6 GHz BSs assigned to the SP. When the UE wants to access the mmW BSs, it sends a request to the sub-6 GHz BS. Upon receiving the request, the sub-6 GHz BS informs all of its associated mmW BSs that are assigned to the SP to switch on their beams. The UE starts to scan the availability of the mmW beams. In each resource allocation cycle/time period, the UE sends its mmW beam availability information to the sub-6 GHz BS. If there is no mmW beam available for the UE, the sub-6 GHz BS is assigned to the UE. If more than one mmW beam is available for the UE, the legacy BS assigns the most stable beam to the UE.

Chapter 4

Deriving Downlink Rate Coverage Probability of Sub-6 GHz Cellular Networks[1]

4.1 Introduction

One important performance metric for a cellular network is its downlink rate coverage probability, defined as the probability of an arbitrarily chosen UE achieving a certain downlink rate. In this chapter, we derive a closed-form expression of the downlink rate coverage probability of sub-6 GHz cellular network.

Due to UE mobility and various stochastic channel effects (such as multipath fading, shadowing, intra- and inter-cell interference), the rate coverage probability analysis of a network is extremely challenging. Stochastic geometry has emerged as an efficient and tractable approach for analyzing rate coverage probability [63]. Existing stochastic geometry works analyze the rate coverage probability assuming uncertainty in the locations of both UEs and sub-6 GHz BSs. sub-6 GHz BS locations were modeled stochastically in existing works in order to obtain analytical results that are valid for a variety of sub-6 GHz BS deployments. In contrast, in this chapter, we answer a new question: Considering a set of sub-6 GHz BSs

[1]Material in this chapter was published in [38].

deployed by RPs, in which the BS locations are known, what is the performance (in terms of the rate coverage probability) of the deployed network in the presence of uncertainty in UE locations and channel conditions? Answering this question is of great importance for VNBs to know the probabilistic QoS level (as measured by the rate coverage) that they can provide to their SPs.

With this motivation, in this chapter, we present a tractable mathematical expression for the downlink rate coverage probability of a sub-6 GHz network with known BS locations. The rest of the chapter is organized as follows. We describe the BS rate allocation model in Section 4.2. The rate coverage analysis is presented in Section 4.3. In Section 4.4, we discuss our numerical results. Finally, we conclude the chapter in Section 4.5.

4.2 BS Rate Allocation Model

We assume each BS in $\mathcal{B}$ performs a proportional rate allocation for its UEs, i.e., the sub-6 GHz rate allocated to each UE is proportional to its spectral efficiency. Hence, assuming a saturated UE queue, the sub-6 GHz rate of a typical UE associated with BS b, $b \in \mathcal{B}$, is given by:

$$\tilde{R}_b = \frac{W_b}{\tilde{N}_b} \underbrace{\log_2\left(1 + \tilde{\text{SINR}}_b\right)}_{\text{spectral efficiency}} \tag{4.1}$$

where $\tilde{N}_b$ is the load of BS b, defined as the total number of UEs associated with BS b.

4.3 Rate Coverage Analysis

4.3.1 Preliminaries

Definition 1 (Rate Coverage Probability): The rate coverage probability is the probability that an arbitrarily chosen UE of the network can have a data rate of at least κ bps. Let $\tilde{R}$

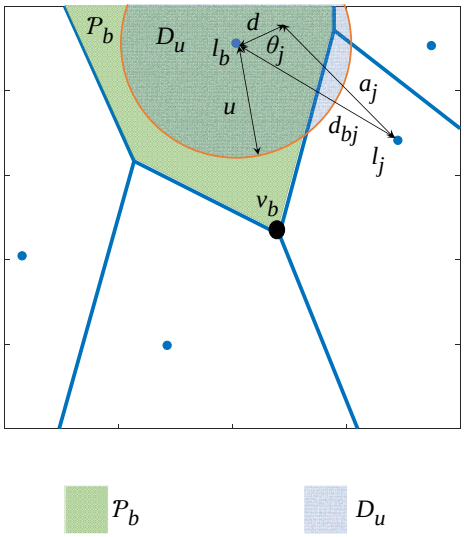

Figure 4.1: Voronoi tessellation of a set of sub-6 GHz BSs.

be the sub-6 GHz data rate of an arbitrary UE of the network. Then, the sub-6 GHz rate coverage probability, denoted by $\mathcal{R}$, is expressed as:

$$\mathcal{R} \triangleq \Pr\left\{\tilde{R} \geq \kappa\right\}. \tag{4.2}$$

Definition 2 (Association Region): The association region of sub-6 GHz BS $b, b \in \mathcal{B}$, denoted by $\mathcal{P}_b$, is the region in $\mathcal{A}$ in which all UEs are served by BS b. As mentioned in Chapter 3, we assume that each UE is associated with its nearest sub-6 GHz BS.

The tessellation formed by the collection of $\mathcal{P}_b, \forall b \in \mathcal{B}$, forms a Voronoi diagram, an example of which is shown in Figure 4.1. The coverage region of BS b, $\mathcal{P}_b$, can be geometrically represented as a polygon, whose area (denoted by A_b) can be readily calculated since its vertices are known. To calculate A_b, we divide $\mathcal{P}_b$ into multiple triangles by drawing line segments from l_b to the vertices. Then, we calculate the area of each triangle by applying Heron's formula [67].

4.3.2 Probability Distribution of Sub-6 GHz BS Load

Recall from Chapter 3 that the UEs requiring sub-6 GHz connections are assumed to be distributed in $\mathcal{A}$ according to a homogeneous PPP. Let the intensity of the homogeneous PPP be λ. Then, the number of UEs that are served by BS b (i.e., located within $\mathcal{P}_b$) is a Poisson random variable of parameter $\lambda\ A_b$ [63]. Hence, we can express the distribution of the number of UEs served by BS b (i.e., load of BS b), N_b, as:

$$\Pr\{N_b = n\} = \frac{(\lambda\ A_b)^n}{n!} e^{-\lambda\ A_b}. \tag{4.3}$$

4.3.3 Probability Distribution of the Distance to the Nearest Sub-6 GHz BS

Consider BS b. Since we assumed a homogeneous PPP, the UEs are uniformly distributed in the polygon $\mathcal{P}_b$. To compute the cumulative distribution function (CDF) of $\tilde{d}$, the distance of a typical UE from its associated sub-6 GHz BS (say b), let us define D_u to be a circular disc of radius u centered at l_b as shown in Figure 4.1. Then,

$$\Pr\{d \leq u\} = \begin{cases} \frac{\nabla\{\mathcal{P}_b \cap D_u\}}{A_b}, & \text{for } 0 \leq u \leq |l_b - v_b| \\ 1, & \text{otherwise} \end{cases} \tag{4.4}$$

where $\nabla\{\mathcal{P}_b \cap D_u\}$ denotes the overlapping area between polygon $\mathcal{P}_b$ and disc D_u, and v_b denotes the farthest vertex of polygon $\mathcal{P}_b$ from BS b (i.e., l_b). $\nabla\{\mathcal{P}_b \cap D_u\}$ is found by following the algorithm proposed in [68]. To calculate $\nabla\{\mathcal{P}_b \cap D_u\}$, we divide $\mathcal{P}_b$ into multiple triangles by drawing line segments from l_b to the vertices. In each triangle, we have an overlapping area with D_u. The overlapping area contains a circular sector under the arc of D_u and occasionally some triangular areas. Since we know the coordinates of the vertices

of the triangles as well as the intersecting points between D_u and the triangles, we are able to calculate the overlapping area in each triangle. Finally, we add all of these overlapping areas of the triangles to obtain $\nabla\{\mathcal{P}_b \cap D_u\}$.

From the CDF (4.4), the probability density function (PDF) of $\tilde{d}$ can be obtained as follows:

$$\begin{aligned} f_d(u) &= \frac{\mathrm{d}\Pr\{d \le u\}}{\mathrm{d}u} \\ &= \begin{cases} \frac{1}{A_b}\frac{\mathrm{d}[\nabla\{\mathcal{P}_b \cap D_u\}]}{\mathrm{d}u}, & \text{for } 0 \le u \le |l_b - v_b| \\ 0, & \text{otherwise.} \end{cases} \end{aligned} \tag{4.5}$$

4.3.4 Probability Distribution of Sub-6 GHz Downlink Interference

Consider a typical UE located at distance d from its associated sub-6 GHz BS b, experiencing a downlink interference $\tilde{I}_j$ from another sub-6 GHz BS j, which is located at l_j in $\mathcal{A}$. Let $d_{b,j}$ be the distance between BSs b and j and $\tilde{\theta}_j$ be the angle shown in Figure 4.1. Then, the distance of this typical UE from BS j is given by $\tilde{a}_j = \sqrt{\tilde{d}^2 + d_{b,j}^2 - 2\,\tilde{d}\,d_{b,j}\cos\tilde{\theta}_j}$. Therefore, for a constant transmit power $1/\mu_j$ of BS j, and in a Rayleigh fading channel, the CDF of $\tilde{I}_j$ for given d and θ_j can be expressed as:

$$\begin{aligned} F_{I_j}(c \mid d, \theta_j) &= \Pr\{I_j \le c \mid d, \theta_j\} = \Pr\left\{h_j\, a_j^{-\alpha} \le c \mid d, \theta_j\right\} = \Pr\left\{h_j \le c\, a_j^{\alpha} \mid d, \theta_j\right\} \\ &= 1 - \exp\left(-c\,\mu_j\, a_j^{\alpha}\right) \end{aligned} \tag{4.6}$$

for any real number c within the support of $\tilde{I}_j$.

The PDF of $\tilde{I}_j$ for given d and θ_j can be found as:

$$f_{I_j}\left(c \mid d, \theta_j\right) = \frac{\mathrm{d}F_{I_j}\left(c \mid d, \theta_j\right)}{\mathrm{d}c} = \mu_j \; a_j^{\alpha} \; \exp\left(-c \; \mu_j \; a_j^{\alpha}\right). \tag{4.7}$$

Note that for a given d, $\tilde{\theta}_j$ varies within a range between 0 and 2π, following a uniform distribution [69]. Then, the marginal PDF of I_j for a given d can be found as:

$$f_{I_j}\left(c \mid d\right) = \int f_{I_j}\left(c \mid d, v\right) \; f_{\theta_j}\left(v \mid d\right) \mathrm{d}v = \frac{1}{2\pi} \int_0^{2\pi} \mu_j \; a_j^{\alpha} \; \exp\left(-c \; \mu_j \; a_j^{\alpha}\right) \mathrm{d}v. \tag{4.8}$$

The characteristic function of $\tilde{I}_j$ for a given d can be found as [69]:

$$\begin{aligned} \phi_{I_j}\left(\omega\right) &= \int_0^{\infty} f_{I_j}\left(c \mid d\right) \; e^{i\omega c} \, \mathrm{d}c = \int_0^{\infty} \frac{1}{2\pi} \left\{ \int_0^{2\pi} \mu_j \; a_j^{\alpha} \; \exp\left(-c \; \mu_j \; a_j^{\alpha}\right) \mathrm{d}v \right\} \; e^{i\omega c} \, \mathrm{d}c \\ &= \frac{1}{2\pi} \int_0^{2\pi} \frac{\mu_j \; a_j^{\alpha}}{\mu_j \; a_j^{\alpha} - i\omega} \, \mathrm{d}v \end{aligned} \tag{4.9}$$

where $i = \sqrt{-1}$.

Assuming that all neighboring sub-6 GHz BSs cause interference independently, the PDF of the cumulative interference experienced by a typical UE located at distance d from its associated sub-6 GHz BS b can be expressed as:

$$f_I\left(c \mid d\right) = \frac{1}{2\pi} \int_{-\infty}^{\infty} \left\{ e^{-i\omega c} \prod_{j \in \mathcal{B} \setminus b} \phi_{I_j}\left(\omega\right) \; \mathrm{d}\omega \right\}. \tag{4.10}$$

4.3.5 Probability Distribution of Sub-6 GHz Downlink SINR

The CDF of the received SINR by a typical UE located at distance d from its associated sub-6 GHz BS b, which experiences a cumulative downlink interference I from its neighboring

sub-6 GHz BSs can be derived as:

$$\Pr\left\{\mathrm{SINR}_b \leq \gamma \mid I, d\right\} = \Pr\left\{h \leq \gamma d^{\alpha}\left(\sigma^2 + I\right) \mid I, d\right\} = 1 - \exp\left(-\mu_b\, \gamma\, d^{\alpha}\left(\sigma^2 + I\right)\right).$$

Hence, the PDF of $\tilde{\mathrm{SINR}}_b$ for given I and d is given by:

$$\begin{aligned} f_{\mathrm{SINR}_b}\left(\gamma \mid I, d\right) &= \frac{\mathrm{d}\Pr\left\{\mathrm{SINR}_b \leq \gamma \mid I, d\right\}}{\mathrm{d}\gamma} \\ &= \mu_b\, d^{\alpha}\left(\sigma^2 + I\right) \exp\left(-\mu_b\, \gamma\, d^{\alpha}\left(\sigma^2 + I\right)\right). \end{aligned} \tag{4.11}$$

The joint PDF of $\tilde{\mathrm{SINR}}_b$, d and I is given by:

$$f_{\mathrm{SINR}_b, I, d}\left(\gamma, c, u\right) = f_{\mathrm{SINR}_b}\left(\gamma \mid c, u\right)\, f_I\left(c \mid u\right) f_d\left(u\right). \tag{4.12}$$

Therefore, the marginal PDF of the received SINR by a typical UE associated with BS b is given by (4.13).

4.3.6 Sub-6 GHz Downlink Rate Coverage Probability

Theorem 4.1. *The rate coverage probability of a sub-6 GHz cellular network with the BS rate allocation model characterized as in Section 4.2 is given by* (4.14).

Proof. Let Z be a stochastic variable defined as $Z = W_b \log_2\left(1 + \gamma\right)$, where the distribution of γ is $f_{\mathrm{SINR}_b}\left(\gamma\right)$ in (4.13). Then, the PDF of Z is given by [69]:

$$\begin{aligned} f_Z\left(z\right) &= \left(f_{\mathrm{SINR}_b}\left(\gamma\right) \left|\frac{\mathrm{d}\gamma}{\mathrm{d}z}\right|\right)_{\gamma = \left(2^{\frac{z}{W_b}} - 1\right)} \\ &= \frac{\left(2^{\frac{z}{W_b}}\right) \log 2}{W_b} f_{\mathrm{SINR}_b}\left(2^{\frac{z}{W_b}} - 1\right). \end{aligned} \tag{4.15}$$

From (4.1), the distribution of the sub-6 GHz rate achieved by an arbitrarily chosen UE in $\mathcal{A}$, which is associated with BS b, can be expressed as:

$$f_{\text{Rate}_b}(\rho) = f_{\text{Rate}_b}\left(\frac{Z}{N_b}\right) = \sum_{n=0}^{\infty} \Pr\{N_b = n\}\; n\, f_Z(n\rho). \tag{4.16}$$

Hence, the probability that an arbitrarily chosen UE in $\mathcal{A}$ achieves a minimum sub-6 GHz rate of κ bps while being associated with BS b is given by:

$$\Pr\left\{\tilde{R}_b \geq \kappa\right\} = 1 - \int_0^{\kappa} f_{\text{Rate}_b}(\rho)\; \mathrm{d}\rho. \tag{4.17}$$

Recall from Chapter 3 that UEs are assumed to be associated with the nearest sub-6 GHz BS. Therefore, when choosing a UE arbitrarily from $\mathcal{A}$ (whose area is denoted by A), it

---

$$\begin{aligned} f_{\text{SINR}_b}(\gamma) &= \int\int f_{\text{SINR}_b,I,d}(\gamma, c, u)\; \mathrm{d}u\; \mathrm{d}c \\ &= \frac{1}{2\pi A_b} \int_0^{\infty} \int_0^{|l_b - v_b|} \mu_b u^{\alpha} \left(\sigma^2 + c\right) \exp\left(-\mu_b\, \gamma\, u^{\alpha} \left(\sigma^2 + c\right)\right) \\ &\times \left\{ \int_{-\infty}^{\infty} \left\{ e^{-i\omega c} \prod_{j \in \mathcal{B}\setminus b} \int_0^{2\pi} \frac{\mu_j\; a_j^{\alpha}}{2\pi\left(\mu_j\; a_j^{\alpha} - i\omega\right)}\; \mathrm{d}v \right\} \mathrm{d}\omega \right\} \frac{\mathrm{d}\left[\nabla\left\{\mathcal{P}_b \cap D_u\right\}\right]}{\mathrm{d}u}\, \mathrm{d}u\, \mathrm{d}c. \end{aligned} \tag{4.13}$$

$$\begin{aligned} \mathcal{R} = 1 - \frac{1}{2\pi A} \sum_{b \in \mathcal{B}} \Bigg[& e^{-\lambda A_b}\, \frac{\log 2}{W_b} \sum_{n=0}^{\infty} \frac{\lambda^n A_b^n}{(n-1)!} \int_0^{\kappa} 2^{\frac{n\rho}{W_b}} \int_0^{\infty} \int_0^{|l_b - v_b|} \mu_b\; u^{\alpha} \left(\sigma^2 + c\right) \\ & \times \exp\left(-\mu_b\; u^{\alpha}\; \left(2^{\frac{n\rho}{W_b}} - 1\right)\; \left(\sigma^2 + c\right)\right) \\ & \times \left\{ \int_{-\infty}^{\infty} \left\{ e^{-i\omega c} \prod_{j \in \mathcal{B}\setminus b} \int_0^{2\pi} \frac{\mu_j\; a_j^{\alpha}}{2\pi\left(\mu_j\; a_j^{\alpha} - i\omega\right)}\; \mathrm{d}v \right\} \mathrm{d}\omega \right\} \frac{\mathrm{d}\left[\nabla\left\{\mathcal{P}_b \cap D_u\right\}\right]}{\mathrm{d}u}\, \mathrm{d}u\, \mathrm{d}c\, \mathrm{d}\rho \Bigg]. \end{aligned} \tag{4.14}$$

---

is more likely to be associated with the sub-6 GHz BS which has a larger association region. In other words, the probability of a UE being associated with a given sub-6 GHz BS is the fraction of the total area covered by the association region of that sub-6 GHz BS. Hence, considering a set of sub-6 GHz BSs $\mathcal{B}$, the sub-6 GHz rate coverage probability, defined in (4.2), is given by:

$$\mathcal{R} = \sum_{b\in\mathcal{B}} \frac{A_b}{A} \Pr\left\{\tilde{R}_b \geq \rho_s\right\} = 1 - \sum_{b\in\mathcal{B}} \frac{A_b}{A} \int_0^{\kappa} f_{\text{Rate}_b}(\rho)\, \mathrm{d}\rho. \tag{4.18}$$

Substituting (4.16) in (4.18), we obtain the result in (4.14). □

4.4 Numerical Analysis

In this section, we validate the rate coverage probability expression given by Theorem 4.1 (for deterministically known locations of sub-6 GHz BSs), and compare it with an existing rate coverage probability result, which assumes that the sub-6 GHz BS locations form a homogeneous PPP [63]. We consider a geographical area of 5×5 km^2, where 50 sub-6 GHz BSs are located as shown in Figure 4.2. To compare with [63], the sub-6 GHz BS locations are generated as a realization of a homogeneous PPP of intensity 2/km^2. All sub-6 GHz BSs operate over a bandwidth of 10 MHz. The sub-6 GHz BSs transmission power is set to 40 dBm and σ^2 is set to -104 dBm. We compare our result in Theorem 4.1 with a simulation-based result. In simulations, we took a random realization of UE locations. For each realization, we calculate the sub-6 GHz rate achieved by each UE using (4.1). Finally, we compute the fraction of the UEs that achieved the sub-6 GHz rate threshold.

First, in Figure 4.3 we vary the sub-6 GHz rate threshold (κ) and plot the sub-6 GHz rate coverage probability ($\mathcal{R}$) for different values of α, while fixing λ at 50/km^2. It can be seen that the sub-6 GHz rate coverage probability obtained from Theorem 4.1 closely

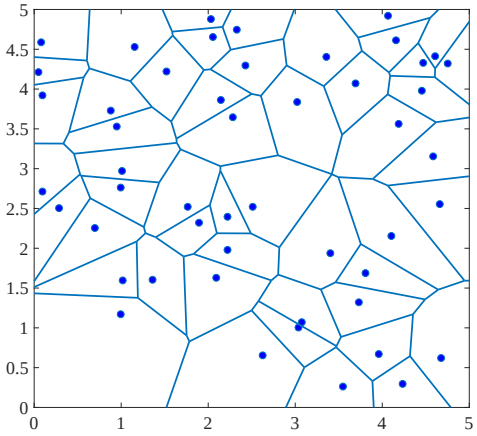

Figure 4.2: Locations of 50 sub-6 GHz BSs, as obtained from a realization of a homogeneous PPP of intensity $2/\text{km}^2$.

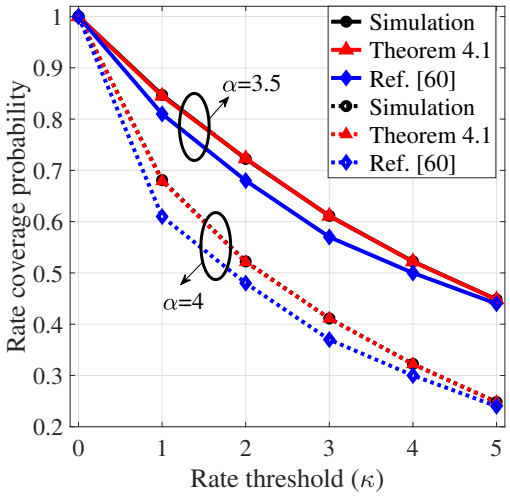

Figure 4.3: $\mathcal{R}$ vs. κ for different values of α ($\lambda = 50/\text{km}^2$).

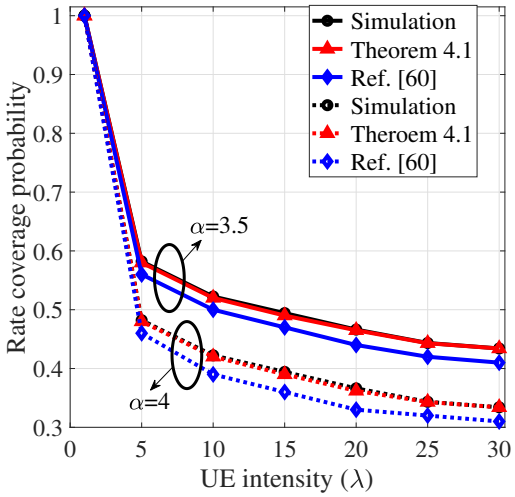

Figure 4.4: $\mathcal{R}$ vs. the UEs intensity for different values of α ($\kappa = 5$ Mbps).

matches the actual sub-6 GHz rate coverage probability obtained from the simulations.

Next, in Figure 4.4 we plot $\mathcal{R}$ vs. the UEs intensity for different values of α, while fixing κ at 5 Mbps. Since the bandwidth of the sub-6 GHz BSs are fixed, as the number of UE increases, the sub-6 GHz rate coverage probability decreases.

Note that, in both Figures, the sub-6 GHz rate coverage probability computed by Theorem 4.1 is always higher than [63]. The reason is as follows. Recall that in [63] the authors assume that the sub-6 GHz BS locations form a homogeneous PPP. The authors computed the sub-6 GHz rate coverage probability based on the intensity of the sub-6 GHz BS distribution whereas, in Theorem 4.1, we computed the sub-6 GHz rate coverage probability based on the deterministically known sub-6 GHz BS locations. In other words, the sub-6 GHz rate coverage probability computed from [63] is an average of all possible realizations of the PPP for sub-6 GHz BS locations, whereas the sub-6 GHz rate coverage probability computed from Theorem 4.1 is for one particular realization of the PPP for sub-6 GHz BS locations. Essentially, the results in [63] include realizations of the PPP in which the sub-6 GHz rate coverage probability is extremely bad, because the sub-6 GHz BSs are poorly

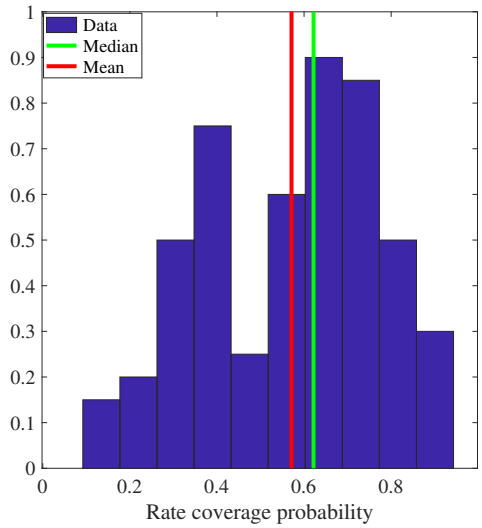

Figure 4.5: Histogram of the sub-6 GHz rate coverage probabilities of 1000 realizations of the PPP for sub-6 GHz BS locations.

spread. These pull down the average. On the other hand, the realization of the PPP that we choose happened to result in a sub-6 GHz rate coverage probability that is higher than the average. In fact, a typical realization of the PPP provides a higher than average sub-6 GHz rate coverage probability, because the median sub-6 GHz rate coverage probability is higher than the mean. Let us take an example. Consider 1000 realizations of the PPP for sub-6 GHz BS locations. For each realization, we compute the sub-6 GHz rate coverage probability through pure simulations. Then, we plot the histogram of the sub-6 GHz rate coverage probabilities of the 1000 realizations of the PPP for sub-6 GHz BS locations, as shown in Figure 4.5. As can be seen, the median sub-6 GHz rate coverage probability is higher than the mean. This shows that, a typical realization of the PPP for sub-6 GHz BS locations produces rate coverage probability that is higher than the mean. Consequently, when we compute the rate coverage probability for a typical realization of the PPP for sub-6 GHz BS locations, Theorem 4.1 results in higher than average rate coverage probability.

4.5 Summary

In this chapter, we provided the first expression for the downlink sub-6 GHz rate coverage probability of a cellular network with *deterministically known sub*-6 *GHz BS locations*. We numerically validate our results. We have shown that by stochastically modeling the sub-6 GHz BS locations, we would underestimate the true achievable downlink sub-6 GHz rate coverage probability. Consequently, there is a trade off between desired accuracy and required complexity for the computation of the sub-6 GHz rate coverage probability.

Chapter 5

Sub-6 GHz Virtual Resource Allocation[1]

5.1 Introduction

In this chapter, we design an efficient scheme that is to be executed at the VNB to build sub-6 GHz virtual networks for the SPs to meet their sub-6 GHz downlink rate coverage probability demands with affordable network overhead and reasonable computation complexity. Specifically, we design a chance-constrained stochastic optimization framework that optimally aggregates the sub-6 GHz BSs from the RPs, *slices* them, and then allocates the sliced BSs to the SPs in such a way that the SPs' sub-6 GHz rate coverage probability demands are satisfied, isolation among the slices are maintained, and resource over-provisioning is minimized in the presence of the uncertainty in UE locations and channel conditions. Towards designing this framework, we derive the sub-6 GHz downlink rate coverage probability obtained from a set of *sliced* sub-6 GHz BSs by modifying the closed-form expression of the sub-6 GHz downlink rate coverage probability obtained from a set of non-sliced sub-6 GHz BSs derived in the last chapter. After that, with this expression, we design a low-complexity algorithm to build sub-6 GHz virtual networks for the SPs. Furthermore, considering the possibility of the optimization model being infeasible due to lack of sufficient resources in

[1]Part of the material in this chapter was published in [70] and additional material was published in [71].

the resource pool, we propose a prioritized sub-6 GHz virtual resource allocation mechanism where virtual networks are sequentially built for SPs based on given priorities.

The rest of the chapter is organized as follows. In Section 5.2, we characterize the SP demands and describe our virtual resource allocation model. In Section 5.3, we present the details of our optimal virtual resource allocation framework. The numerical analysis is presented and discussed in Section 5.4. Finally, the chapter is concluded in Section 5.5.

5.2 SP Demands Characterization, Framework Overview, and Problem Statement

5.2.1 SP Demands Characterization

SP $s, s \in \mathcal{S}$, characterizes its sub-6 GHz demand as follows: If we arbitrarily choose a UE of SP s in $\mathcal{A}$ that requires sub-6 GHz connection, the probability that this UE receives a sub-6 GHz data rate of at least κ_s bps needs to be at least β_s. Let $\tilde{R}_s$ be the sub-6 GHz data rate of an arbitrarily chosen UE of SP s located in $\mathcal{A}$. Then, the sub-6 GHz data rate demand of SP s can be expressed as

$$\Pr\left\{\tilde{R}_s \geq \kappa_s\right\} \geq \beta_s.$$

Let us call $\Pr\left\{\tilde{R}_s \geq \kappa_s\right\}$ the sub-6 GHz virtual network downlink rate coverage probability.

5.2.2 Framework Overview

Upon receiving the sub-6 GHz demands from SPs, VNB leases a subset of sub-6 GHz BSs from $\mathcal{B}$ and slices them among the SPs such that their demands are satisfied. A slice of a

BS provides a fraction of capacity of the BS [72]. For example, let $\delta_{bs} \in [0,1]\,,\ b \in \mathcal{B},\ s \in \mathcal{S}$, be a slice of sub-6 GHz BS b allocated to SP s. In that case, δ_{bs} represents the fraction of the capacity of BS b that SP s is the only SP to access. If SP s is the only SP associated with BS b, then $\delta_{bs} = 1$. Likewise, if SP s is not to be associated with BS b at all, then $\delta_{bs} = 0$. Recall from Chapter 3 that we assume each sub-6 GHz BS performs a proportional rate allocation for its UEs, i.e., the sub-6 GHz rate allocated to each UE is proportional to its spectral efficiency. Hence, the sub-6 GHz rate of a typical UE of SP s associated with BS b can be expressed from (4.1) as:

$$\tilde{R}_{bs} = \delta_{bs} \left(\frac{W_b}{\tilde{N}_{bs}} \underbrace{\log_2\left(1 + \tilde{\text{SINR}}_b\right)}_{\text{spectral efficiency}} \right) \tag{5.1}$$

where $\tilde{N}_{bs}$ is the total number of UEs of SP s associated with BS b.

The slicing is implemented on a sub-6 GHz BS as follows. The VNB associates SPs with the BS and dictates the BS to reserve the fractions of its resources (e.g., service time, operating bandwidth, number of resource blocks in each resource allocation cycle [72]) for each of the associated SPs. Now, the BS while serving the UEs of the associated SPs, ensures that each SP gets its share. Hence, in terms of slicing sub-6 GHz BSs, the VNB's job is to determine the fractions of the capacity of the BSs to be allocated to SPs.

5.2.3 Problem Statement

Our goal is to design a scheme to be executed at the VNB to optimally perform the sub-6 GHz virtual resource allocation, i.e., determining the optimal subset of BSs to be leased from the sub-6 GHz BS pool $\mathcal{B}$ and determining the optimal fractions of capacity of the leased BSs to be allocated to the SPs. Our optimality criterion is to minimize the costs of BS aggregation (i.e., maximize the utilization of the resources) while satisfying the SP

demands. Hence, we define the optimal sub-6 GHz virtual resource allocation problem as: *For given sub-6 GHz demands of the SPs in $\mathcal{S}$, determine the cheapest subset of BSs to be leased from $\mathcal{B}$ such that, when sliced among SPs, these BSs can meet the sub-6 GHz demands of all SPs.*

5.3 Optimization Framework

In this section, we propose an optimization framework that is executed at the VNB to optimally perform the virtual resource allocation. First, we formulate the problem.

5.3.1 Problem Formulation

Let $x_b,\ b \in \mathcal{B}$, be a binary decision variable indicating whether to lease sub-6 GHz BS b or not. x_b equals one if BS b will be selected and it equals zero otherwise. The cost for leasing BS $b,\ b \in \mathcal{B}$, is c_b. Then, the optimal sub-6 GHz virtual resource allocation problem for the VNB can be formulated as:

Problem 5.1: Optimal Sub-6 GHz Virtual Resource Allocation

$$\underset{\left\{\substack{x_b,\delta_{bs} \\ b\in\mathcal{B},s\in\mathcal{S}}\right\}}{\text{minimize}} \sum_{b\in\mathcal{B}} c_b\, x_b \tag{5.2}$$

subject to:

$$\Pr\left\{\tilde{R}_s \geq \kappa_s\right\} \geq \beta_s,\ \ \forall s \in \mathcal{S} \tag{5.3}$$

$$\sum_{s\in\mathcal{S}} \delta_{bs} \leq 1,\ \ \forall b \in \mathcal{B} \tag{5.4}$$

$$x_b = \mathbb{1}_{\left\{\sum_{s\in\mathcal{S}} \delta_{bs} > 0\right\}},\ \ \forall b \in \mathcal{B} \tag{5.5}$$

$$\delta_{bs} \geq 0,\ \ \forall b \in \mathcal{B},\ \ \forall s \in \mathcal{S} \tag{5.6}$$

$$x_b \in \{0,1\}, \forall b \in \mathcal{B}. \tag{5.7}$$

$$
\begin{aligned}
f_{\mathrm{SINR}_b}(\gamma) &= \int\int f_{\mathrm{SINR}_b,\mathrm{I,d}}(\gamma,c,u)\ \mathrm{d}u\ \mathrm{d}c = \int\int f_{\mathrm{SINR}_b|\mathrm{I,d}}(\gamma|c,u)\, f_{\mathrm{I|d}}(c|u)\, f_{\mathrm{d}}(u)\ \mathrm{d}u\ \mathrm{d}c \\
&= \int_0^{\infty}\int_0^{|l_b-v_b|} \underbrace{\mu_b\, u^{\alpha}\left(\sigma^2+c\right)\exp\left(-\mu_b\,\gamma\, u^{\alpha}\left(\sigma^2+c\right)\right)}_{(i)} \\
&\quad \times \underbrace{\left\{\int_{-\infty}^{\infty}\frac{e^{-i\omega c}}{2\pi}\prod_{j\in\mathcal{B}\setminus b}\left(\Phi_{I_j}(\omega)\right)\mathrm{d}\omega\right\}}_{(ii)} \underbrace{\frac{\mathrm{d}\left[\nabla\left\{\mathcal{P}_b\cap D_u\right\}\right]}{\mathrm{d}u\ A_b}}_{(iii)}\mathrm{d}u\ \mathrm{d}c. \qquad (5.8)
\end{aligned}
$$

The objective function (5.2) represents the cost of the leased sub-6 GHz BSs. Constraint (5.3) ensures the sub-6 GHz demand satisfaction of the SPs in $\mathcal{S}$. Constraint (5.4) ensures that the utilization of the leased sub-6 GHz BSs does not exceed 100%. Constraint (5.5) relates between the two decision variables x_b and δ_{bs}. Here, $\mathbb{1}_{\{\}}$ is the indicator function.

In order to solve Problem 5.1, the key challenge is to derive a closed-form expression of the sub-6 GHz rate coverage probability in (5.3).

5.3.2 Sub-6 GHz Virtual Network Rate Coverage Probability

In Chapter 4, we have derived a closed-form expression of downlink rate coverage probability obtained from non-shared sub-6 GHz BSs. From Chapter 4, the PDF of the sub-6 GHz downlink SINR received by a typical UE of an SP associated with sub-6 GHz BS $b, b\in\mathcal{B}$, can be given by (5.8) for any real number γ within the support of $\tilde{\mathrm{SINR}}_b$ where $\mathcal{P}_b$ is the region of the Voronoi cell of BS b, A_b is the area of the Voronoi cell $\mathcal{P}_b$, A is the area of the geographical area $\mathcal{A}$, D_u is a circular disc of radius u centered at l_b, d_{bj} is the distance between BS b and an interfering sub-6 GHz BS j, and $\Phi_{I_j}(\omega)=\int_0^{2\pi}\frac{1}{2\pi}\frac{\mu_j\left(u^2+d_{bj}^2-2u\,d_{bj}\,\cos\theta\right)^{\alpha/2}}{\mu_j\left(u^2+d_{bj}^2-2u\,d_{bj}\,\cos\theta\right)^{\alpha/2}-i\,\omega}\,\mathrm{d}\theta$ is the characteristic function of $\tilde{I}_j$ (the interference caused by BS j).

Note that in (5.8), part (i) is the PDF of the SINR received by a typical UE located at

distance u from its associated BS b and experiencing cumulative interference c, denoted by $f_{\tilde{\text{SINR}}_b|\tilde{\text{I}},\tilde{\text{d}}}(\gamma|c,u)$ for any real number γ within the support of $\tilde{\text{SINR}}_b$. Part (ii) is the PDF of $\tilde{I}$, the cumulative interference experienced by a typical UE located at distance u from its associated BS b, denoted by $f_{\text{I}|\text{d}}(c|u)$ for any real number c within the support of $\tilde{I}$. Finally, part (iii) is the PDF of $\tilde{d}$, the distance of a typical UE of SP s from its associated BS b, denoted by $f_{\text{d}}(u)$, for any real number u within the support of $\tilde{d}$.

Now, in our proposed virtualized wireless network model, the VNB aggregates a subset of BSs from $\mathcal{B}$ and slices them among the SPs in $\mathcal{S}$. Here, $x_b, b \in \mathcal{B}$, represents the selection of BS b. In that case, to compute the PDF of SINR received by a typical UE of an SP associated with BS b from (5.8), we need to express $f_{\text{I}|\text{d}}(c|u)$, the cumulative interference experienced by a typical UE located at distance u from its associated BS b, as a function of $x_j, \forall j \in \mathcal{B} \setminus b$. Specifically, if $x_j = 1$ (i.e., BS j is selected) then $\tilde{I}_j$ (the interference caused by that BS on BS b) needs to be considered in $f_{\text{I}|\text{d}}(c|u)$. On the other hand, if $x_j = 0$, $\tilde{I}_j$ needs to be ignored. Hence, $f_{\text{I}|\text{d}}(c|u)$ can be expressed as a function of $x_j, \forall j \in \mathcal{B} \setminus b$, as:

$$f_{\text{I}|\text{d}}(c|u) = \int_{-\infty}^{\infty} \frac{e^{-i\omega c}}{2\,\pi} \left\{ \prod_{j \in \mathcal{B} \setminus b} \left(1 - x_j \left(1 - \phi_{I_j}(\omega)\right)\right) \right\} \text{d}\omega. \tag{5.9}$$

We apply these modifications on (5.8) and express $f_{\text{SINR}_b}(\gamma)$, the PDF of downlink SINR received by a typical UE associated with BS $b, b \in \mathcal{B}$, as function of $x_j, \forall j \in \mathcal{B} \setminus b$. Then, from $f_{\text{SINR}_b}(\gamma)$, we derive the virtual network rate coverage probability as follows.

Let $\tilde{Z}$ be a stochastic variable defined as $\tilde{Z} = \delta_{bs} W_b \log_2\left(1 + \tilde{\text{SINR}}_b\right)$. Then, the PDF of $\tilde{Z}$ is given by [69]:

$$f_Z(z) = \left(f_{\text{SINR}_b}(\gamma) \left| \frac{\text{d}\gamma}{\text{d}z} \right| \right)_{\gamma = \left(2^{\frac{z}{\delta_{bs} W_b}} - 1\right)} = \frac{\left(2^{\frac{z}{\delta_{bs} W_b}}\right) \log 2}{\delta_{bs} W_b} f_{\text{SINR}_b}\left(2^{\frac{z}{\delta_{bs} W_b}} - 1\right). \tag{5.10}$$

Now, from (5.1), the PDF of $\tilde{R}_{bs}$, the sub-6 GHz rate allocated to a typical UE of SP $s, s \in \mathcal{S}$, in the considered geographical area $\mathcal{A}$, which is associated with BS b, can be expressed in terms of $f_Z(z)$ as:

$$f_{\mathrm{R}_{bs}}(\rho) = f_{\mathrm{R}_{bs}}\left(\frac{Z}{\tilde{N}_{bs}}\right) = \sum_{n=0}^{\infty} \Pr\left\{\tilde{N}_{bs} = n\right\} n\, f_Z(n\rho) \tag{5.11}$$

where $\tilde{N}_{bs}$ is the number of UEs of SP s associated with BS b.

Since the UEs of SP s are distributed in $\mathcal{A}$ according to a homogeneous PPP of intensity λ_s, the number of UEs that are served by BS b (i.e., located within $\mathcal{P}_b$) is a Poisson random variable of parameter $\lambda_s A_b$. Hence, we can express the distribution of the number of UEs served by BS b (i.e., load of BS b), $\tilde{N}_{bs}$, as:

$$\Pr\left\{\tilde{N}_{bs} = n\right\} = e^{-\lambda_s A_b}\, \frac{\lambda_s^n A_b^n}{n!}. \tag{5.12}$$

Next, recall that UEs of an SP are assumed to be associated with the nearest sub-6 GHz BS among the set of sub-6 GHz BSs allocated to the SP. Therefore, when choosing a UE arbitrarily from $\mathcal{A}$ (whose area is denoted by A), it is more likely to be associated with the sub-6 GHz BS which has a larger association region. In other words, the probability of a UE being associated with a given sub-6 GHz BS is the fraction of the total area covered by the association region of that sub-6 GHz BS. This leads us to the following Theorem.

Theorem 5.1. *In the sub-6 GHz virtual resource allocation model described in Section 5.2.2, for a set of sub-6 GHz BSs $\mathcal{B}$, the downlink rate coverage probability achieved by the sub-6 GHz virtual network of SP s, $s \in \mathcal{S}$, is given by (5.13).*

$$\Pr\left\{\tilde{R}_s \geq \kappa_s\right\} = \sum_{b\in\mathcal{B}} \frac{A_b}{A} \Pr\left\{\tilde{R}_s^{(b)} \geq \kappa_s\right\} = 1 - \sum_{b\in\mathcal{B}} \frac{A_b}{A} \int_0^{\kappa_s} f_{\mathrm{R}_{bs}}(\rho)\, \mathrm{d}\rho$$

$$= 1 - \underbrace{\frac{A_b(\boldsymbol{x})}{A}}_{(i)} \Bigg[\sum_{b\in\mathcal{B}} \underbrace{e^{-\lambda_s A_b(\boldsymbol{x})} \sum_{n=0}^{\infty} \frac{\lambda_s^n A_b^n(\boldsymbol{x})}{(n-1)!}}_{(ii)} \int_0^{\kappa_s} \int_0^{\infty} \int_0^{|l_b - v_b|} \underbrace{\frac{\log 2}{\delta_{bs} W_b}\, 2^{\frac{n\rho}{\delta_{bs} W_b}}\, \mu_b\, u^{\alpha} \left(\sigma^2 + c\right)}$$

$$\underbrace{\times \exp\left(-\mu_b u^{\alpha} \left(2^{\frac{n\rho}{\delta_{bs} W_b}} - 1\right) \left(\sigma^2 + c\right) \right)}_{(iii)} \underbrace{\int_{-\infty}^{\infty} \frac{e^{-i\omega c}}{2\pi} \prod_{j\in\mathcal{B}\setminus b} \left(1 - x_j \left(1 - \Phi_{I_j}(\omega)\right)\right) \mathrm{d}\omega}_{(iv)}$$

$$\times \underbrace{\frac{\mathrm{d}\left[\nabla\left\{\mathcal{P}_b \cap D_u\right\}(\boldsymbol{x})\right]}{A_b(\boldsymbol{x})\, \mathrm{d}u}}_{(v)} \mathrm{d}u\, \mathrm{d}c\, \mathrm{d}\rho \Bigg]. \tag{5.13}$$

5.3.3 Solution Approach

In this subsection, we discuss how to efficiently solve Problem 5.1. First, we state the following theorem regarding the computation complexity of Problem 5.1.

Theorem 5.2. *Problem 5.1, i.e., the optimal sub-6 GHz virtual resource allocation problem is NP-complete.*

Proof. Note that Problem 5.1 is a combinatorial optimization problem that has continuous decision variables $\delta_{bs},\ \forall b \in \mathcal{B}, \forall s \in \mathcal{S}$. Hence, there is no algorithm that can guarantee to optimally solve the problem in polynomial time. However, we can verify feasibility of a given instance of the decision variables δ_{bs} and $x_b,\ \forall b \in \mathcal{B}, \forall s \in \mathcal{S}$, in polynomial times. Hence, Problem 5.1 is NP.

Now, we show that Problem 5.1 is NP-hard by a straightforward reduction from the Capacity-limited Facility Location Problem (CFLP) which is known to be NP-hard [73]. In CFLP, the goal is to optimally place a set of facilities with limited capacity in a geographical

area to serve a set of demand-points. Given an instance of the CFLP problem, we construct an instance of Problem 5.1 as follows:

- The set of capacity-limited facilities $\rightarrow \mathcal{B}$, i.e., the set of sub-6 GHz BSs,
- The set of demand points $\rightarrow$ Demands of the SPs in $\mathcal{S}$,
- Total cost (i.e., facility cost + service cost) $\rightarrow \sum_{b\in\mathcal{B}} c_b\, x_b$, i.e., the cost of leasing sub-6 GHz BSs,
- Assignment function $\rightarrow \mathbb{1}_{\{\delta_{bs}>0\}}, \forall b \in \mathcal{B}, \forall s \in \mathcal{S}$.

Then, it is easy to see that a solution of an instance of the CFLP problem that costs C exists if and only if there exists a solution of the corresponding instance of Problem 5.1 (as described above) that costs $C + n$ where $n \geq 0$, i.e., Problem 1 $\geq_P$ CFLP. Thus, Problem 5.1 is NP-complete. □

In addition to NP-completeness of the problem, note that the closed-form expression of the rate coverage probability (RCP) achieved by SP s, $s \in \mathcal{S}$, (i.e., (5.13)) has seven sources of non-linearity with respect to the decision variables δ_{bs} and x_b, $\forall b \in \mathcal{B}$. One non-linearity is due to having the continuous decision variables δ_{bs} in the denominator term in part (iii) of the expression, two non-linearity terms are in the form of a continuous decision variables appearing in exponent terms in part (iii) of the expression, one non-linearity is in the form of a product of different subsets of binary decision variables in part (iv) of the expression, and three non-linearity terms are in part (i), (ii), and (v) in the form of a binary decision variables defining shapes and areas of the Voronoi cells. Since the non-linear terms appear in the exponents and the denominator of the RCP expression, it is extremely challenging to reformulate the expression as a linear or the non-linear expression that is accepted by optimizers like CPLEX and GUROBI (e.g., semi-definite, second-order cone, and quadratic expressions [74]). Furthermore, due to the combinatorial feature of the RCP expression, it is

difficult to address the non-linearity issue based on standard linear-approximation techniques (e.g., piecewise-linear approximation [75]). For example, the sub-6 GHz RCP achieved by SP s from BS b depends on the slicing decision variable δ_{bs} as well as the shape of the Voronoi cell of BS b that depends on the selection of other sub-6 GHz BSs, i.e., $x_j, j \in \mathcal{B} \setminus b$. In that case, to linearly approximate the expression of the sub-6 GHz RCP achieved by SP s from BS b with respect to δ_{bs}, we need to fix $x_j, j \in \mathcal{B} \setminus b$. However, it is not computationally reasonable to consider each possible subset of BSs from $\mathcal{B}$ and approximate the sub-6 GHz RCP expression with respect to the slicing decision variables. Hence, we develop our solution approach based on an efficient greedy algorithm that can find good solutions with affordable computation complexity.

Our algorithm can be summarized as follows. Initially, we have an empty set (say, $\mathcal{B}^*$) of candidate sub-6 GHz BSs. Then, in each iteration, we perform two steps. In the first step, we optimally select a sub-6 GHz BS from $\mathcal{B} \setminus \mathcal{B}^*$ and add it to $\mathcal{B}^*$ such that the added BS would minimize the demand deficit of the SP with the highest sub-6 GHz demand deficit in $\mathcal{S}$. In the next step, we optimally slice the BSs in $\mathcal{B}^*$ among the SPs in $\mathcal{S}$ to satisfy their demands. In this way, we continue adding sub-6 GHz BSs in $\mathcal{B}^*$ in each iteration until $\mathcal{B}^*$ meets the sub-6 GHz demands of all the SPs in $\mathcal{S}$.

Let us describe the functionality of the two steps in details.

Sub-6 GHz BS Aggregation:

Initially, we have an empty set of candidate sub-6 GHz BSs $\mathcal{B}^*$. Then, in each iteration, we select a sub-6 GHz BS from $\mathcal{B} \setminus \mathcal{B}^*$ such that when its full capacity is allocated to the SP with highest sub-6 GHz demand deficit in $\mathcal{S}$, it minimizes the sub-6 GHz demand deficit of that SP per unit cost. The sub-6 GHz demand deficit of an SP (say, s) is the difference between β_s, the sub-6 GHz RCP demand of the SP, and $\Pr\left\{\tilde{R}_s \geq \kappa_s\right\}$, the sub-6 GHz RCP

achieved by the SP from the slices of the BSs of $\mathcal{B}^*$ allocated to the SP. Note that in the first iteration, the SP with highest sub-6 GHz RCP demand has the highest demand deficit. However, from the next iterations, demand deficits of the SPs are computed based on the slices of the BSs of $\mathcal{B}^*$ allocated to the SP in the previous iteration. Let SP s', $s' \in \mathcal{S}$, be the SP with the highest demand deficit. Then, we add to $\mathcal{B}^*$ the sub-6 GHz BS b^* that satisfies:

$$b^* = \underset{b' \in \mathcal{B} \setminus \mathcal{B}^*}{\operatorname{argmax}} \left\{ \frac{\Pr\left\{ \tilde{R}_{s'} \geq \kappa_{s'} \right\}_{(\mathcal{B}^* \cup b')}}{\hat{c}_{b'}} \right\} \tag{5.14}$$

where $\hat{c}_{b'}$ is the normalized cost of leasing sub-6 GHz BS b', i.e., $\hat{c}_{b'} = \frac{c_{b'}}{\sum\limits_{j \in \mathcal{B} \setminus \mathcal{B}^*} c_j}$.

In (5.14), $\Pr\left\{ \tilde{R}_{s'} \geq \kappa_{s'} \right\}_{(\mathcal{B}^* \cup b')}, b' \in \mathcal{B} \setminus \mathcal{B}^*$, can be computed from (5.13) by setting the decision variables x_b and $\delta_{bs'}$, $\forall b \in \mathcal{B}^*$, to the solutions obtained in the previous iteration and the decision variables $x_{b'}$ and $\delta_{b's'}$ to 1. In the case of the first iteration, decision variables x_b and $\delta_{bs'}$, $\forall b \in \mathcal{B}^*$, are to be set to zero. However, in order to solve (5.14) from (5.13), we have to generate Voronoi cells for the subset of sub-6 GHz BSs $(\mathcal{B}^* \cup b')$, $\forall b \in \mathcal{B} \setminus \mathcal{B}^*$. Consequently, we would experience high computation complexity for a large set of BSs in $\mathcal{B}$. To overcome this complexity issue, we want to simplify the sub-6 GHz RCP expression in (5.13) with the following approximations and modifications.

First, we will approximate the coverage region of sub-6 GHz BS b, $b \in (\mathcal{B}^* \cup b')$, as a circular area of radius q_b, where $q_b = \min\limits_{j \in (\mathcal{B}^* \cup b') \setminus b} \frac{d_{bj}}{2}$ and d_{bj} is the distance between sub-6 GHz BSs b and j.

In that case, the area of the coverage region of BS b can be expressed as $\pi\, q_b^2$. Moreover, the CDF of $\tilde{d}$, the distance of a typical UE from its associated sub-6 GHz BS (say b), can

be written as:

$$\Pr\left\{\tilde{d} \leq u\right\} = \begin{cases} \frac{u^2}{q_b^2}, & \text{for } 0 \leq u \leq q_b \\ 1, & \text{otherwise.} \end{cases} \tag{5.15}$$

From the CDF (5.15), the PDF of $\tilde{d}$ can be obtained as follows:

$$f_d(u) = \frac{\mathrm{d}\Pr\left\{\tilde{d} \leq u\right\}}{\mathrm{d}u} = \begin{cases} \frac{2u}{q_b^2}, & \text{for } 0 \leq u \leq q_b \\ 0, & \text{otherwise.} \end{cases} \tag{5.16}$$

Next, we approximate the load of a sub-6 GHz BS for SP $s, s \in \mathcal{S}$, by the average number of UEs of SP s served by that BS. Since UEs of SP s are distributed according to a homogeneous PPP of intensity λ_s, the number of UEs of SP s served by a sub-6 GHz BS (say, b) will be a Poisson random variable with parameter $\lambda_s\ \pi\ q_b^2$. Hence, the load of BS b for SP s is approximated by $\lambda_s\ \pi\ q_b^2$.

With these approximations, we can state the following corollary of Theorem 5.1.

Corollary 5.3. *In the sub-6 GHz virtual resource allocation model described in Section 5.2.2, for a set of sub-6 GHz BSs $\mathcal{B}$, if the coverage regions of the BSs are approximated as circular areas and the load of the BSs are approximated by the mean load, the downlink rate coverage probability achieved by the sub-6 GHz virtual network of SP $s, s \in \mathcal{S}$, can be approximated by (5.17) where q_b, $b \in \mathcal{B}$, is the radius of the coverage region of BS b.*

In order to avoid confusion between the left-hand-side terms in (5.13) and (5.17), we refer to the exact virtual network rate coverage probability by $\Pr\left\{\tilde{R}_s \geq \kappa_s\right\}$ in (5.13) and refer to the approximated virtual network rate coverage probability by $\Pr_{\text{appr}}\left\{\tilde{R}_s \geq \kappa_s\right\}$ in (5.17).

$$\Pr_{\text{appr}}\left\{\tilde{R}_s \geq \kappa_s\right\} = 1 - \sum_{b\in\mathcal{B}} \frac{\pi {q_b}^2}{A}\Bigg\{\frac{\lambda_s \log 2}{\delta_{bs} W_b}\int_0^{\kappa_s}\left(2^{\frac{\lambda_s \pi {q_b}^2 \rho}{\delta_{bs} W_b}}\right)\int_0^{\infty}\int_0^{q_b}\mu_b\, u^{\alpha+1}\left(\sigma^2+c\right)$$
$$\times \exp\left(-\mu_b\left(2^{\frac{\lambda_s \pi {q_b}^2 \rho}{\delta_{bs} W_b}}-1\right)u^{\alpha}\left(\sigma^2+c\right)\right)$$
$$\times\left\{\int_{-\infty}^{\infty} e^{-i\omega c}\prod_{j\in\mathcal{B}\setminus b}\left(1-x_j\left(1-\phi_{I_j}(\omega)\right)\right)\mathrm{d}\omega\right\}\mathrm{d}u\,\mathrm{d}c\,\mathrm{d}\rho\Bigg\}. \quad (5.17)$$

With the simplified expression of sub-6 GHz RCP in (5.17), we can solve (5.14) in standard optimizers (e.g., CPLEX) with affordable computation complexity.

Note that due to the approximations related to the load and coverage regions of the sub-6 GHz BSs, the load of a sub-6 GHz BS becomes a deterministic parameter. Moreover, due to the approximations related to the coverage regions of the sub-6 GHz BSs, some portions of $\mathcal{A}$ is excluded from the sub-6 GHz RCP computation. However, channel conditions (i.e., SINR) experienced by the UEs remain stochastic. Furthermore, this is an intermediate step. In this step, we wish to select a sub-6 GHz BS that has high capacity but causes minimum interference to the other sub-6 GHz BSs in the candidate set. Hence, the approximations related to the load and coverage regions will not heavily tamper our final solutions.

Sub-6 GHz BS Slicing:

In each iteration, the VNB slices the sub-6 GHz BSs in the candidate set $\mathcal{B}^*,\ \mathcal{B}^* \subseteq \mathcal{B}$, among the SPs in $\mathcal{S}$ as follows:

Problem 5.2: Optimal Sub-6 GHz BS Slicing

$$\underset{\left\{\substack{\delta_{bs}\\ b\in\mathcal{B}^*, s\in\mathcal{S}}\right\}}{\text{maximize}} \sum_{s\in\mathcal{S}}\sum_{b\in\mathcal{B}^*}\frac{A_b}{A}\Pr\left\{\tilde{R}_{bs}\geq\kappa_s\right\} \quad \text{subject to:} \quad \sum_{s\in\mathcal{S}}\delta_{bs}\leq 1,\ \ \forall b\in\mathcal{B}^*.$$

The objective function represents the aggregated sub-6 GHz RCP achieved by the SPs in $\mathcal{S}$ from the aggregated subset of sub-6 GHz BSs $\mathcal{B}^*$, $\mathcal{B}^* \subseteq \mathcal{B}$. The constraint ensures that the utilization of the sub-6 GHz BSs does not exceed 100%.

We compute $\Pr\left\{\tilde{R}_s \geq \kappa_s\right\}$ from (5.13) by setting $x_b = 1,\ \forall b \in \mathcal{B}^*$, and $x_j = 0,\ \delta_{js} = 0,\ \forall j \in \mathcal{B} \setminus \mathcal{B}^*,\ s \in \mathcal{S}$. As can be seen from (5.13), if we fix the binary decision variables $x_b,\ \forall b \in \mathcal{B}^*$, we have non-linearity only with respect to the continuous decision variables. Specifically, here we have three sources of non-linearity. One non-linearity is due to having the continuous decision variables δ_{bs} in the denominator term in part (iii) of the expression, two non-linearity terms are in the form of a continuous decision variables appearing in exponent terms in part (iii) of the expression. To address the non-linearity issue, first, we study the behavior of (5.13) with respect to the decision variable δ_{bs} for a particular sub-6 GHz BS $b, b \in \mathcal{B}^*$, and for a particular SP $s, s \in \mathcal{S}$. We consider a simple set up as follows. BS b is located in a geographical area of 2×2 km^2 as shown in Figure 5.1 and 5.2. It has two sets of neighbor sub-6 GHz BSs. In the first set, there are three neighbor sub-6 GHz BSs as shown in Figure 5.1. In the second set, there are five neighbor sub-6 GHz BSs as shown in Figure 5.2. All sub-6 GHz BSs transmit with a constant power of 23 dBm and operate over a bandwidth of 20 MHz. Noise variance (σ^2) is set to -174 dBm/Hz. Pathloss exponent (α) is set to 4. SP s wishes to provide wireless services within the geographical area shown in Figures 5.1 and 5.2. SP s has UE intensity (λ_s) of 5 /km^2 and minimum sub-6 GHz data rate demand (κ_s) of 1 Mbps. In this set up, we plot $\text{RCP}_s^{(b)} \stackrel{def}{=} \Pr\left\{\tilde{R}_{bs} \geq \kappa_s\right\}$, the sub-6 GHz RCP achieved by SP s from BS b vs. δ_{bs} in Figure 5.3. As can be seen that $\text{RCP}_s^{(b)}$ is a non-convex and non-concave function of δ_{bs}. From this observation, we can sate the following proposition:

Proposition 1. In the virtualized wireless network model described in Section 5.2, for an aggregated subset of sub-6 GHz BSs $\mathcal{B}^*, \mathcal{B}^* \subseteq \mathcal{B}$, the downlink sub-6 GHz rate coverage

probability achieved by SP s, $s \in \mathcal{S}$, from BS $b, b \in \mathcal{B}^*$, is a sigmoidal, i.e., non-convex, non-concave, and non-decreasing function of the slicing decision variable δ_{bs}.

Due to the sigmoidal nature of the objective function, it becomes extremely challenging to solve Problem 5.2. One potential approach is to approximate the sigmoid function by a piecewise-linear function where the sigmoid function is divided into pieces and each piece is approximated by a linear function [75]. In order to perform the piecewise-linear approximation, the key step is the selection of the breakpoints. In [75], the authors computed a set of breakpoints for a sigmoid function that expands from $(-6, 0)$ to $(6, 1)$. Taking this into consideration, we construct a piecewise-linear approximation of $\text{RCP}_s^{(b)}$, $b \in \mathcal{B}^*, s \in \mathcal{S}$, the sub-6 GHz RCP achieved by SP s from BS b denoted by $\text{RCP}_s^{(b)}$, from the breakpoints computed in [75] with making the following changes. Consider a breakpoint computed in [75] with an x-axis value of $a, a \in (-6, 6)$. Then, we select the x-axis value of a breakpoint for the $\text{RCP}_s^{(b)}$ function as: $a' = \left(\left(\frac{a+6}{12} + \Delta\right) \mod 1\right)$ where Δ is the difference between the value of δ_{bs} at the transition point of the $\text{RCP}_s^{(b)}$ function and 0.5. The purpose of adding Δ is that the $\text{RCP}_s^{(b)}$ function does not have a fixed transition point at $(0.5, 0.5)$ like the sigmoid function at $(0, 0.5)$. Therefore, we need to add the difference between the value of δ_{bs} at the transition point of the $\text{RCP}_s^{(b)}$ function and 0.5 while using breakpoints of the sigmoid function. In this way, we can obtain x-axis values of breakpoints. Then, from the x-axis values of breakpoints, we compute the corresponding y-axis values by using (5.13).

We evaluate the piecewise-linear-approximation technique in Figure 5.4. As can be seen that there exists moderately low approximation error between the exact function and its piecewise-linear approximation.

In this way, we approximate $\text{RCP}_s^{(b)}, \forall b \in \mathcal{B}^*, \forall s \in \mathcal{S}$, as a set of $\mathcal{M}_{bs}$ linear functions of the slicing decision variable δ_{bs}. Let $p_{bs}^{(m)}, m \in \mathcal{M}_{bs}$, and $q_{bs}^{(m)}, m \in \mathcal{M}_{bs}$, be the coefficients of the linear sub-6 GHz RCP function m of δ_{bs}. Let $K_{bs}, b \in \mathcal{B}, s \in \mathcal{S}$, be an auxiliary decision

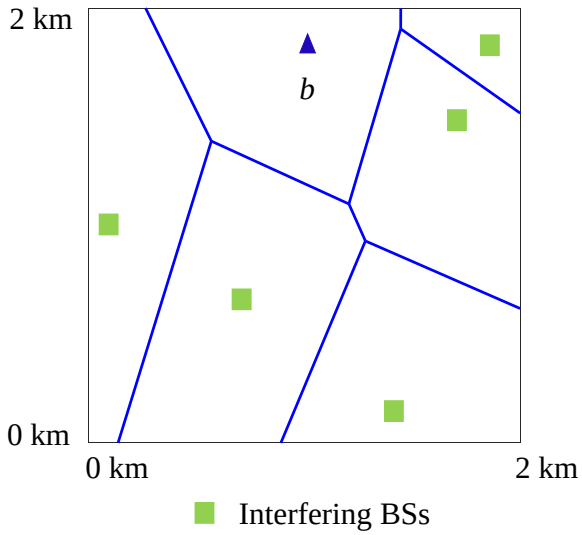

Figure 5.1: Locations of five interfering sub-6 GHz BSs.

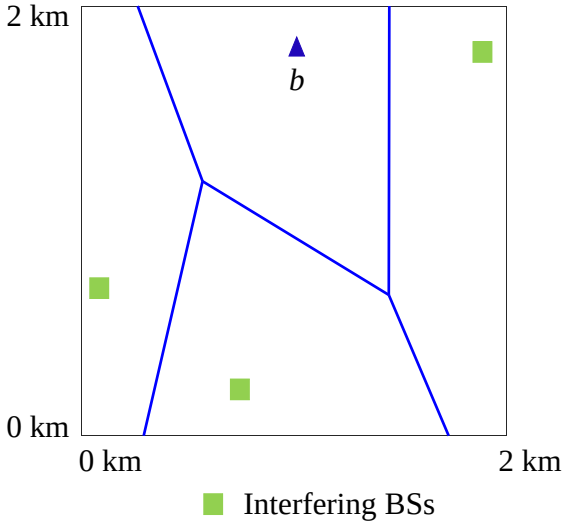

Figure 5.2: Locations of three interfering sub-6 GHz BSs.

variable. Then, the piecewise linear approximation of Problem 5.2 can be given as:

$$\underset{\left\{b\in\mathcal{B}^*,s\in\mathcal{S}\right\}}{\text{maximize}} \sum_{s\in\mathcal{S}}\sum_{b\in\mathcal{B}^*} K_{bs} \tag{5.18}$$

subject to:

$$p_{bs}^{(m)}\delta_{bs} + q_{bs}^{(m)} \geq K_{bs}, \quad \forall m \in \mathcal{M}_{bs}, \forall b \in \mathcal{B}^*, \forall s \in \mathcal{S} \tag{5.19}$$

$$\sum_{s\in\mathcal{S}} \delta_{bs} \leq 1, \quad \forall b \in \mathcal{B}^*. \tag{5.20}$$

The piecewise linear approximation of Problem 5.2 is a linear program that can be solved in polynomial time using some of the state-of-the-art solution techniques, such as the path following method as described in [76]. The overall idea of the path following method is to iteratively moving towards the optimal solution by computing gradients of the constraints and the objective function in the polytope. For v constraints, w variables, and L coefficients, the complexity of the path following method is given as $\mathcal{O}\left((v+w)^{1.5}wL\right)$[76]. Now, consider that in our piecewise linear approximation of Problem 5.2 there are B^* sub-6 GHz BSs in

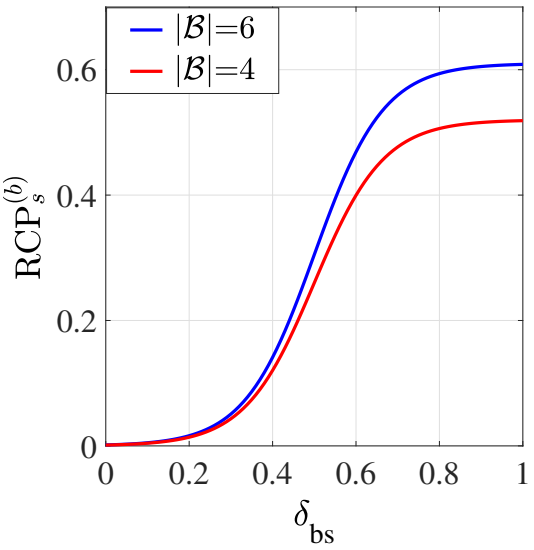

Figure 5.3: Sub-6 GHz Rate coverage probability achieved from BS b vs. δ_{bs}.

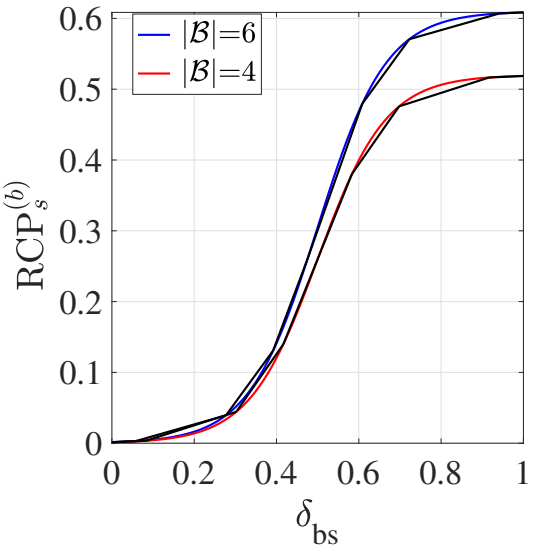

Figure 5.4: Piecewise-linear approximation of the sub-6 GHz RCP achieved from BS b.

$\mathcal{B}^*$, S SPs in $\mathcal{S}$, and M linear functions in $\mathcal{M}_{bs}, b \in \mathcal{B}^*, s \in \mathcal{S}$. In that case, (5.19) produces a total of MB^*S constraints and (5.20) produces B^* constraints. There are a total of B^*S decision variables. The objective function (5.18) has a total of B^*S coefficients. Constraint (5.19) has a total of $3MB^*S$ coefficients and constraint (5.20) has a total of B^*S coefficients. Hence, the complexity for solving the piecewise linear approximation of Problem 5.2 using the path following method can be given as $\mathcal{O}\left((MB^*S + B^* + B^*S)^{1.5} B^*S(3MB^*S + 2B^*S)\right)$ or $\mathcal{O}\left(M^{2.5}S^{3.5}B^{*3.5}\right)$.

With the solutions of Problem 5.2, we compute the sub-6 GHz RCP achieved by each SP in $\mathcal{S}$ from the candidate set $\mathcal{B}^*$ by using (5.13). If each SP obtains sub-6 GHz RCP higher than its demand, i.e., constraint (5.3) in Problem 5.1 is satisfied, we stop the iterations. Otherwise, we continue the iterations until the SP demands are satisfied.

We summarize the overall solution scheme in Algorithm 1. As can be seen in each iteration, the VNB computes (5.14) and adds a sub-6 GHz BS in the candidate set. Then, it

Algorithm 1 Sub-6 GHz Virtual Resource Allocation

Input: $\mathcal{A}$, $\mathcal{B}$, $\mathcal{S}$, $c_b,\ \forall b \in \mathcal{B}$, $\mu_b,\ \forall b \in \mathcal{B}$, $W_b,\ \forall b \in \mathcal{B}$, $\kappa_s,\ \forall s \in \mathcal{S}$, $\beta_s,\ \forall s \in \mathcal{S}$, $\lambda_s,\ \forall s \in \mathcal{S}$

Output: $x_b^*, \delta_{bs}^*,\ \forall b \in \mathcal{B}, \forall s \in \mathcal{S}$

$x_b^* \leftarrow 0,\ \delta_{bs}^* \leftarrow 0,\ \forall b \in \mathcal{B}, \forall s \in \mathcal{S}$, $\mathcal{B}^* \leftarrow \emptyset$

repeat

  Select the SP with highest sub-6 GHz demand deficit in $\mathcal{S}$

  Consider SP $s', s' \in \mathcal{S}$, has the highest sub-6 GHz demand deficit. Then, select a sub-6 GHz BS from $\mathcal{B} \setminus \mathcal{B}^*$ by:

$$b^* \leftarrow \underset{b' \in \mathcal{B} \setminus \mathcal{B}^*}{\operatorname{argmax}} \left\{ \frac{\Pr_{\text{approx}} \left\{ \tilde{R}_{s'} \geq \kappa_{s'} \right\}_{(\mathcal{B}^* \cup b')}}{\hat{c}_{b'}} \right\}$$

  $\mathcal{B}^* \leftarrow (\mathcal{B}^* \cup b^*)$

  $x_b^* \leftarrow 1,\ \ \forall b \in \mathcal{B}^*$

  Solve Problem 5.2 for candidate set $\mathcal{B}^*$ and store the solutions in $\delta_{bs}^*,\ \forall b \in \mathcal{B}^*, \forall s \in \mathcal{S}$

  Compute sub-6 GHz demand deficit $\left(\beta_s - \Pr\left\{\tilde{R}_s \geq \kappa_s\right\}\right)$ with $x_b^*, \delta_{bs}^*,\ \forall b \in \mathcal{B}, \forall s \in \mathcal{S}$

until $\left(\beta_s - \Pr\left\{\tilde{R}_s \geq \kappa_s\right\}\right) \leq 0,\ \ \forall s \in \mathcal{S}$ **Or**, $\mathcal{B}^* = \mathcal{B}$

Report $x_b^*, \delta_{bs}^*,\ \forall b \in \mathcal{B}, \forall s \in \mathcal{S}$

solves Problem 5.2 for this candidate set of sub-6 GHz BSs. With the solutions obtained from Problem 5.2, it evaluates constraint (5.3) of Problem 5.1. In this way, the VNB continues the iterations until it finds a feasible solution for constraint (5.3) of Problem 5.1.

We state the following theorem regarding the complexity of Algorithm 1.

Theorem 5.4. *If we solve the piecewise linear approximation of Problem 5.2 using the path following method [76] then, for S SPs in $\mathcal{S}$, B BSs in $\mathcal{B}$, and $(M+1)$ breakpoints or M linear RCP functions for each of the slicing decision variables $\delta_{bs}, \forall b \in \mathcal{B}, \forall s \in \mathcal{S}$, the complexity of Algorithm 1 is $\mathcal{O}\left(M^{2.5}S^{3.5}B^{5}\right)$, i.e., in polynomial time.*

Proof. First, note that for B BSs, the outer loop of Algorithm 1 runs in the worst case for B times. Moreover, at l^{th} iteration of the outer loop, we have $(B-l)$ choices to select a BS. Hence, at the worst case, for B iterations of the outer loop, the complexity for aggregating BSs can be given as:

$$\begin{aligned} T_{\text{agg.}}(B) &= B + (B-1) + (B-2) + (B-3) + \ldots + 1 \\ &= \frac{B(B+1)}{2} = \mathcal{O}\left(B^2\right). \end{aligned} \tag{5.21}$$

Next, note that we perform the piecewise linear optimization in each iteration after adding a BS in the candidate set of BSs. Therefore, for B BSs in $\mathcal{B}$, S SPs in $\mathcal{S}$, and M linear RCP functions for each of the slicing decision variables $\delta_{bs}, \forall b \in \mathcal{B}, \forall s \in \mathcal{S}$, the complexity for slicing BSs for B iterations of the outer loop can be given as:

$$T_{\text{slc.}}(B, S, M) = \sum_{b=1}^{B} \mathcal{O}\left(M^{2.5}S^{3.5}b^{3.5}\right). \tag{5.22}$$

Since $\sum_{b=1}^{B} b^{3.5} < \sum_{b=1}^{B} b^4$ and we know that $\sum_{b=1}^{B} b^4 = \frac{1}{30}B(B+1)(2B+1)(3B^2+3B-1) = \mathcal{O}\left(B^5\right)$, we have

$$T_{\text{slc.}}(B,S,M) = \sum_{b=1}^{B} \mathcal{O}\left(M^{2.5}S^{3.5}b^{3.5}\right) = \mathcal{O}\left(M^{2.5}S^{3.5}B^5\right). \tag{5.23}$$

Therefore, the complexity of Algorithm 1 can be given as:

$$\begin{aligned} T_{\text{agg.}}(B) + T_{\text{slc.}}(B,S,M) &= \mathcal{O}\left(B^2\right) + \mathcal{O}\left(M^{2.5}S^{3.5}B^5\right) \\ &= \mathcal{O}\left(M^{2.5}S^{3.5}B^5\right). \end{aligned} \tag{5.24}$$

□

5.3.4 Special Case: Infeasibility

We identify Problem 5.1 as 'infeasible' when all BSs in $\mathcal{B}$ are not sufficient to meet the sub-6 GHz demands of all SPs in $\mathcal{S}$. In that case, the VNB can either minimize the aggregated demand deficit of the SPs in $\mathcal{S}$ or completely satisfy some SPs considering their priorities. To minimize the aggregated demand deficit of the SPs, the VNB leases all the BSs from $\mathcal{B}$ and executes Problem 5.2. On the other hand, to completely satisfy prioritized SP demands, SPs are ranked based on their priorities and the VNB builds their virtual networks one by one sequentially according to their ranks as long as the resources are available in $\mathcal{B}$. Let us discuss this sequential virtual network building process in details. First, note that there is lack of sufficient resources in $\mathcal{B}$ to meet all SP demands in the first place. Hence, we can assume that the VNB would eventually select all the BSs in $\mathcal{B}$ to satisfy all (or as many as possible) SP demands. In other words, the set of sub-6 GHz BSs to be leased is fixed, i.e., $x_b = 1,\ \forall b \in \mathcal{B}$. In that case, to build virtual network for an SP (say, SP s, $s \in \mathcal{S}$),

the VNB only needs to determine the slices of the BSs of $\mathcal{B}$ to be allocated to SP s. Let $\alpha_b \in [0,1],\ b \in \mathcal{B}$, denotes the remaining fraction of capacity of BS b. Then, we formulate a problem for allocating virtual resources to SP s as follows:

Problem 5.3: Sequential Virtual Resource Allocation

$$\underset{\{\delta_{bs}, b\in\mathcal{B}\}}{\text{minimize}} \sum_{b\in\mathcal{B}} \delta_{bs} \tag{5.25}$$

$$\text{subject to: } \Pr\left\{\tilde{R}_s \geq \kappa_s\right\} \geq \beta_s \tag{5.26}$$

$$0 \leq \delta_{bs} \leq \alpha_b, \quad \forall b \in \mathcal{B}. \tag{5.27}$$

The objective function (5.25) represents the total amount of sub-6 GHz virtual resources to be allocated to SP s. Constraint (5.26) ensures the sub-6 GHz demand satisfaction of SP s. Constraint (5.27) ensures that the utilization of the sub-6 GHz BSs does not exceed 100%.

Note that in Problem 5.3, the set of BSs to be leased is fixed. Hence, we solve Problem 5.3 following an approach similar to the solution approach of Problem 5.2. Specifically, we approximate constraint (5.26) following the piecewise-linear-approximation technique described in the solution approach of Problem 5.2. Consider $\text{RCP}_s^{(b)},\ b \in \mathcal{B}^*, s \in \mathcal{S}$, the sub-6 GHz RCP achieved by SP s from BS b is approximated as a set of $\mathcal{M}_{bs}$ linear functions of the slicing decision variable δ_{bs}. Let $p_{bs}^{(m)}, m \in \mathcal{M}_{bs}, b \in \mathcal{B}^*, s \in \mathcal{S}$, and $q_{bs}^{(m)}, m \in \mathcal{M}_{bs}, b \in \mathcal{B}^*, s \in \mathcal{S}$, be the coefficients of the linear RCP function m of δ_{bs}. Then, we can write the piecewise linear approximation of constraint (5.26) by introducing an auxiliary variable $K_{bs}, b \in \mathcal{B}, s \in \mathcal{S}$, as:

$$p_{bs}^{(m)}\delta_{bs} + q_{bs}^{(m)} \geq K_{bs}, \quad \forall m \in \mathcal{M}_{bs}, \forall b \in \mathcal{B} \tag{5.28}$$

$$\sum_{b\in\mathcal{B}} K_{bs} \geq \beta_s. \tag{5.29}$$

Now, the piecewise linear approximation of Problem 5.3, i.e., an LP can be solved in polynomial time by the state-of-the-art solution techniques such as the the path following method (as described in [76]).

If Problem 5.3 is infeasible, the VNB allocates all of the remaining capacity of the BSs to SP s. In that case, SP s is partially satisfied.

To summarize these steps, we provide Algorithm 2. As can be seen when Problem 5.1

Algorithm 2 Sequential Virtual Resource Allocation

Input: $\mathcal{A}$, $\mathcal{B}$, $\mathcal{S}$, c_b, $\forall b \in \mathcal{B}$, μ_b, $\forall b \in \mathcal{B}$, W_b, $\forall b \in \mathcal{B}$, κ_s $\forall s \in \mathcal{S}$, β_s $\forall s \in \mathcal{S}$, λ_s $\forall s \in \mathcal{S}$
Output: x_b^*, δ_{bs}^*, $\forall b \in \mathcal{B}, \forall s \in \mathcal{S}$
\\ When Problem 5.1 is 'infeasible' \\
Sort SPs in $\mathcal{S}$ according to their ranks. Let $\mathcal{S}[i]$ be the i^{th} SP in the ranked set of SPs.
$i \leftarrow 1$, $\alpha_b \leftarrow 1$, $\forall b \in \mathcal{B}$, $x_b^* \leftarrow 1$, $\delta_{bs}^* \leftarrow 0$, $\forall b \in \mathcal{B}, \forall s \in \mathcal{S}$
while $\sum_{b \in \mathcal{B}} \alpha_b \neq 0$ **do**
  $s \leftarrow \mathcal{S}[i]$
  Set the range of δ_{bs} to be $[0, \alpha_b]$, $\forall b \in \mathcal{B}$
  Solve Problem 5.3 for SP s and store the solutions in δ_{bs}^*, $\forall b \in \mathcal{B}$
  if Problem 5.3 is 'infeasible' **then**
    $\delta_{bs}^* \leftarrow \alpha_b$, $\forall b \in \mathcal{B}$
    EXIT
  end if
  $\alpha_b \leftarrow 1 - \delta_{bs}^*$, $\forall b \in \mathcal{B}$, $i \leftarrow i + 1$
end while
Report x_b^*, $\delta_{bs}^*, \forall b \in \mathcal{B}, \forall s \in \mathcal{S}$

is infeasible, the VNB executes Problem 5.3. In each iterations, based on the solutions of Problem 5.3, i.e., δ_{bs}^*, $\forall b \in \mathcal{B}$, the VNB updates α_b, $\forall b \in \mathcal{B}$. In this way, the VNB continues allocating virtual resources to the SPs according to their ranks as long as the resources are available in $\mathcal{B}$.

We state the following theorem regarding the complexity of Algorithm 2.

Theorem 5.5. *If we solve the piecewise linear approximation of Problem 5.3 using the path following method [76] then, for S SPs in $\mathcal{S}$, B BSs in $\mathcal{B}$, and $(M+1)$ breakpoints or M linear*

RCP functions for each of the slicing decision variables $\delta_{bs}, \forall b \in \mathcal{B}, \forall s \in \mathcal{S}$, the complexity of Algorithm 2 is $\mathcal{O}\left(SM^{2.5}B^{3.5}\right)$, i.e., in polynomial time.

Proof. Note that for B BSs in $\mathcal{B}$ and M linear RCP functions for each of the slicing decision variables $\delta_{bs}, \forall b \in \mathcal{B}, s \in \mathcal{S}$, the piecewise linear approximation of constraint (5.26) produces a total of $(MB+1)$ constraints. There are total B decision variables. The objective function (5.25) has a total of B coefficients. The piecewise linear approximation of constraint (5.26) produces a total of $(3MB + B + 1)$ coefficients. Hence, the complexity for solving the piecewise linear approximation of Problem 5.3 using the path following method [76], can be given as $\mathcal{O}\left((MB+1+B)^{1.5}B(B+3MB+B+1)\right)$ or $\mathcal{O}\left(M^{2.5}B^{3.5}\right)$.

Note that for S SPs in $\mathcal{S}$, we solve the piecewise linear approximation of Problem 5.3 in the worst case for S times. Therefore, the complexity for allocating virtual resources for S iterations can be given as: $T_{\text{sequential}}(B,S,M) = \sum_{s=1}^{S} \mathcal{O}\left(M^{2.5}B^{3.5}\right) = \mathcal{O}\left(SM^{2.5}B^{3.5}\right)$. □

5.4 Performance Evaluation

In this section, we evaluate the performances of our proposed virtual resource allocation schemes. We implement our algorithms using Visual C++, CPLEX, and MATLAB.

5.4.1 Evaluation Setup

We consider three RPs that make a total of ten sub-6 GHz BSs available in an area of 2×2 km^2, as shown in Figure 5.5. Based on the conventional assumption that the sub-6 GHz BS locations form a homogeneous PPP, we obtain the sub-6 GHz BS locations as a realization of a homogeneous PPP of intensity 2.5/km^2. All three sub-6 GHz BSs of RP 1 transmit with a constant power of 23 dBm (e.g., femto-cell). All six sub-6 GHz BSs of RP 2 transmit with a constant power of 30 dBm (e.g., pico-cell). The sub-6 GHz BS of

RP 3 transmits with a constant power of 46 dBm (e.g., macro-cell). All ten sub-6 GHz BSs operate over a bandwidth of 20 MHz. Noise variance (σ^2) is set to -174 dBm/Hz. Pathloss exponent (α) is set to 4. As an example, we picked the cost of leasing a sub-6 GHz BS to be 100 from RP 1, 200 from RP 2, and 300 from RP 3.

5.4.2 Precision of the Virtual Network Rate Coverage Probability Expressions

In this subsection, we demonstrate the preciseness of Theorem 1, i.e., (5.13), and Corollary 1, i.e., (5.17) for computing the virtual network rate coverage probability as compared to Monte-Carlo simulation. In the Monte-Carlo simulation, we take 1000 random realizations of UE locations and channel conditions. For each realization, we calculate the sub-6 GHz rate allocated to each UE using (5.1). Finally, we compute the fraction of the UEs that achieved the sub-6 GHz rate threshold.

We consider there is an SP that wishes to provide wireless services in the geographical area shown in Figure 5.5. The SP accesses full capacity of all ten sub-6 GHz BSs, i.e., $\delta_{bs} = 1,\ x_b = 1,\ \forall b \in \mathcal{B}$. Figure 5.6 shows the virtual network rate coverage probability achieved by the SP as computed from (5.13), (5.17), and simulations for two different sub-6 GHz rate demands (κ). As can be seen that the virtual network rate coverage probability computed from (5.13) is closely matched with the simulations-based results. Furthermore, note that the difference between the virtual network rate coverage probability computed from the approximated expression in (5.17) and the exact expression in (5.13) is moderate.

5.4.3 Evaluation of Algorithm 1

In this subsection, we demonstrate the performance of Algorithm 1 in terms of SP demands satisfaction and costs minimization. Specifically, we benchmark the performance

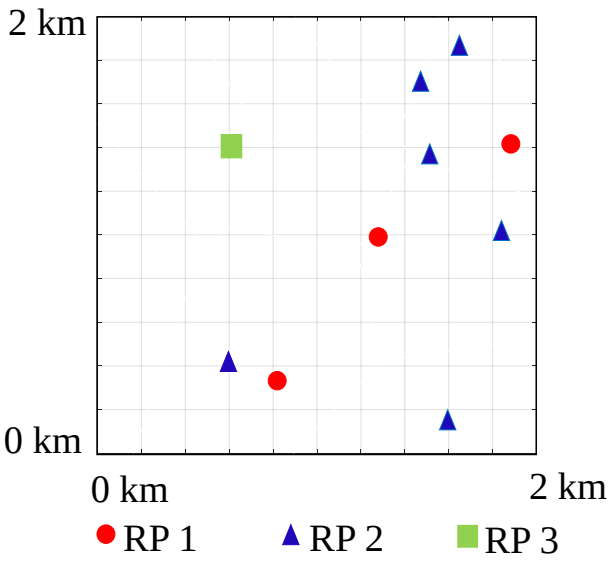

Figure 5.5: Locations of sub-6 GHz BSs.

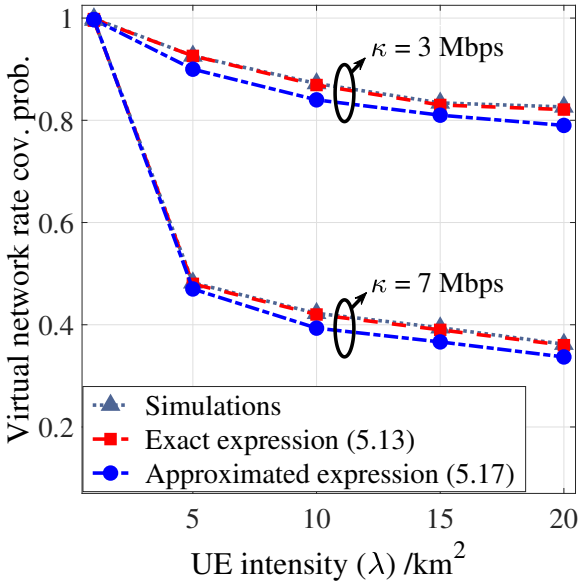

Figure 5.6: Sub-6 GHz RCP vs. UE intensity.

of Algorithm 1 against the brute-force-search (BFS) in terms of finding optimal solutions for Problem 5.1. We implement the BFS as follows. Note that the slicing decision variable is a continuous variable. Therefore, BFS should ideally have an infinite search space. To have a finite computation time, we assume that each of the slicing decision variables $\delta_{bs}, \forall b \in \mathcal{B}, \forall s \in \mathcal{S}$, has 1000 monotonically increasing discrete values between 0 and 1 with a step size of 0.001. Then, we search through all possible combinations of the values of $\delta_{bs}, \forall b \in \mathcal{B}, \forall s \in \mathcal{S}$, to find the cheapest subset of sub-6 GHz BSs that can satisfy the SP demands in $\mathcal{S}$.

To conduct this experiment, we consider that there are two SPs who wish to provide wireless services within the geographical area shown in Figure 5.5. Both SPs have the same UE intensity λ. Each SP requires its UEs to have a minimum sub-6 GHz data rate of κ with a minimum probability of β. Both SPs have the same priority, i.e., if Problem 5.1 is infeasible, then the VNB minimizes the aggregated demand deficits of the SPs.

In this set up, we evaluate Algorithm 1 and the BFS by varying the UE intensity λ and

demand parameters κ and β. Specifically, we perform the following three evaluations. In the first evaluation, we fix κ as 1 Mbps and β as 0.95. We vary λ and plot the virtual network rate coverage probability achieved by the SPs in Figure 5.7, and the costs of leasing sub-6 GHz BSs in Figure 5.8. In the second evaluation, we fix λ as 5/ km^2 and β as 0.95, and vary κ. Figure 5.9 shows the virtual network rate coverage probability achieved by the SPs and Figure 5.10 shows the costs of leasing sub-6 GHz BSs. In the last evaluation, we fix λ as 20/ km^2 and κ as 1 Mbps, and vary β. Figure 5.11 shows the virtual network rate coverage probability achieved by the SPs and Figure 5.12 shows the costs of leasing sub-6 GHz BSs.

Based on these evaluations, we can see that as long as sufficient resources are available in the resource pool, Algorithm 1 ensures the SPs' sub-6 GHz rate coverage probability demands satisfaction as well as isolation among the virtual networks in the presence of uncertainty in UE locations and channel conditions. Furthermore, the optimality gap between Algorithm 1 and the BFS is moderate. This shows the efficiency of Algorithm 1 for obtaining good solutions. Furthermore, as the demands increase, the number of feasible solutions decreases. As a result, the optimality gap between Algorithm 1 and the BFS gradually reduces as the demand parameters increase.

Next, we plot the required CPU-time of Algorithm 1 and the BFS by varying the number of SPs in Figure 5.13. We ran the two algorithms in a i7-2.4 GHz processor. It can be seen from Figure 5.13 that Algorithm 1 has significantly lower complexity than the BFS.

5.4.4 Comparison Between Stochastic Virtualization and Deterministic Virtualization

In this subsection, we illustrate the gains brought by our stochastic-optimization-based virtual resource allocation, as compared to the deterministic-optimization-based virtual resource allocation that is commonly adopted in the exiting works (e.g., [10, 11, 33, 34]). Specif-

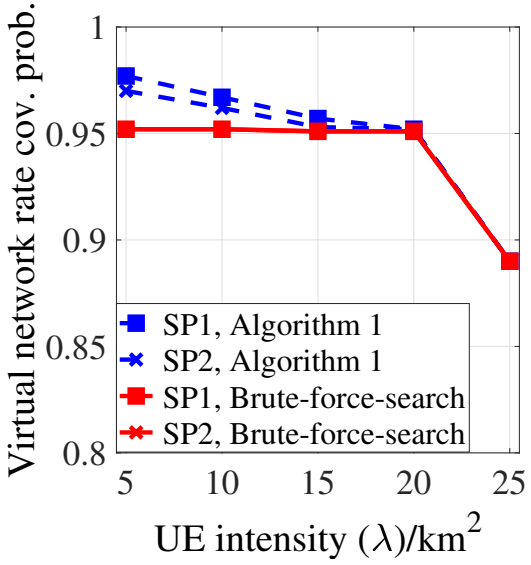

Figure 5.7: Sub-6 GHz RCP achieved by the SPs vs. UE intensity of the SPs.

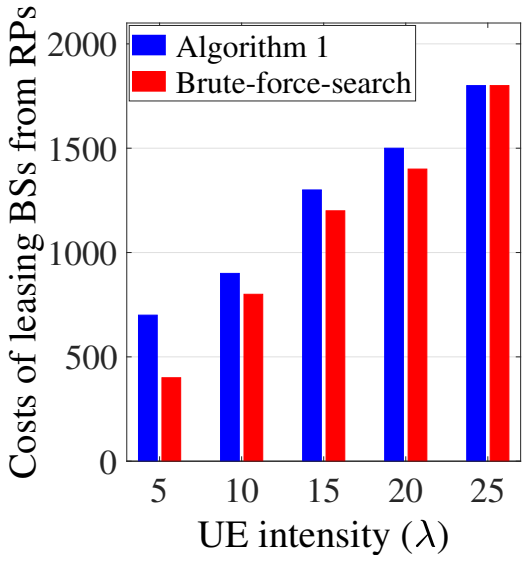

Figure 5.8: Cost of leasing sub-6 GHz BSs vs. UE intensity of the SPs.

ically, we design a deterministic version of Problem 5.1 by following the similar approach as proposed in the existing deterministic-optimization-based virtual resource allocation schemes and compare the performance of Problem 5.1 with its deterministic version.

Let us briefly describe the deterministic version of Problem 5.1. We consider SP $s, s \in \mathcal{S}$, characterize its demand as the average sum-rate needs to be at least T_s bps. Specifically, we generate a set of scenarios (i.e., realizations) Ω of UE locations and channel conditions and replace constraint (5.3) in Problem 5.1 with:

$$\frac{1}{|\Omega|}\sum_{\omega\in\Omega}\sum_{b\in\mathcal{B}}\delta_{bs}^{(\omega)}\sum_{n\in\mathcal{N}_{bs}^{(\omega)}}\left(\frac{W_b}{\left|\mathcal{N}_{bs}^{(\omega)}\right|}\log_2\left(1+\frac{h_n^{(\omega)}\left(d_n^{(\omega)}\right)^{-\alpha}}{\sigma^2+\sum_{j\in\mathcal{B}/b}x_j g_{nj}{}^{(\omega)}\left(a_{nj}^{(\omega)}\right)^{-\alpha}}\right)\right)\geq T_s,\ \forall s\in\mathcal{S} \tag{5.30}$$

where $\mathcal{N}_{bs}^{(\omega)}$ is the set of UEs of SP s associated with sub-6 GHz BS b in scenario ω, $h_n^{(\omega)}$ is the channel gain experienced by UE n of SP s from BS b in scenario ω, W_b is the operating

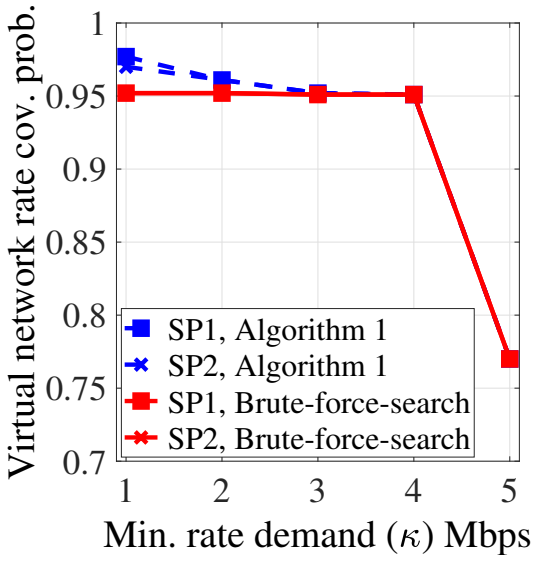

Figure 5.9: Sub-6 GHz RCP achieved by the SPs vs. minimum sub-6 GHz rate demand of the SPs.

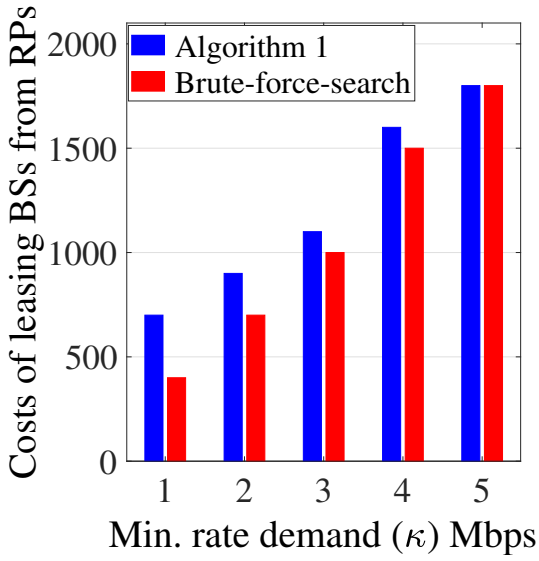

Figure 5.10: Cost of leasing sub-6 GHz BSs vs. minimum sub-6 GHz rate demand of the SPs.

bandwidth BS b, σ^2 is the variance of the additive noise, α is the pathloss exponent, ${a_{nj}}^{(\omega)}$ is the distance between UE n and the interfering sub-6 GHz BS j in scenario ω, and ${g_{nj}}^{(\omega)}$ is the gain of the channel between them in scenario ω.

Furthermore, we replace constraint (5.5) with $x_b = \mathbb{1}_{\left\{\sum_{\omega\in\Omega}\sum_{s\in\mathcal{S}}\delta_{bs}^{(\omega)}>0\right\}}, \quad \forall b \in \mathcal{B}$.

Note that the deterministic version of Problem 5.1 is a non-linear problem since (5.30) is a non-linear function of the decision variables δ_{bs} and x_b, $\forall b \in \mathcal{B}, \forall\ s \in \mathcal{S}$. We solve the problem following the similar greedy scheme as described in Algorithm 1.

In order to compare the performances of Problem 5.1 with its deterministic version, we consider the following set up. There are two SPs who wish to provide wireless services within the considered geographical area shown in Figure 5.5. Each SP has same UE intensity of λ. Each SP requires its UEs to have minimum sub-6 GHz data rate of κ with probabilistic guarantee of 0.95. Each SP has same priority. For the deterministic scheme, we consider 1000 scenarios. Furthermore, we set the minimum average sub-6 GHz sum-rate demand

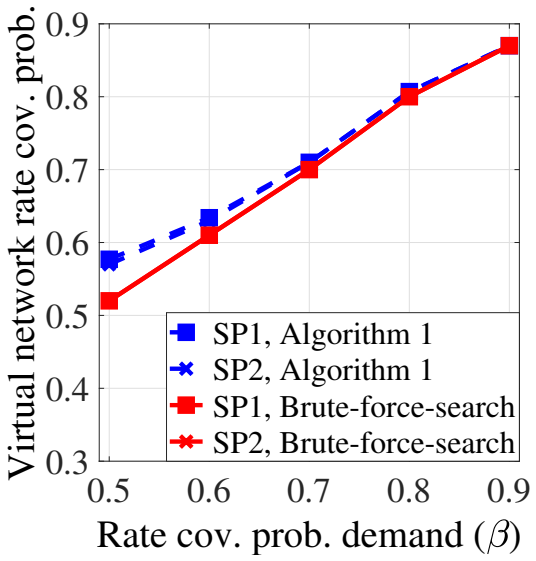

Figure 5.11: Sub-6 GHz RCP achieved by the SPs vs. minimum sub-6 GHz RCP demand of the SPs.

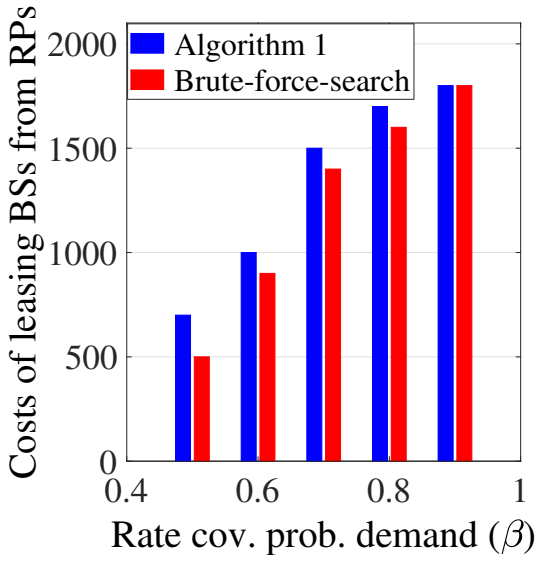

Figure 5.12: Cost of leasing sub-6 GHz BSs vs. minimum sub-6 GHz RCP demand of the SPs.

$T_s, s \in \mathcal{S}$, as $T_s = \frac{1}{|\Omega|}\left(\kappa \sum_{\omega\in\Omega} \mathcal{N}_s^{(\omega)}\right)$ where $\mathcal{N}_s^{(\omega)}$ is the total number of UEs of SP s in the considered geographical area in scenario ω.

In this set up, we compare the virtual network rate coverage probability obtained from the solutions of Algorithm 1 and the deterministic scheme while varying the UE intensity λ and the minimum sub-6 GHz rate demand κ. First, we fix κ as 1 Mbps and vary λ and plot the virtual network rate coverage probability achieved by the SPs in Figure 5.14. Next, we fix λ as 10/ km^2 and vary κ and plot the virtual network rate coverage probability achieved by the SPs in Figure 5.15.

As can be seen in Figures 5.14 and 5.15, the average virtual network rate coverage probability achieved by the SPs based on the deterministic scheme are inconsistent. The reason is that in the deterministic model, the virtual network is built based on one scenario, i.e., one random realization of UE locations and channel conditions. If the considered scenario is bad (i.e., bad channel conditions and/or large number of UEs), we allocate large amount

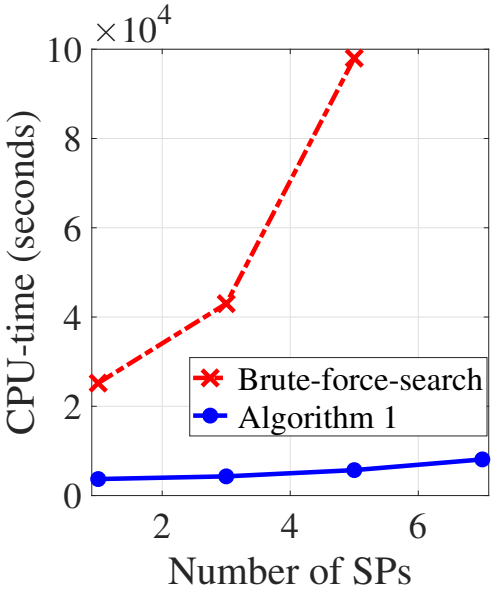

Figure 5.13: Required computation time vs. the number of SPs.

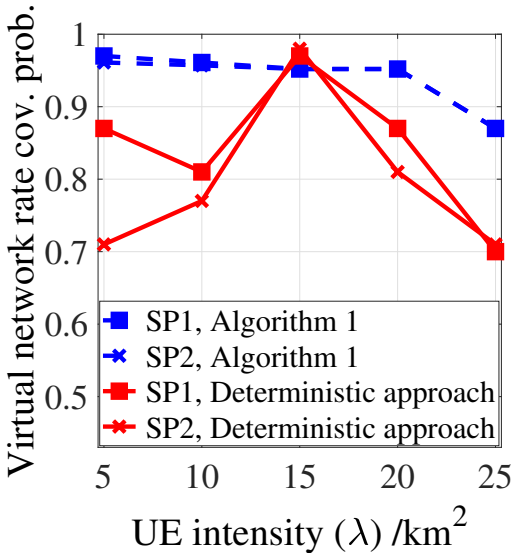

Figure 5.14: Sub-6 GHz RCP achieved by the SPs vs. UE intensity of the SPs.

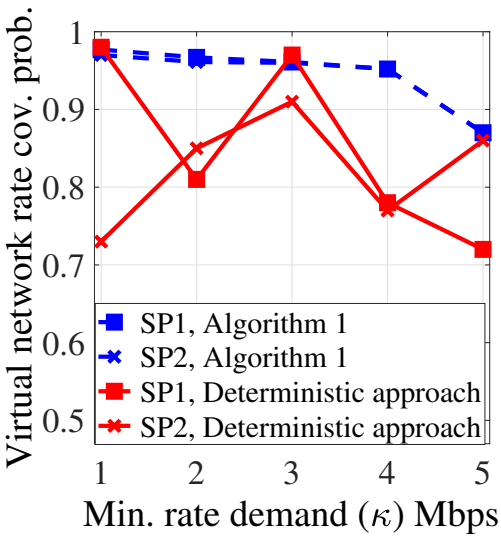

Figure 5.15: Sub-6 GHz RCP achieved by the SPs vs. minimum sub-6 GHz rate demand of the SPs.

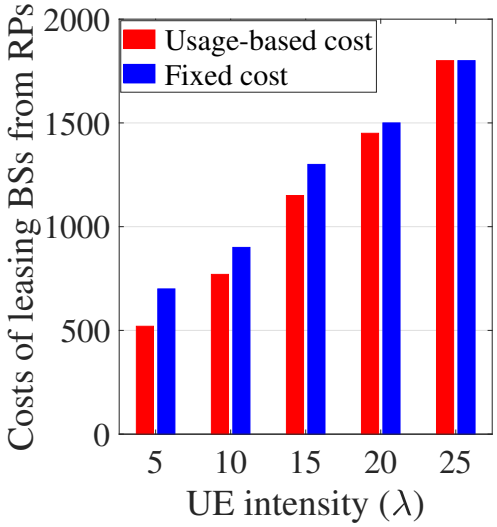

Figure 5.16: Cost of leasing sub-6 GHz BSs vs. UE intensity of the SPs.

of resources to build the virtual network that can satisfy the sum-rate demand of the SP. As a result, the virtual network has high virtual network rate coverage probability. On the other hand, if the considered scenario is good (i.e., good channel conditions and/or small number of UEs), we allocate small amount of resources to build the virtual network, resulting in low virtual network rate coverage probability. In other words, the virtual networks built based on the deterministic model cannot provide any guarantee of individual UEs sub-6 GHz rate demand satisfaction in the presence of the uncertainty in UE locations and channel conditions. Whereas, the virtual networks built based on our proposed stochastic demand model provide probabilistic guarantees of individual UEs sub-6 GHz rate demand satisfaction as long as sufficient resources are available in the resource pool.

5.4.5 Studying Other Sub-6 GHz BS Pricing Models

In our proposed virtual resource allocation framework, we considered a fixed-pricing model where RPs lease entire sub-6 GHz BSs to the VNB, i.e., charge full price of a sub-6 GHz BS to the VNB, regardless of the fraction of the BS that is needed to satisfy the minimum virtual network rate coverage probability demands of the SPs. In this subsection, we show that other pricing models such as usage-based pricing model (where RPs lease the required slice of sub-6 GHz BSs to the VNB, i.e., charge the VNB based on the amount of slices of sub-6 GHz BSs it uses) can also be studied using our proposed framework. We implement the usage-based pricing model as follows. First, we execute Algorithm 1 to obtain the cheapest subset of sub-6 GHz BSs that can satisfy the SP demands. Then, we solve a modified version of Problem 5.1 for this cheapest subset of BSs (say, $\mathcal{B}^*$). Specifically, we replace the objective function (5.2) of Problem 5.1 as: $\underset{\{\delta_{bs}\atop b\in\mathcal{B}^*,s\in\mathcal{S}\}}{\text{minimize}} \sum_{b\in\mathcal{B}} c_b \sum_{s\in\mathcal{S}} \delta_{bs}$. Furthermore, we remove constraint (5.5). Then, we solve the modified version of Problem 5.1 for $\mathcal{B}^*$ set of BSs using the piecewise linear approximation approach.

We compare the two pricing models in our evaluation set up by considering two SPs with same demand parameters, i.e., $\kappa = 1$ Mbps and $\beta = 0.95$ and varying λ. As can be seen in Figure 5.16, the performance gap between the two pricing models is moderate. Moreover, as the SP demands increase, the performance gap between the two pricing models reduces. This is expected since with higher demands, usage-based model also utilizes the entire capacity of the leased sub-6 GHz BSs.

5.4.6 Evaluation of Algorithm 2

In this subsection, we demonstrate the performance of our sequential virtual resource allocation scheme described in Algorithm 2. We consider four SPs who wish to provide wireless services within the considered geographical area shown in Figure 5.5. SP 1 requires its UEs to have a minimum sub-6 GHz data rate of 64 Kbps with probabilistic guarantee of 0.95. SP 2 requires its UEs to have a minimum sub-6 GHz data rate of 256 Kbps with probabilistic guarantee of 0.9. SP 3 requires its UEs to have a minimum sub-6 GHz data rate of 512 Kbps with probabilistic guarantee of 0.85. SP 4 requires its UEs to have a minimum sub-6 GHz data rate of 1 Mbps with probabilistic guarantee of 0.8. Each SP has same UE intensity. The SPs are ranked as follows. SP 1 is ranked as first. SP 2 is ranked as second. SP 3 is ranked as third and SP 4 is ranked as fourth.

In this set up, we evaluate Algorithm 2 by varying the UE intensity of the SPs. Table 5.1, shows the satisfied SPs. As can be seen that the SP demands are satisfied based on their ranks. This validates our proposed sequential virtual resource allocation scheme.

5.4.7 Comparison of Algorithm 1 with other Heuristics

In this subsection, we compare the performance of our suboptimal scheme described in Algorithm 1 with a meta-heuristic scheme, the differential evolutionary (DE) algorithm [77].

Table 5.1: Satisfaction of the SP demands according to their ranks.

UE intensity of the SPs	Satisfied SPs
10 /km^2	SP 1, SP 2, SP 3, SP 4
20 /km^2	SP 1, SP 2, SP 3
40 /km^2	SP 1, SP 2
80 /km^2	SP 1

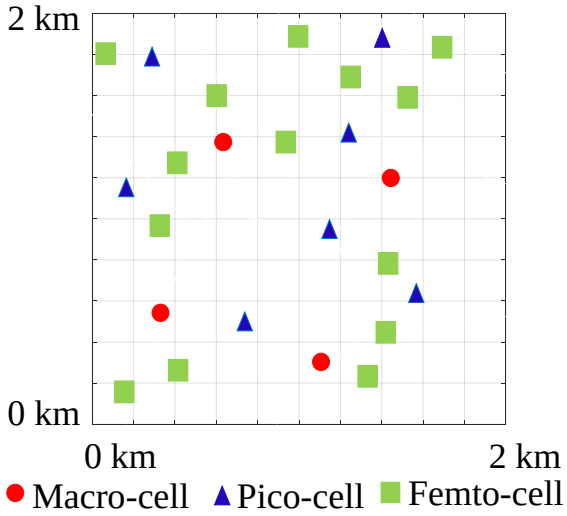

Figure 5.17: Locations of sub-6 GHz BSs.

To conduct this experiment, we consider a real scenario of sub-6 GHz BS deployment as shown in Figure 5.17. It is part of a map of real 4G network deployment [78]. As can be seen that there are total 25 sub-6 GHz BSs within an area of 2×2 km^2. There are three SPs who wish to provide wireless services within the geographical area. SP 1 requires its UEs to have a minimum sub-6 GHz data rate of 256 Kbps with probabilistic guarantee of 0.95. SP 2 requires its UEs to have a minimum sub-6 GHz data rate of 1 Mbps with probabilistic guarantee of 0.9. Both SPs have the same UE intensity. Moreover, both SPs have the same priority. To implement the DE algorithm, we generate a set $\mathcal{N}$ of candidate solutions of

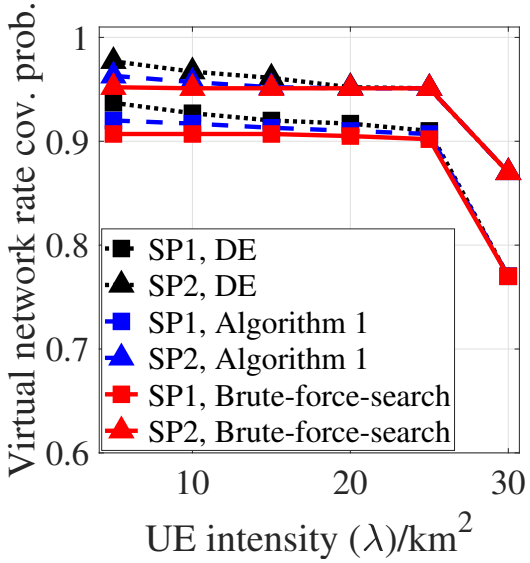

Figure 5.18: Sub-6 GHz RCP achieved by the SPs vs. UE intensity of the SPs.

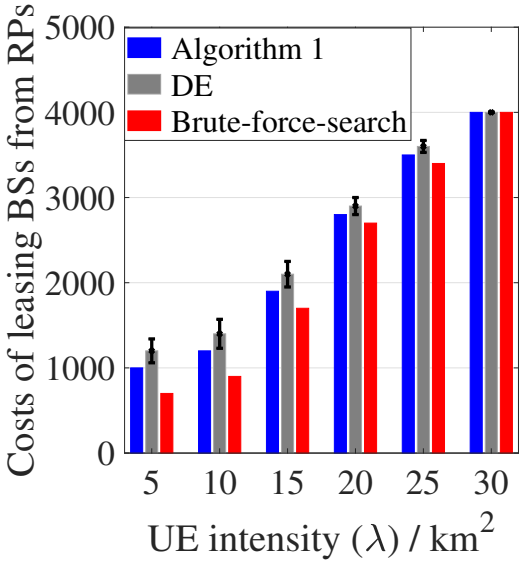

Figure 5.19: Cost of leasing sub-6 GHz BSs vs. UE intensity of the SPs.

the slicing decision variables δ_{bs}, $\forall b \in \mathcal{B}$, $\forall s \in \mathcal{S}$. Then, for a candidate solution, say, $X, X \in \mathcal{N}$, we define a fitness function as: $f(X) = C(X) + \eta(X)$ where $C(X)$ denotes the cost of leasing sub-6 GHz BSs for candidate solution X and $\eta(X)$ denotes the penalty for violating constraint (5.3) for candidate solution X. The elitist solution X^* is determined as: $\underset{\{X \in \mathcal{N}\}}{\text{argmax}}\{-f(X)\}$. We set the cross-over rate as 0.5, the mutation rate as 0.1, the population size as 10^4 and the maximum number of iterations as 10^3 which results in a reasonable CPU-time.

In this set up, we benchmark the performance of Algorithm 1 and DE with the BFS. In Figure 5.18, we plot the virtual network rate coverage probability achieved by the SPs and in Figure 5.19, we plot the cost of leasing sub-6 GHz BSs. As can be seen the optimality gap between Algorithm 1 and the BFS is much lower compare to the optimality gap between DE and the BFS.

5.5 Summary

In this chapter, we provided a chance-constrained virtualization framework that probabilistically satisfies SPs' sub-6 GHz rate coverage demands while minimizing resource over-provisioning in virtual networks. Through extensive simulations, we demonstrated the gains brought by our proposed stochastic-optimization-based virtual resource allocation schemes. Furthermore, note that the network overhead of our proposed framework and the computation load of the VNB are both reasonable since the proposed approach does not require the SPs, the VNB, and the RPs to interact to identify the instantaneous demands of individual UEs. This optimization framework can be used also for other service specific design criteria (e.g., delay, jitter).

Chapter 6

Sub-6 GHz Virtual Resource Allocation with Adaptive Statistical Multiplexing[1]

6.1 Introduction

In the previous chapter, we have presented a sub-6 GHz virtual resource allocation framework that aggregates and slices the sub-6 GHz BSs based on the distributions of the UE locations and channel conditions, before the UE locations and channel conditions are revealed. As a result, when a slice of a BS serves its associated UEs, it can be over-satisfied (i.e., resources left after satisfying the minimum sub-6 GHz rate demands of all UEs of the SP assigned to the slice) or under-satisfied (i.e., lack of resources to satisfy the minimum sub-6 GHz rate demands of all UEs of the SP assigned to the slice). Taking this into consideration, in this chapter, we develop an efficient scheme that performs the virtual resource allocation in two phases, i.e., virtual network deployment phase (static) and statistical multiplexing phase (adaptive), shown in Figure 6.1. In the virtual network deployment phase, the VNB statically aggregates, slices, and allocates sub-6 GHz BSs to SPs in the presence of uncertainty in UE locations and channel conditions, without knowing which realization of UE locations

[1]The material in this chapter is submitted to [79].

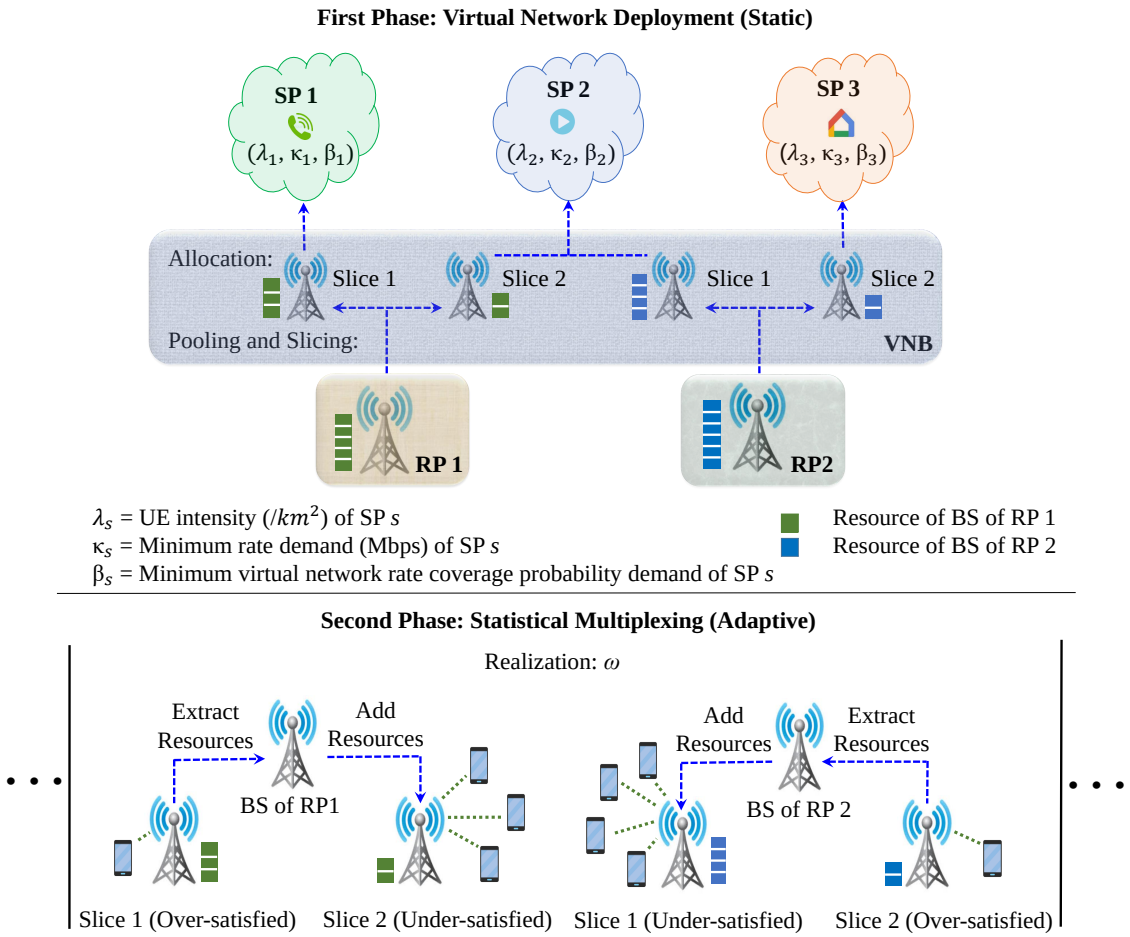

Figure 6.1: Wireless network virtualization architecture enabled with statistical multiplexing.

and channel conditions will occur. After the virtual networks are deployed, each of the aggregated sub-6 GHz BSs statistically multiplexes its associated SP demands, i.e., allocates excess resources from the over-satisfied slices to the under-satisfied slices, according to the realized channel conditions of associated UEs.

Towards developing this framework, first, we formulate a joint stochastic optimization problem for the VNB to jointly aggregate a set of sub-6 GHz BSs, slice them among the SPs, and determine their statistical multiplexing decisions with a finite set of realizations of UE locations and channel conditions of SPs. In the joint optimization problem, the deployment

decisions (i.e., the required set of sub-6 GHz BSs and how they are sliced and allocated) are static and are taken before knowing which realization of UE locations and channel conditions will occur. The statistical multiplexing decisions are adaptively taken according to the realized UE locations and channel conditions. The optimality criterion of our joint framework is to minimize resource over-provisioning while probabilistically satisfying SPs' sub-6 GHz rate and coverage demands. To solve our joint stochastic virtual resource allocation problem for a finite set of realizations of UE locations and channel conditions, we design a greedy algorithm in which, we allocate sub-6 GHz virtual resources gradually for the SPs until we probabilistically satisfy a minimum sub-6 GHz rate and coverage to all SPs in the considered set of realizations. Furthermore, taking into account the possibility of the joint optimization model being infeasible in the considered set of realizations due to a lack of sufficient sub-6 GHz resources, we propose a prioritized sub-6 GHz virtual resource allocation mechanism where sub-6 GHz resources are sequentially allocated for SPs based on given priorities. Next, considering the possibility of the deployed virtual networks encountering realizations of UE locations and channel conditions that were not considered in the joint optimization problem, we propose an efficient online statistical multiplexing scheme for the deployed sub-6 GHz BSs. Finally, we study the quality of the deployment decisions taken considering a finite set of realizations of UE locations and channel conditions in terms of meeting SPs' sub-6 GHz rate and coverage demands in any arbitrary set of realizations where each of the deployed sub-6 GHz BSs statistically multiplexes its associated SP demands.

The rest of the chapter is organized as follows. In Section 6.2, we describe our proposed model for sub-6 GHz virtual resource allocation and adaptive statistical multiplexing. In Section 6.3, we present our joint optimization model. In Section 6.4, we present our online statistical multiplexing scheme. In Section 6.5, we study the quality of the solutions in terms of meeting SPs' sub-6 GHz rate coverage demands in any arbitrary set of realizations. The

numerical analysis is presented and discussed in Section 6.6. Finally, the chapter is concluded in Section 6.7.

6.2 Framework Overview and Problem Statement

6.2.1 Framework Overview

Recall from Chapter 5 that we characterize the sub-6 GHz demands of SPs in $\mathcal{S}$ in the following way. If we arbitrarily choose a UE of SP s, $s \in \mathcal{S}$, that requires sub-6 GHz connections, the probability that this UE receives a sub-6 GHz data rate of at least κ_s bps needs to be at least β_s.

Upon receiving the sub-6 GHz demands from SPs, VNB leases a subset of sub-6 GHz BSs from $\mathcal{B}$ and slices them among the SPs in the presence of uncertainty in UE locations and channel conditions, before knowing which realization of UE locations and channel conditions will occur. A slice of a BS provides a fraction of capacity of the BS. For example, let $\delta_{bs} \in [0, 1]$, $b \in \mathcal{B}$, $s \in \mathcal{S}$, be a slice of BS b allocated to SP s. In that case, δ_{bs} represents the fraction of the capacity of BS b that SP s is the only SP to access. If SP s is the only SP associated with BS b, then $\delta_{bs} = 1$. Likewise, if SP s is not to be associated with BS b at all, then $\delta_{bs} = 0$.

After that, each of the aggregated sub-6 GHz BSs *corrects* its slicing according to the realized channel conditions of associated UEs. Specifically, UEs of the SPs share their CSI with their associated sub-6 GHz BSs. Each of these BSs upon receiving the CSI of UEs, identifies over-satisfied and under-satisfied slices, extracts resources from the over-satisfied slices as long as the slices do not become under-satisfied, and allocates these excess resources to the under-satisfied slices.

A slice of a sub-6 GHz BS allocated to an SP is identified as *over-satisfied* in a realization

of UE locations and channel conditions if the UE of the SP with the worst channel condition obtains a sub-6 GHz data rate higher than the minimum sub-6 GHz data rate requested by the SP. Likewise, a slice of a BS allocated to an SP is identified as *under-satisfied* in a realization if the UE of the SP with the worst channel conditions obtains a sub-6 GHz data rate lower than the minimum sub-6 GHz data rate requested by the SP.

Recall from the previous chapters that we assume each sub-6 GHz BS performs a proportional rate allocation for its UEs, i.e., the sub-6 GHz rate allocated to each UE is proportional to its spectral efficiency. Let $\hat{\delta}_{bs} \in [-1, 1]\,,\ b \in \mathcal{B},\ s \in \mathcal{S}$, be the correction factor for slice δ_{bs}. Then, the sub-6 GHz rate of a typical UE of SP s associated with BS b can be expressed from (6.1) as:

$$\tilde{R}_{bs} = (\delta_{bs} + \hat{\delta}_{bs}) \left(\frac{W_b}{\tilde{N}_{bs}} \underbrace{\log_2 \left(1 + \tilde{\text{SINR}}_b\right)}_{\text{spectral efficiency}} \right) \tag{6.1}$$

where $\tilde{N}_{bs}$ is the total number of UEs of SP s associated with BS b.

6.2.2 Problem Statement

Our goal is to (i) *aggregate the cheapest subset of sub-6 GHz BSs from* $\mathcal{B}$ and (ii) *optimally slice them among the SPs in* $\mathcal{S}$ *in the presence of uncertainty in UE locations and channel conditions*, and (iii) *optimally correct the slices according to the realized UE locations and channel conditions in order to meet the minimum sub-6 GHz virtual network rate coverage probability demands of the SPs in* $\mathcal{S}$.

6.3 Joint Optimization Model

In this section, we describe our centralized joint optimization framework that is executed at the VNB to jointly determine sub-6 GHz BS aggregation, slicing, allocation, and statistical

multiplexing decisions for a finite set of realizations of UE locations and channel conditions of SPs in $\mathcal{S}$.

6.3.1 Scenario Generation

We generate a finite set Ω of independent and identically distributed (i.i.d.) samples ("scenarios") of (i) the locations of the UEs of the SPs in $\mathcal{S}$ and (ii) their channel conditions from their respective distributions, described in Section III, by Monte Carlo sampling. A scenario $\omega,\ \omega \in \Omega$, represents a realization of the locations of the UEs of the SPs in $\mathcal{S}$ and their channel conditions.

6.3.2 Problem Formulation

Let $R_s^{(\omega)},\ s \in \mathcal{S},\ \omega \in \Omega$, be the sub-6 GHz rate obtained by an arbitrarily chosen UE of SP s in scenario ω from the sub-6 GHz virtual network of SP s. Then, sub-6 RCP achieved by the virtual network of SP $s,\ s \in \mathcal{S}$, (i.e., the probability of an arbitrarily chosen UE of SP s obtaining the minimum sub-6 rate κ_s), considering the set of scenarios Ω, can be expressed as:

$$\Pr_{\Omega}\left\{\tilde{R}_s \geq \kappa_s\right\} = \frac{1}{|\Omega|}\sum_{\omega\in\Omega}\mathbb{1}_{\left\{R_s^{(\omega)} \geq \kappa_s\right\}} \tag{6.2}$$

where $\mathbb{1}_{\{.\}}$ is an indicator function which equals one if the condition inside the brackets $\{.\}$ is satisfied and it equals zero otherwise.

However, (6.2) does not give us the information regarding the sub-6 GHz RCP achieved from individual BSs in $\mathcal{B}$. This necessitates a further detailed derivation of the sub-6 GHz RCP achieved by SP $s,\ s \in \mathcal{S}$, from the BSs in $\mathcal{B}$. Let $R_{bs}^{(\omega)},\ b \in \mathcal{B},\ s \in \mathcal{S},\ \omega \in \Omega$, be the sub-6 GHz rate obtained by an arbitrarily chosen UE of SP s associated with BS b in scenario ω. Let the distances of the arbitrarily chosen UE from BS b be $d_{bs}^{(\omega)}$ and from

interfering sub-6 GHz BS $j,\ j \in \mathcal{B}/b$, be $a_{js}^{(\omega)}$ in scenario ω. Let the channel gains experienced in scenario ω by the arbitrarily chosen UE from BS b be $h_{bs}^{(\omega)}$ and from interfering BS j be $g_{js}^{(\omega)}$. Let the total number of UEs of SP s associated with BS b in scenario ω be $N_{bs}^{(\omega)}$. Let $\hat{\delta}_{bs}^{(\omega)} \in [-1, 1]\,,\ b \in \mathcal{B},\ s \in \mathcal{S},\ \omega \in \Omega$, be the correction factor for δ_{bs}, the slice of BS b allocated to SP s, in scenario ω. Let $x_b \in \{0, 1\}\,,\ b \in \mathcal{B}$, be a binary decision variable indicating whether to lease BS b or not. x_b equals one if BS b will be selected and it equals zero otherwise. Then, $R_{bs}^{(\omega)},\ b \in \mathcal{B},\ s \in \mathcal{S},\ \omega \in \Omega$, the sub-6 GHz rate of the arbitrarily chosen UE of SP s associated with BS b in scenario ω is given by:

$$R_{bs}^{(\omega)} = \left(\delta_{bs} + \hat{\delta}_{bs}^{(\omega)}\right) \left(\frac{W_b}{N_{bs}^{(\omega)}} \log_2\left(1 + \frac{h_{bs}^{(\omega)} \left(d_{bs}^{(\omega)}\right)^{-\alpha}}{\sigma^2 + \sum_{j \in \mathcal{B}/b} x_j\ g_{js}^{(\omega)} \left(a_{js}^{(\omega)}\right)^{-\alpha}}\right)\right). \tag{6.3}$$

With (6.3), the sub-6 GHz RCP achieved by SP s from BS b in the set of scenarios Ω can be expressed as:

$$\Pr_{\Omega}\left\{\tilde{R}_{bs} \geq \kappa_s\right\} = \frac{1}{|\Omega|} \sum_{\omega \in \Omega} \mathbb{1}_{\left\{R_{bs}^{(\omega)} \geq \kappa_s\right\}}. \tag{6.4}$$

Now, recall that UEs of an SP are assumed to be associated with the nearest sub-6 GHz BS among the set of sub-6 GHz BSs allocated to the SP. Therefore, when choosing a UE arbitrarily from $\mathcal{A}$ (whose area is denoted by A), it is more likely to be associated with the sub-6 GHz BS which has a larger association region. In other words, the probability of a UE being associated with a given sub-6 GHz BS is the fraction of the total area covered by the association region of that BS. Then, the sub-6 GHz RCP achieved by SP s from the BSs in

$\mathcal{B}$ considering the set of scenarios Ω, can be expressed as:

$$\Pr_{\Omega}\left\{\tilde{R}_s \geq \kappa_s\right\} = \sum_{b\in\mathcal{B}} \frac{A_b}{A} \Pr_{\Omega}\left\{\tilde{R}_{bs} \geq \kappa_s\right\} = \frac{1}{|\Omega|} \sum_{b\in\mathcal{B}} \frac{A_b}{A} \sum_{\omega\in\Omega} \mathbb{1}_{\left\{R_{bs}^{(\omega)} \geq \kappa_s\right\}}. \tag{6.5}$$

Next, let $r_{bs}^{(\omega)},\ b \in \mathcal{B},\ s \in \mathcal{S},\ \omega \in \Omega$, be the sub-6 GHz rate of the UE of SP s associated with BS b with the worst channel conditions in scenario ω. Let the distances of the UE from BS b be $d_{bs}^{\prime(\omega)}$ and from interfering sub-6 GHz BS $j,\ j \in \mathcal{B}/b$, be $a_{js}^{\prime(\omega)}$ in scenarios ω. Let the channel gain experienced in scenario ω by the UE from BS b be $h_{bs}^{\prime(\omega)}$ and from interfering BS $j,\ j \in \mathcal{B}/b$, be $g_{js}^{\prime(\omega)}$. Then, $r_{bs}^{(\omega)},\ b \in \mathcal{B},\ s \in \mathcal{S},\ \omega \in \Omega$, the sub-6 GHz rate of the UE of SP s associated with BS b with the worst channel conditions in scenario ω is given by:

$$r_{bs}^{(\omega)} = \left(\delta_{bs} + \hat{\delta}_{bs}^{(\omega)}\right) \left(\frac{W_b}{N_{bs}^{(\omega)}} \log_2\left(1 + \frac{h_{bs}^{\prime(\omega)} \left(d_{bs}^{\prime(\omega)}\right)^{-\alpha}}{\sigma^2 + \sum_{j\in\mathcal{B}^*/b} x_j\ g_{js}^{\prime(\omega)} \left(a_{js}^{\prime(\omega)}\right)^{-\alpha}}\right)\right). \tag{6.6}$$

Likewise, the sub-6 GHz rate of the UE of SP s associated with uncorrected slice δ_{bs} of BS b with the worst channel condition in scenario ω is given by:

$$\hat{r}_{bs}^{(\omega)} = \delta_{bs} \left(\frac{W_b}{N_{bs}^{(\omega)}} \log_2\left(1 + \frac{h_{bs}^{\prime(\omega)} \left(d_{bs}^{\prime(\omega)}\right)^{-\alpha}}{\sigma^2 + \sum_{j\in\mathcal{B}^*/b} x_j\ g_{js}^{\prime(\omega)} \left(a_{js}^{\prime(\omega)}\right)^{-\alpha}}\right)\right). \tag{6.7}$$

With (6.5), (6.6), and (6.7), we formulate our joint stochastic sub-6 GHz virtual resource allocation problem as follows. Let $y_{bs}^{(\omega)} \in \{0,1\},\ b \in \mathcal{B},\ s \in \mathcal{S},\ \omega \in \Omega$, be a binary decision variable indicating the over-satisfaction of the uncorrected slice δ_{bs}. $y_{bs}^{(\omega)}$ equals one if $\hat{r}_{bs}^{(\omega)}$ greater than κ_s, the minimum sub-6 GHz rate requested by SP s, and it equals zero otherwise. Then, we can write the joint stochastic sub-6 GHz virtual resource allocation problem considering a set of Ω UE locations and channel conditions as follows:

Problem 6.1: Joint Aggregation, Slicing, Allocation, and Statistical Multiplexing

$$\underset{\substack{\{x_b, \delta_{bs}, \hat{\delta}_{bs}^{(\omega)}, \\ b\in\mathcal{B},\ s\in\mathcal{S},\ \omega\in\Omega\}}}{\text{minimize}} \left\{ \sum_{b\in\mathcal{B}} c_b\ x_b + \frac{1}{|\Omega|} \sum_{\omega\in\Omega} \sum_{b\in\mathcal{B}} \sum_{s\in\mathcal{S}} \left| \hat{\delta}_{bs}^{(\omega)} \right| \right\} \tag{6.8}$$

$$\text{subject to: } \frac{1}{|\Omega|} \sum_{b\in\mathcal{B}} \frac{A_b}{A} \sum_{\omega\in\Omega} \mathbb{1}_{\left\{R_{bs}^{(\omega)} \geq \kappa_s\right\}} \geq \beta_s, \quad \forall s \in \mathcal{S} \tag{6.9}$$

$$\sum_{s\in\mathcal{S}} \delta_{bs} \leq x_b, \quad \forall b \in \mathcal{B} \tag{6.10}$$

$$\sum_{s\in\mathcal{S}} \hat{\delta}_{bs}^{(\omega)} \leq 0, \quad \forall b \in \mathcal{B},\ \forall \omega \in \Omega \tag{6.11}$$

$$\left(\hat{r}_{bs}^{(\omega)} - \kappa_s\right) \left(2\ y_{bs}^{(\omega)} - 1\right) > 0, \quad \forall b \in \mathcal{B},\ \forall s \in \mathcal{S},\ \forall \omega \in \Omega \tag{6.12}$$

$$-\ y_{bs}^{(\omega)} \leq \hat{\delta}_{bs}^{(\omega)} \leq \left(1 - y_{bs}^{(\omega)}\right), \quad \forall b \in \mathcal{B},\ \forall s \in \mathcal{S},\ \forall \omega \in \Omega \tag{6.13}$$

$$r_{bs}^{(\omega)} \geq y_{bs}^{(\omega)}\ \kappa_s, \quad \forall b \in \mathcal{B},\ \forall s \in \mathcal{S},\ \forall \omega \in \Omega. \tag{6.14}$$

The first term in the objective function (6.8) represents the cost of the leased sub-6 GHz BSs and the second term in the objective function (6.8) represents the average amount of corrected (i.e., extracted/added) resources in the slices. Constraint (6.9) ensures that the sub-6 GHz RCP demand satisfaction of the SPs in $\mathcal{S}$ in the set of scenarios Ω. Constraints (6.10) and (6.11) ensure that the utilization of the leased sub-6 GHz BSs does not exceed 100%. Constraint (6.12) ensures that $y_{bs}^{(\omega)}$ equals one if $\hat{r}_{bs}^{(\omega)}$ is higher than κ_s and it equals zero otherwise. Constraint (6.13) ensures that the resources can be extracted only from the over-satisfied slices and the resources can be added only to the under-satisfied slices. Constraint (6.14) ensures that the resources can be extracted from the over-satisfied slices as long as they are not becoming under-satisfied.

6.3.3 Solution Approach

Theorem 6.1. *Problem 6.1, i.e., the joint sub-6 GHz resource aggregation, slicing, allocation, and statistical multiplexing problem is NP-complete.*

Proof. Note that Problem 6.1 is a combinatorial optimization problem that has continuous decision variables $\delta_{bs},\ \hat{\delta}_{bs}^{(\omega)},\ \forall b \in \mathcal{B},\ \forall s \in \mathcal{S},\ \omega \in \Omega$. Hence, there is no algorithm that can guarantee to optimally solve the problem in polynomial time. However, we can verify feasibility of a given instance of the decision variables $\delta_{bs},\ \hat{\delta}_{bs}^{(\omega)}$, and $x_b,\ \forall b \in \mathcal{B},\ \forall s \in \mathcal{S},\ \omega \in \Omega$, in the set of scenarios Ω in polynomial times. Hence, Problem 6.1 is NP.

Now, we show that Problem 6.1 is NP-hard by a straightforward reduction from the Capacity-limited Facility Location Problem (CFLP) which is known to be NP-hard [73]. In CFLP, the goal is to optimally place a set of facilities with limited capacity in a geographical area to serve a set of demand-points. Given an instance of the CFLP problem, we construct an instance of Problem 6.1 as follows:

- The set of capacity-limited facilities $\rightarrow \mathcal{B}$, i.e., the set of sub-6 GHz BSs,
- The set of demand points $\rightarrow$ Demands of the SPs in $\mathcal{S}$,
- Total cost (i.e., facility cost + service cost) $\rightarrow \sum_{b \in \mathcal{B}} c_b\, x_b$, i.e., the cost of leasing sub-6 GHz BSs,
- Assignment function $\rightarrow \mathbb{1}_{\left\{\sum_{s \in \mathcal{S}} \delta_{bs} > 0\right\}},\ \forall b \in \mathcal{B},\ \forall s \in \mathcal{S}$.

Then, it is easy to see that a solution of an instance of the CFLP problem that costs C exists if and only if there exists a solution of the corresponding instance of Problem 6.1 (as described above) that costs $C + n$ where $n \geq 0$, i.e., Problem 6.1 $\geq_P$ CFLP. Thus, Problem 6.1 is NP and NP-hard, i.e., NP-complete. □

In addition to NP-completeness of the problem, as can be seen that the binary decision

variables $x_b,\ b \in \mathcal{B}$, appears in the denominator term inside of the logarithmic function of $R_{bs}^{(\omega)},\ s \in \mathcal{S},\ b \in \mathcal{B},\ \omega \in \Omega$, the sub-6 GHz rate of an arbitrarily chosen UE of SP s associated with BS b in scenario ω in constraint (6.9), $\hat{r}_{bs}^{(\omega)},\ s \in \mathcal{S},\ b \in \mathcal{B},\ \omega \in \Omega$, the sub-6 GHz rate the UE of SP s associated with uncorrected slice δ_{bs} of BS b with the worst channel condition in scenario ω in constraint (6.12), and $r_{bs}^{(\omega)},\ s \in \mathcal{S},\ b \in \mathcal{B},\ \omega \in \Omega$, the sub-6 GHz rate the UE of SP s associated with corrected slice $(\delta_{bs} + \hat{\delta}_{bs}^{(\omega)})$ of BS b with the worst channel condition in scenario ω in constraint (6.14). As a result, it is extremely challenging to reformulate Problem 6.1 as a linear or the non-linear expression that is accepted by optimizers like CPLEX and GUROBI (e.g., semi-definite, second-order cone, and quadratic expressions [74]). Furthermore, due to the combinatorial nature of the problem, it is difficult to linearize the expression of the rate obtained by a UE from a sub-6 GHz BS. For example, the sub-6 GHz rate obtained by a UE of SP s from BS b depends on the shape of the Voronoi cell of BS b, which depends on the selection of the other sub-6 GHz BSs, i.e., $x_j,\ j \in \mathcal{B}/b$. In that case, to linearize the expression of the rate obtained by a UE (arbitrarily chosen or with the worst channel condition) of SP s from BS b with respect to δ_{bs} and $\hat{\delta}_{bs}^{(\omega)}$, we need to fix $x_j,\ j \in \mathcal{B}/b$. However, it is not computationally reasonable to consider each possible subset of sub-6 GHz BSs from $\mathcal{B}$ and linearize the rate expressions with respect to the slicing decision variables. Hence, we develop our solution approach based on an efficient greedy algorithm that can find good solutions with affordable computation complexity.

Our algorithm can be summarized as follows. Initially, we have an empty set (say, $\mathcal{B}^*$) of candidate sub-6 GHz BSs. Then, in each iteration, we perform two steps. In the first step, we select a BS from $\mathcal{B} \setminus \mathcal{B}^*$ and add it to $\mathcal{B}^*$ such that when its full capacity is allocated to the SP with highest sub-6 GHz RCP demand deficit in $\mathcal{S}$, it minimizes the demand deficit of that SP. In the next step, we slice and perform the statistical multiplexing among the slices of the BSs in $\mathcal{B}^*$ to satisfy the sub-6 GHz RCP demands of the SPs in $\mathcal{S}$. In this way,

we continue adding sub-6 GHz BSs in $\mathcal{B}^*$ in each iteration until $\mathcal{B}^*$ meets all the sub-6 GHz RCP demands of the SPs in $\mathcal{S}$. Let us explain the steps in details.

Sub-6 GHz BS Aggregation:

Note that in the first iteration, the SP with highest sub-6 GHz RCP demand has the highest demand deficit. However, from the next iterations, sub-6 GHz RCP demand deficits of the SPs are computed based on the slices of the BSs of $\mathcal{B}^*$ allocated to the SP in the previous iteration. Let SP s', $s' \in \mathcal{S}$, be the SP with the highest sub-6 GHz RCP demand deficit. Then, we add to $\mathcal{B}^*$ the sub-6 GHz BS b^* that satisfies:

$$b^* = \underset{b' \in \mathcal{B} \setminus \mathcal{B}^*}{\operatorname{argmax}} \left\{ \frac{\Pr_{\Omega} \left\{ \tilde{R}_{s'} \geq \kappa_{s'} \right\}_{(\mathcal{B}^* \cup b')}}{\hat{c}_{b'}} \right\} \tag{6.15}$$

where $\hat{c}_{b'}$ is the normalized cost of leasing BS b', i.e., $\hat{c}_{b'} = \frac{c_{b'}}{\sum\limits_{j \in \mathcal{B} \setminus \mathcal{B}^*} c_j}$.

In (6.15), $\Pr \left\{ \tilde{R}_{s'} \geq \kappa_{s'} \right\}_{(\mathcal{B}^* \cup b')}$, $b' \in \mathcal{B} \setminus \mathcal{B}^*$, is computed from (6.5) by setting the decision variables x_b and $\delta_{bs'}$, $\forall b \in \mathcal{B}^*$, to the solutions obtained in the previous iteration and the decision variables $x_{b'}$ and $\delta_{b's'}$ to one. In the case of the first iteration, decision variables x_b and $\delta_{bs'}$, $\forall b \in \mathcal{B}^*$, are to be set to zero since no sub-6 GHz BSs are added to $\mathcal{B}^*$ so far.

Sub-6 GHz BS Slicing and Statistical Multiplexing:

In each iteration, the VNB slices the BSs in the candidate set $\mathcal{B}^*$, $\mathcal{B}^* \subseteq \mathcal{B}$, among the SPs in $\mathcal{S}$ and performs the statistical multiplexing among the slices in order to satisfy the sub-6 GHz RCP demands of as many SPs as possible. Then, we can write the joint slicing and statistical multiplexing problem for the VNB as follows:

Problem 6.2: Joint Slicing, Allocation, and Statistical Multiplexing

$$\underset{\substack{\{\delta_{bs},\, \hat{\delta}_{bs}^{(\omega)},\\ b\in\mathcal{B}^*,\, s\in\mathcal{S},\, \omega\in\Omega\}}}{\text{maximize}} \left\{ \sum_{s\in\mathcal{S}} \mathbb{1}_{\left\{\Pr_{\Omega}\left\{\tilde{R}_s \geq \kappa_s\right\} \geq \beta_s\right\}} - \frac{1}{|\Omega|} \sum_{\omega\in\Omega} \sum_{b\in\mathcal{B}^*} \sum_{s\in\mathcal{S}} \left| \hat{\delta}_{bs}^{(\omega)} \right| \right\} \tag{6.16}$$

$$\text{subject to:} \quad \sum_{s\in\mathcal{S}} \delta_{bs} \leq 1, \quad \forall b \in \mathcal{B}^* \tag{6.17}$$

$$\sum_{s\in\mathcal{S}} \hat{\delta}_{bs}^{(\omega)} \leq 0, \quad \forall b \in \mathcal{B}^*, \ \forall \omega \in \Omega \tag{6.18}$$

$$\left(\hat{r}_{bs}^{(\omega)} - \kappa_s\right)\left(2\, y_{bs}^{(\omega)} - 1\right) > 0, \quad \forall b \in \mathcal{B}^*, \ \forall s \in \mathcal{S}, \ \forall \omega \in \Omega \tag{6.19}$$

$$-\, y_{bs}^{(\omega)} \leq \hat{\delta}_{bs}^{(\omega)} \leq \left(1 - y_{bs}^{(\omega)}\right), \quad \forall b \in \mathcal{B}^*, \ \forall s \in \mathcal{S}, \ \forall \omega \in \Omega \tag{6.20}$$

$$r_{bs}^{(\omega)} \geq y_{bs}^{(\omega)}\, \kappa_s, \quad \forall b \in \mathcal{B}^*, \ \forall s \in \mathcal{S}, \ \forall \omega \in \Omega. \tag{6.21}$$

The first term in the objective function (6.16) represents the number of SPs satisfied with their minimum sub-6 GHz RCP demands. Rest of the terms and constraints are similar to Problem 6.1.

As can be seen that the objective function (6.16) is nonlinear with respect to the decision variables δ_{bs} and $\hat{\delta}_{bs}^{(\omega)}$, $\forall b \in \mathcal{B}^*$, $\forall s \in \mathcal{S}$, $\forall \omega \in \Omega$. Let $e_{bs}^{(\omega)} \in \{0, 1\}$, $b \in \mathcal{B}$, $s \in \mathcal{S}$, $\omega \in \Omega$, be an auxiliary binary decision variable that denotes whether any correction is made on slice δ_{bs} in scenario ω or not. $e_{bs}^{(\omega)}$ is one if a correction is made on slice δ_{bs} in scenario ω and it equals zero otherwise. Let $z_s \in \{0, 1\}$, $s \in \mathcal{S}$, be a binary decision variable that denotes whether the sub-6 GHz RCP demand β_s of SP s is satisfied or not. z_s equals one if SP s obtains a sub-6 GHz RCP of at least β_s and it equals zero otherwise. Furthermore, let $v_{bs}^{(\omega)} \in \{0, 1\}$, $b \in \mathcal{B}$, $s \in \mathcal{S}$, $\omega \in \Omega$, be a binary decision variable that denotes whether $R_{bs}^{(\omega)}$, the sub-6 GHz rate obtained by an arbitrarily chosen UE of SP s associated with BS b in scenario ω is at least κ_s or not. $v_{bs}^{(\omega)}$ equals one if $R_{bs}^{(\omega)}$ is greater than or equal to κ_s and it equals zero otherwise. Then, we can replace the objective function (6.16) in Problem 6.2

with the following objective function and by adding the following constraints.

$$\underset{\substack{\{\delta_{bs},\, \hat{\delta}_{bs}^{(\omega)},\, z_s,\, e_{bs}^{(\omega)},\, v_{bs}^{(\omega)} \\ s\in\mathcal{S},\, b\in\mathcal{B}^*,\, \omega\in\Omega\}}}{\text{maximize}} \left\{ \sum_{s\in\mathcal{S}} z_s - \frac{1}{|\Omega|} \sum_{\omega\in\Omega} \sum_{b\in\mathcal{B}^*} \sum_{s\in\mathcal{S}} e_{bs}^{(\omega)} \right\} \tag{6.22}$$

$$\text{subject to:} \quad \left(\sum_{b\in\mathcal{B}^*} \sum_{\omega\in\Omega} v_{bs}^{(\omega)} - |\Omega|\, \beta_s \right) (2\, z_s - 1) \geq 0, \quad \forall s \in \mathcal{S} \tag{6.23}$$

$$\left(R_{bs}^{(\omega)} - \kappa_s \right) \left(2\, v_{bs}^{(\omega)} - 1 \right) \geq 0, \quad \forall b \in \mathcal{B}^*,\ \forall s \in \mathcal{S},\ \forall \omega \in \Omega \tag{6.24}$$

$$e_{bs}^{(\omega)} \geq -\hat{\delta}_{bs}^{(\omega)}, \quad \forall b \in \mathcal{B}^*,\ s \in \mathcal{S},\ \forall \omega \in \Omega \tag{6.25}$$

$$e_{bs}^{(\omega)} \geq \hat{\delta}_{bs}^{(\omega)}, \quad \forall b \in \mathcal{B}^*,\ s \in \mathcal{S},\ \forall \omega \in \Omega. \tag{6.26}$$

The product of the binary decision variables, z_s and $v_{bs}^{(\omega)}$, $b \in \mathcal{B},\ s \in \mathcal{S},\ \omega \in \Omega$, in constraint (6.23) can be equivalently expressed in a linear form by (i) introducing a new auxiliary non-negative decision variable, say Z, (ii) replacing $z_s\, v_{bs}^{(\omega)}$ by Z, and (iii) adding the following constraints:

$$Z \leq z_s, \quad Z \leq v_{bs}^{(\omega)}, \quad Z \geq z_s + v_{bs}^{(\omega)} - 1, \quad Z \geq 0. \tag{6.27}$$

The product of the binary and continuous decision variables $y_{bs}^{(\omega)}$ and $\hat{\delta}_{bs}^{(\omega)}$ (or δ_{bs}) in $\hat{r}_{bs}^{(\omega)}$, $b \in \mathcal{B},\ s \in \mathcal{S},\ \omega \in \Omega$, in constraint (6.19) can be equivalently expressed in a linear form by (i) introducing a new auxiliary non-negative decision variable, say Y, (ii) replacing $y_{bs}^{(\omega)}\ \hat{\delta}_{bs}^{(\omega)}$ by Y and (iii) adding the following constraints:

$$Y \leq y_{bs}^{(\omega)}, \quad Y \leq \hat{\delta}_{bs}^{(\omega)}, \quad Y \geq \hat{\delta}_{bs}^{(\omega)} - (1 - y_{bs}^{(\omega)}), \quad Y \geq 0. \tag{6.28}$$

Similarly, the product of binary and continuous decision variables $v_{bs}^{(\omega)}$ and $\hat{\delta}_{bs}^{(\omega)}$ (or δ_{bs}) of $R_{bs}^{(\omega)}$, $b \in \mathcal{B},\ s \in \mathcal{S},\ \omega \in \Omega$, in constraint (6.24) can be equivalently expressed in a linear

form. In this way Problem 6.2 can be reformulated as an MILP and it can be solved using the state-of-the-art solution techniques, such as branch and cut techniques [74]. With the solutions of Problem 6.2, say, $\delta^*_{bs},\ \hat{\delta}^{(\omega)}_{bs},\ \forall b \in \mathcal{B}^*,\ \forall s \in \mathcal{S},\ \forall \omega \in \Omega$, we compute the sub-6 GHz RCP achieved by each SP in $\mathcal{S}$ from the candidate set $\mathcal{B}^*$ using (6.2). If each SP obtains sub-6 GHz RCP higher than its demand, i.e., Constraint (6.9) in Problem 6.1 is satisfied, we stop the iterations. Otherwise, we continue the iterations until the SP demands are satisfied. We summarize the solution procedure in Algorithm 3.

Algorithm 3 Sub-6 GHz Virtual Resource Allocation with Statistical Multiplexing

1: Input: $\mathcal{A}$, $\mathcal{B}$, $\mathcal{S}$, $c_b,\ \forall b \in \mathcal{B}$, $\mu_b,\ \forall b \in \mathcal{B}$, $W_b,\ \forall b \in \mathcal{B}$, $\kappa_s,\ \forall s \in \mathcal{S}$, $\beta_s,\ \forall s \in \mathcal{S}$, Ω
2: Output: $x^*_b,\ \delta^*_{bs},\ \hat{\delta}^{(\omega)}_{bs},\ \forall b \in \mathcal{B},\ \forall s \in \mathcal{S},\ \forall \omega \in \Omega$
3: $x^*_b \leftarrow 0,\ \delta^*_{bs} \leftarrow 0,\ \hat{\delta}^{(\omega)}_{bs} \leftarrow 0,\ \forall b \in \mathcal{B},\ \forall s \in \mathcal{S},\ \forall \omega \in \Omega,\ \mathcal{B}^* \leftarrow \emptyset$
4: **repeat**
5: Select the SP with highest sub-6 GHz RCP demand deficit in $\mathcal{S}$
6: Consider SP $s',\ s' \in \mathcal{S}$, has the highest demand deficit. Then, select a sub-6 GHz BS from $\mathcal{B} \setminus \mathcal{B}^*$ by:

$$b^* \leftarrow \underset{b' \in \mathcal{B} \setminus \mathcal{B}^*}{\operatorname{argmax}} \left\{ \frac{\Pr_{\Omega}\left\{\tilde{R}_{s'} \geq \kappa_{s'}\right\}_{(\mathcal{B}^* \cup b')}}{\hat{c}_{b'}} \right\}$$

7: $\mathcal{B}^* \leftarrow (\mathcal{B}^* \cup b^*)$
8: Solve Problem 6.2 for candidate set $\mathcal{B}^*$ and store the solutions in $\delta^*_{bs},\ \hat{\delta}^{(\omega)}_{bs},\ \forall b \in \mathcal{B}^*,\ \forall s \in \mathcal{S},\ \forall \omega \in \Omega$
9: Compute demand deficit $\left(\beta_s - \Pr_{\Omega}\left\{\tilde{R}_s \geq \kappa_s\right\}\right)$ with $\delta^*_{bs},\ \hat{\delta}^{(\omega)}_{bs},\ \forall b \in \mathcal{B}^*,\ \forall s \in \mathcal{S},\ \forall \omega \in \Omega$, from (6.2)
10: **until** $\left(\beta_s - \Pr_{\Omega}\left\{\tilde{R}_s \geq \kappa_s\right\}\right) \leq 0,\ \ \forall s \in \mathcal{S}$ **Or**, $\mathcal{B}^* = \mathcal{B}$
11: Report $x^*_b,\ \delta^*_{bs},\ \hat{\delta}^{(\omega)}_{bs},\ \forall b \in \mathcal{B},\ \forall s \in \mathcal{S},\ \forall \omega \in \Omega$.

6.3.4 Infeasibility

We identify Problem 6.1 as 'infeasible' when all BSs in $\mathcal{B}$ are not sufficient to meet all SP demands in the set of scenarios Ω. In that case, the VNB can satisfy as many SPs as possible by solving Problem 6.2 or satisfy SPs considering their priorities. To satisfy prioritized SP

demands, SPs are ranked based on their priorities and the VNB builds their virtual networks one by one sequentially according to their ranks as long as the resources are available in $\mathcal{B}$. Let us discuss this sequential virtual network building process in details. Note that there is a lack of sufficient resources in $\mathcal{B}$ to meet all SP demands in the first place. Hence, we can assume that the VNB would eventually select all the BSs in $\mathcal{B}$ to satisfy all (or as many as possible) prioritized SP demands. In other words, the set of sub-6 GHz BSs to be leased is fixed, i.e., $x_b^* = 1,\ \forall b \in \mathcal{B}$. Taking this into consideration, we design an iterative algorithm for sequential virtual resource allocation as follows. Initially, we have an empty set (say, $\mathcal{S}^*$) of satisfied SPs. Then, in each iteration, we select the SP with the highest rank from $\mathcal{S} \setminus \mathcal{S}^*$, add it to $\mathcal{S}^*$, and solve Problem 6.1 for the SPs in $\mathcal{S}^*$. In this way, we continue adding SPs in $\mathcal{S}^*$ in each iteration until we find that Problem 6.1 is 'infeasible', i.e., there is not enough resources to satisfy all SP demands in $\mathcal{S}^*$.

Note that with $x_b = 1,\ \forall b \in \mathcal{B}$, we can write Problem 6.1 for the SPs in $\mathcal{S}^*, \mathcal{S}^* \subseteq \mathcal{S}$, as follows:

Problem 6.3: Sequential Virtual Resource Allocation

$$\underset{\left\{\substack{\delta_{bs},\, \hat{\delta}_{bs}^{(\omega)},\\ s\in\mathcal{S}^*,\, b\in\mathcal{B},\, \omega\in\Omega}\right\}}{\text{minimize}} \ \frac{1}{|\Omega|} \sum_{\omega\in\Omega} \sum_{b\in\mathcal{B}} \sum_{s\in\mathcal{S}^*} \left|\hat{\delta}_{bs}^{(\omega)}\right| \tag{6.29}$$

$$\text{subject to:} \ \frac{1}{|\Omega|} \sum_{b\in\mathcal{B}} \frac{A_b}{A} \sum_{\omega\in\Omega} \mathbb{1}_{\left\{R_{bs}^{(\omega)} \geq \kappa_s\right\}} \geq \beta_s, \ \ \forall s \in \mathcal{S}^* \tag{6.30}$$

$$\sum_{s\in\mathcal{S}^*} \delta_{bs} \leq 1, \ \ \forall b \in \mathcal{B} \tag{6.31}$$

$$\sum_{s\in\mathcal{S}^*} \hat{\delta}_{bs}^{(\omega)} \leq 0, \ \ \forall b \in \mathcal{B}, \ \forall \omega \in \Omega \tag{6.32}$$

$$\left(\hat{r}_{bs}^{(\omega)} - \kappa_s\right)\left(2\, y_{bs}^{(\omega)} - 1\right) > 0, \ \ \forall b \in \mathcal{B}, \forall s \in \mathcal{S}^*, \forall \omega \in \Omega \tag{6.33}$$

$$-\, y_{bs}^{(\omega)} \leq \hat{\delta}_{bs}^{(\omega)} \leq \left(1 - y_{bs}^{(\omega)}\right), \ \ \forall b \in \mathcal{B}, \forall s \in \mathcal{S}^*, \forall \omega \in \Omega \tag{6.34}$$

$$r_{bs}^{(\omega)} \geq y_{bs}^{(\omega)} \kappa_s, \quad \forall b \in \mathcal{B}, \forall s \in \mathcal{S}^*, \forall \omega \in \Omega. \tag{6.35}$$

As can be seen that in Problem 6.3, the objective function (6.29) and constraints (6.30) and (6.33) are nonlinear with respect to the decision variables δ_{bs} and $\hat{\delta}_{bs}^{(\omega)}$ $b \in \mathcal{B},\ s \in \mathcal{S}^*,\ \omega \in \Omega$. We can linearize the objective function (6.29) by introducing auxiliary binary decision variables $e_{bs}^{(\omega)}, \in \{0,1\}\,,\ b \in \mathcal{B},\ s \in \mathcal{S},\ \omega \in \Omega$, that indicates whether any correction is made on slice δ_{bs} of BS b or not, and then replacing the objective function (6.29) with the second term in (6.22) and adding constraints (6.25) and (6.26). We can linearize constraint (6.30) by introducing auxiliary binary decision variables $z_s \in \{0,1\}\,,\ s \in \mathcal{S}$, that indicates whether the sub-6 GHz RCP demand β_s of SP s is satisfied or not, and the binary decision variables $v_{bs}^{(\omega)} \in \{0,1\}\,,\ b \in \mathcal{B},\ s \in \mathcal{S},\ \omega \in \Omega$, that indicates whether $R_{bs}^{(\omega)}$, the sub-6 GHz rate obtained by an arbitrarily chosen UE of SP s associated with BS b, is at least κ_s or not in scenario ω. Then, we replace constraint (6.30) with (6.23) and (6.24), and follow the similar steps to linearize them as in (6.28). Similarly, constraint (6.33) can be linearized by following the similar steps as in (6.27) and (6.28). In this way, Problem 6.3 can be reformulated as an MILP and it can be solved using the state-of-the-art solution techniques, such as branch and cut techniques [74].

To summarize the steps, we provide Algorithm 4. As can be seen in each iteration, the VNB adds the SP with the highest rank in $\mathcal{S}^*$ and solve Problem 6.3 with the SPs in $\mathcal{S}^*$. If Problem 6.3 is 'infeasible', i.e., there is not enough resources available in $\mathcal{B}$ to satisfy all the SP demands in $\mathcal{S}^*$, we stop the iterations. Otherwise, we continue the iterations.

Note that Algorithm 3 (or Algorithm 4 in the case of 'infeasibility') provides efficient way to jointly determine the virtual network deployment decisions, which are static, and the statistical multiplexing decisions, which are adaptive, for a finite set of realizations of UE locations and channel conditions. Specifically, the VNB first generates a set of i.i.d.

Algorithm 4 Sequential Virtual Resource Allocation with Statistical Multiplexing

Input: $\mathcal{A}$, $\mathcal{B}$, $\mathcal{S}$, c_b, $\forall b \in \mathcal{B}$, μ_b, $\forall b \in \mathcal{B}$, W_b, $\forall b \in \mathcal{B}$, κ_s, $\forall s \in \mathcal{S}$, β_s, $\forall s \in \mathcal{S}$, Ω
Output: $\delta^*_{bs}, \hat{\delta}^{(\omega)}_{bs}$, $\forall b \in \mathcal{B}, \forall s \in \mathcal{S}, \forall \omega \in \Omega$
\\ When Problem 6.1 is 'infeasible' \\
Sort SPs in $\mathcal{S}$ according to their ranks. Let $\mathcal{S}[i]$ be the i^{th} SP in the ranked set of SPs.
$i \leftarrow 0$, $\delta^*_{bs} \leftarrow 0$, $\hat{\delta}^{(\omega)}_{bs} \leftarrow 0$, $\forall b \in \mathcal{B}$, $\forall s \in \mathcal{S}$, $\forall \omega \in \Omega$, $\mathcal{S}^* \leftarrow \emptyset$
repeat
    $i \leftarrow i + 1$
    $\mathcal{S}^* \leftarrow (\mathcal{S}^* \cup \mathcal{S}[i])$
    Solve Problem 6.3 for SPs in $\mathcal{S}^*$ and store the solutions in δ^*_{bs}, $\hat{\delta}^{(\omega)}_{bs}$, $\forall b \in \mathcal{B}$, $\forall s \in \mathcal{S}^*$, $\forall \omega \in \Omega$
until Problem 6.3 is 'infeasible'
Report $\delta^*_{bs}, \hat{\delta}^{(\omega)}_{bs}$, $\forall b \in \mathcal{B}$, $\forall s \in \mathcal{S}$, $\forall \omega \in \Omega$.

scenarios Ω of the UE locations and the channel conditions of the SPs in $\mathcal{S}$. Then, it executes Algorithm 3 (or Algorithm 4 in the case of 'infeasibility') for the set of scenarios Ω. Based on the solutions obtained from the algorithm, the VNB leases sub-6 GHz BSs from RPs, slices them, and provides the statistical multiplexing decisions to the sub-6 GHz BSs. However, the deployed sub-6 GHz BSs may encounter a realization of UE locations and channel conditions that was not considered in Ω. This necessitates an efficient online scheme that is executed at the deployed sub-6 GHz BSs to correct their slices.

6.4 Online Statistical Multiplexing

Let $\mathcal{S}_b$, $\mathcal{S}_b \subseteq \mathcal{S}$, be the set of SPs associated with BS b, $b \in \mathcal{B}^*$, based on the solutions obtained from Algorithm 3 (or Algorithm 4) for a set of scenarios Ω. Let ω', $\omega' \notin \Omega$, be a realization of UE locations and channel conditions that was not considered in Ω. Let $y^{(\omega')}_{bs} \in \{0, 1\}$, $b \in \mathcal{B}^*$, $s \in \mathcal{S}_b$, be a binary decision variable denoting the over-satisfaction of the uncorrected slice δ_{bs} of BS b in scenario ω'. $y^{(\omega')}_{bs}$ equals one if $\hat{r}^{(\omega')}_{bs}$, the sub-6 GHz rate obtained by the UE of SP s associated with the uncorrected slice δ_{bs} of BS b with the worst channel condition in scenario ω', is higher than κ_s, the minimum sub-6 GHz rate requested by SP s, and it equals zero otherwise. Furthermore, let $\hat{y}^{(\omega')}_{bs} \in \{0, 1\}$, $b \in \mathcal{B}^*$, $s \in \mathcal{S}_b$, be

a binary decision variable denoting the satisfaction of the corrected slice $(\delta_{bs} + \hat{\delta}_{bs}^{(\omega')})$ of BS b in scenario ω'. $\hat{y}_{bs}^{(\omega')}$ equals one if $r_{bs}^{(\omega')}$, the sub-6 GHz rate obtained by the UE of SP s associated with the corrected slice $(\delta_{bs} + \hat{\delta}_{bs}^{(\omega')})$ of BS b with the worst channel condition in scenario ω', is higher than κ_s, and it equals zero otherwise. Then, we can formulate the online statistical multiplexing problem for BS b, $b \in \mathcal{B}^*$, considering the realization of UE locations and channel conditions ω' as follows:

Problem 6.4: Online Statistical Multiplexing

$$\underset{\left\{\hat{\delta}_{bs}^{(\omega')},\, s \in \mathcal{S}_b\right\}}{\text{maximize}} \sum_{s \in \mathcal{S}_b} \hat{y}_{bs}^{(\omega')} \tag{6.36}$$

$$\text{subject to:} \quad \sum_{s \in \mathcal{S}_b} \hat{\delta}_{bs}^{(\omega')} \leq 0 \tag{6.37}$$

$$\left(\hat{r}_{bs}^{(\omega')} - \kappa_s\right)\left(2\, y_{bs}^{(\omega')} - 1\right) > 0, \quad \forall s \in \mathcal{S}_b \tag{6.38}$$

$$\left(r_{bs}^{(\omega')} - \kappa_s\right)\left(2\, \hat{y}_{bs}^{(\omega')} - 1\right) \geq 0, \quad \forall s \in \mathcal{S}_b \tag{6.39}$$

$$-\, y_{bs}^{(\omega')} \leq \hat{\delta}_{bs}^{(\omega')} \leq \left(1 - y_{bs}^{(\omega')}\right), \quad \forall s \in \mathcal{S}_b \tag{6.40}$$

$$r_{bs}^{(\omega')} \geq y_{bs}^{(\omega')}\, \kappa_s, \quad \forall s \in \mathcal{S}_b. \tag{6.41}$$

The objective function (6.36) denotes the number of SPs in $\mathcal{S}_b$ satisfied with the minimum sub-6 GHz rate demands after the slices are corrected. Constraint (6.37) ensures that the utilization of BS b does not exceed 100%. Constraint (6.38) ensures that $y_{bs}^{(\omega')}$ equals one if $\hat{r}_{bs}^{(\omega')}$ is higher than κ_s and it equals zero otherwise. Constraint (6.39) ensures that $\hat{y}_{bs}^{(\omega')}$ equals one if $r_{bs}^{(\omega')}$ is greater than or equal to κ_s and it equals zero otherwise. Constraint (6.40) ensures that the resources can be extracted only from the over-satisfied slices and the resources can be added only to the under-satisfied slices. Constraint (6.41) ensures that the resources can be extracted from the over-satisfied slices as long as they are not becoming under-satisfied.

Problem 6.4 can be reformulated as an MILP by linearizing constraints (6.38) and (6.39) with respect to $\hat{\delta}_{bs}^{(\omega')}$ by following the similar steps as in (6.28). However, it is computationally challenging to solve an MILP in real time. Taking this into consideration, we design a greedy iterative algorithm to solve Problem 6.4 as follows. Let $\mathcal{S}'$, $\mathcal{S}' \subseteq \mathcal{S}_b$, be the set of over-satisfied SPs and $\hat{\mathcal{S}}$, $\hat{\mathcal{S}} \subseteq \mathcal{S}_b$, be the set of under-satisfied SPs. First, we extract resources from all the over-satisfied SPs in $\mathcal{S}'$ as long as they are not becoming under-satisfied. Then, in each iteration, we select the least under-satisfied SP in $\hat{\mathcal{S}}$ and optimally allocate the extracted resources to the SP. In this way, we continue the iterations until we run out of the extracted resources.

We extract resources from over-satisfied SP s, $s \in \mathcal{S}'$, $\mathcal{S}' \subseteq \mathcal{S}_b$, as follows:

Problem 6.5: Resource Extraction from Over-satisfied SPs

$$\text{minimize } \hat{\delta}_{bs}^{(\omega')} \text{ Subject to: } r_{bs}^{(\omega')} \geq \kappa_s,\ \hat{\delta}_{bs}^{(\omega')} \geq -1,\ \hat{\delta}_{bs}^{(\omega')} \leq 0. \tag{6.42}$$

Let $\alpha_b = \sum_{s \in \mathcal{S}'} \hat{\delta}_{bs}^{(\omega')}$ be the extracted resources from the over-satisfied SPs in $\mathcal{S}'$. Then, we add resources to under-satisfied SP s, $s \in \hat{\mathcal{S}}$, $\hat{\mathcal{S}} \subseteq \mathcal{S}_b$, as follows:

Problem 6.6:Resource Addition to Under-satisfied SPs

$$\text{minimize } \hat{\delta}_{bs}^{(\omega')} \text{ Subject to: } r_{bs}^{(\omega')} \geq \kappa_s,\ \hat{\delta}_{bs}^{(\omega')} \geq 0,\ \hat{\delta}_{bs}^{(\omega')} \leq \alpha_b. \tag{6.43}$$

As can be seen that Problems 6.5 and 6.6 are linear problems (LPs) that can be solved in polynomial time using some of the state-of-the-art solution techniques, such as the path following method as described in [76]. The overall idea of the path following method is to iteratively moving towards the optimal solution by computing gradients of the constraints

and the objective function in the polytope. For v constraints, w variables, and L coefficients, the complexity of the path following method is given by $\mathcal{O}\left((v+w)^{1.5}wL\right)$ [76]. Now, as can be seen in Problem 6.5, we have a total of three constraints, one decision variable, and a total of six nonzero coefficients, considering the term $\frac{W}{N}\log_2(.)$ in $r_{bs}^{(\omega')}$ as a single coefficient. Hence, the worst case complexity for solving Problem 6.5 using the path following method can be given as $T_{\text{extraction}} = \left((3+1)^{1.5}\ 1\ (6)\right)K$ or $48K$ where K is a constant denoting the processing time to execute a loop (which is typically in the μs scale) by the processor. Similarly, the worst case complexity for solving Problem 6.6 using the path following method can be given as $T_{\text{allocation}} = \left((3+1)^{1.5}\ 1\ (6)\right)K$ or $48K$.

We summarize the steps of online statistical multiplexing in Algorithm 5. As can be seen, we first solve Problem 6.5 to extract resources from the over-satisfied SPs. After that, in each iteration, we solve Problem 6.6 to add resources to the under-satisfied SPs and compute the remaining excess resources. If we run out of the excess resources, we stop the iterations. Otherwise, we continue the iterations.

Algorithm 5 Online Statistical Multiplexing

Input: $\mathcal{S}_b$, κ_s, $\forall s \in \mathcal{S}_b$, ω'
Output: $\hat{\delta}_{bs}^{(\omega')}$, $\forall s \in \mathcal{S}_b$
$\mathcal{S}' \leftarrow$ Over-satisfied SPs, $\hat{\mathcal{S}} \leftarrow$ Under-satisfied SPs
Solve Problem 6.5 for all SPs in $\mathcal{S}'$ and store solutions in $\hat{\delta}_{bs}^{(\omega')}$, $\forall s \in \mathcal{S}'$
$\alpha_b \leftarrow \sum_{s \in \mathcal{S}'} \hat{\delta}_{bs}^{(\omega')}$
repeat
    Select SP with least sub-6 GHz rate demand deficit from $\hat{\mathcal{S}}$
    Consider SP s' has the least sub-6 GHz rate demand deficit. Solve Problem 6.6 for SP s' and store the solutions in $\hat{\delta}_{bs'}^{(\omega')}$
    if Problem 6.6 is 'infeasible' **then**
        $\hat{\delta}_{bs'}^{(\omega')} \leftarrow \alpha_b$
        EXIT
    end if
    $\alpha_b \leftarrow \alpha_b - \hat{\delta}_{bs'}^{(\omega')}$
until $\alpha_b \leq 0$
Report $\hat{\delta}_{bs}^{(\omega')}$, $\forall s \in \mathcal{S}_b$.

We state the following theorem regarding the complexity of Algorithm 5.

Theorem 6.2. *If we solve Problems 6 and 7 using the path following method [76] then, for S SPs in $\mathcal{S}$, the complexity of Algorithm 5 is $\mathcal{O}(S)$.*

Proof. Note that the first step of the algorithm is to identify the over-satisfaction or the under-satisfaction of each SP in $\mathcal{S}$. Therefore, for S SPs in $\mathcal{S}$, this step has a complexity of $\mathcal{O}(S)$.

Next, note that for S SPs in $\mathcal{S}$, there can be a maximum of $(S-1)$ over-satisfied SPs to extract resources. In that case, Problem 6.5 runs for $(S-1)$ times, which results in a complexity of $\sum_{s=1}^{S-1} 48\ K = (S-1)\ 48\ K$, where K is a constant. Similarly, for S SPs in $\mathcal{S}$, there can be a maximum of $(S-1)$ under-satisfied SPs to add resources. In that case, Problem 6.6 runs for $(S-1)$ times, which results in a complexity of $\sum_{s=1}^{S-1} 48\ K = (S-1)\ 48\ K$, where K is a constant.

Therefore, the complexity of Algorithm 5 is $\mathcal{O}(S) + 2\ (S-1)\ 48\ K$, i.e., $\mathcal{O}(S)$. □

6.5 SP Demands Satisfaction Analysis

In this subsection, we estimate the quality of the static decisions (i.e., sub-6 GHz BS aggregation and slicing decisions) taken for a set of scenarios Ω in Algorithm 3 (or Algorithm 4 in case of 'infeasibility') in terms of satisfying the sub-6 GHz RCP demands of SPs in $\mathcal{S}$ in an arbitrary set of scenarios where the online statistical multiplexing decisions are taken based on Algorithm 5. Let $x_b^*,\ \delta_{bs}^*,\ \forall b \in \mathcal{B},\ \forall s \in \mathcal{S}$, be the static solutions obtained from Algorithm 3 for the set of scenarios Ω. Let $\tilde{\mathcal{C}}$ be an arbitrary set of scenarios. Consider that with the static solutions x_b^* and $\delta_{bs}^*,\ \forall b \in \mathcal{B},\ \forall s \in \mathcal{S}$, we execute Algorithm 5 for each scenario in $\tilde{\mathcal{C}}$ and obtain a set of statistical multiplexing decisions $\hat{\delta}_{bs}^{(\omega)},\ \forall b \in \mathcal{B},\ \forall s \in \mathcal{S},\ \forall \omega \in \tilde{\mathcal{C}}$. With $x_b^*,\ \delta_{bs}^*$, and $\hat{\delta}_{bs}^{(\omega)},\ \forall b \in \mathcal{B},\ \forall s \in \mathcal{S},\ \forall \omega \in \tilde{\mathcal{C}}$, we can compute $R_s^{(\omega)},\ s \in \mathcal{S},\ \omega \in \tilde{\mathcal{C}}$, the sub-6

GHz rate obtained by an arbitrarily chosen UE of SP s from its associated sub-6 GHz BS in scenario ω, from (6.3). Then, we can compute the sub-6 GHz RCP achieved by SP $s,\ s \in \mathcal{S}$, in the set of scenarios $\tilde{\mathcal{C}}$ as:

$$\Pr_{\tilde{\mathcal{C}}}\left\{\tilde{R}_s \geq \kappa_s\right\} = \frac{1}{\left|\tilde{\mathcal{C}}\right|}\sum_{\omega\in\tilde{\mathcal{C}}} \underbrace{\mathbb{1}_{\left\{R_s^{(\omega)} \geq \kappa_s\right\}}}_{\text{independent Bernoulli Trials}}. \tag{6.44}$$

Let $\tilde{\text{RCP}}_s \overset{def}{=} \Pr_{\tilde{\mathcal{C}}}\left\{\tilde{R}_s \geq \kappa_s\right\},\ s \in \mathcal{S}$, denote the sub-6 GHz RCP achieved by SP s in the set of scenarios $\tilde{\mathcal{C}}$. Let $p_s^{(\omega)},\ \omega \in \tilde{\mathcal{C}}$, be the probability of success of the Bernoulli trial, i.e., whether $R_s^{(\omega)}$ is greater than or equal to κ_s or not. Since the Bernoulli trials are nonidentical, it is extremely challenging to find a closed form expression of the distribution of $\widetilde{\text{RCP}}_s,\ s \in \mathcal{S}$. However, we can obtain a lower bound of the distribution of $\widetilde{\text{RCP}}_s,\ s \in \mathcal{S}$, from the Le Cam's Theorem [80] as follows. Let $\tilde{Y}$ be a random variable following a Poisson distribution with mean Λ_s, where $\Lambda_s = \sum_{\omega\in\tilde{\mathcal{C}}} p_s^{(\omega)}$. Then, the lower bound of the distribution of $\widetilde{\text{RCP}}_s,\ s \in \mathcal{S}$, can be given as:

$$\begin{aligned}
&\left|\Pr_{\tilde{\mathcal{C}}}\left\{\sum_{\omega\in\tilde{\mathcal{C}}} p_s^{(\omega)} \ \geq\ \left|\tilde{\mathcal{C}}\right|\ \beta_s\right\} - \Pr\left\{\tilde{Y} \ \geq\ \left|\tilde{\mathcal{C}}\right|\ \beta_s\right\}\right| \leq \epsilon_s, \\
\Rightarrow &\Pr_{\tilde{\mathcal{C}}}\left\{\tilde{\text{RCP}}_s \ \geq\ \beta_s\right\} \geq 1 - \frac{\Gamma\left(\left\lfloor\left|\tilde{\mathcal{C}}\right|\ \beta_s + 1\right\rfloor,\ \Lambda_s\right)}{\left\lfloor\left|\tilde{\mathcal{C}}\right|\ \beta_s\right\rfloor} - \epsilon_s
\end{aligned} \tag{6.45}$$

where $\Gamma(.)$ denotes the gamma function and $\epsilon_s = 2\sum_{\omega\in\tilde{\mathcal{C}}}\left(p_s^{(\omega)}\right)^2$.

Now, we estimate Λ_s and ϵ_s in the following way. We generate sets of i.i.d. scenarios $\mathcal{C} = \left\{\Omega^{(1)}, \Omega^{(1)}, \ldots, \Omega^{(C)}\right\}$, each of cardinality K' following the similar procedure described in Section 6.3.1. Then, with the static solutions x_b^* and $\delta_{bs}^*,\ \forall b \in \mathcal{B},\ \forall s \in \mathcal{S}$, we execute Algorithm 5 for each scenario in $\mathcal{C}$. Let $\hat{\delta}_{bs}^{(\omega)},\ \forall b \in \mathcal{B},\ \forall s \in \mathcal{S},\ \forall \omega \in \Omega^{(c)},\ c \in \mathcal{C}$, be

the solutions obtained from Algorithm 5 for the set of scenarios $\Omega^{(c)}$. With x_b^*, δ_{bs}^*, and $\hat{\delta}_{bs}^{(\omega)}$, $\forall b \in \mathcal{B}$, $\forall s \in \mathcal{S}$, $\forall \omega \in \Omega^{(c)}$, we first compute $R_s^{(\omega)}$ from (6.3), and then estimate $p_s^{(c)}$, $c \in \mathcal{C}$, as:

$$p_s^{(c)} = \frac{1}{K'} \sum_{\omega \in \Omega^{(c)}} \mathbb{1}_{\left\{R_s^{(\omega)} \geq \kappa_s\right\}}. \tag{6.46}$$

After obtaining $p_s^{(c)}$, $\forall c \in \mathcal{C}$, we compute $\Lambda_s = \sum_{c \in \mathcal{C}} p_s^{(c)}$ and $\epsilon_s = 2 \sum_{c \in \mathcal{C}} \left(p_s^{(c)}\right)^2$. By substituting the values of Λ_s and ϵ_s in (6.45), we estimate the probability of the static decisions taken for a set of scenarios Ω meeting the sub-6 GHz RCP demand of SP s in an arbitrary set of scenarios where the online statistical multiplexing decisions have been taken based on Algorithm 5.

Next, in Algorithm 6, we summarize the procedure to obtain the static decisions, i.e., x_b and δ_{bs}, $\forall b \in \mathcal{B}$, $\forall s \in \mathcal{S}$, such that in an arbitrary set of scenarios, the static decisions combined with the online statistical multiplexing decisions can ensure the probability of meeting the sub-6 GHz RCP demands of the SPs in $\mathcal{S}$ to be at least τ. As can be seen that in each iteration, we increase the number of scenarios in Ω and solve Problem 6.1 with Algorithm 3 (or Problem 6.3 in case of 'infeasibility' with Algorithm 4). If the solutions obtained from the set of scenarios Ω ensure that the probability of meeting the sub-6 GHz RCP demand of each SP in an arbitrary set of scenarios is at least τ, we stop the iterations. Otherwise, we continue the iterations.

6.6 Performance Evaluation

In this section, we evaluate the performance of our proposed virtual resource allocation schemes. We implement our algorithms using Visual C++, CPLEX, and MATLAB.

Algorithm 6 Robust Sub-6 GHz Virtual Resource Allocation with Statistical Multiplexing

Input: $\mathcal{A}$, $\mathcal{B}$, $\mathcal{S}$, c_b, $\forall b \in \mathcal{B}$, μ_b, $\forall b \in \mathcal{B}$, W_b, $\forall b \in \mathcal{B}$, κ_s, $\forall s \in \mathcal{S}$, β_s, $\forall s \in \mathcal{S}$, τ
Output: x_b^*, δ_{bs}^*, $\forall b \in \mathcal{B}, \forall s \in \mathcal{S}^*, \mathcal{S}^* \subseteq \mathcal{S}$
Initialize: Cardinality K and K' where $K' >> K$
repeat
    Generate a set Ω of cardinality K of i.i.d. scenarios of the UE locations and the channel conditions as described in Section 6.3.1
    Solve Problem 6.1 for the set of scenarios Ω with Algorithm 3 and store the solutions in x_b^*, δ_{bs}^*, $\hat{\delta}_{bs}^{(\omega)}$, $\forall b \in \mathcal{B}^*$, $\forall s \in \mathcal{S}^*$, $\forall \omega \in \Omega$
    if Problem 6.1 is 'infeasible' **then**
        $x_b^* \leftarrow 1$, $\forall b \in \mathcal{B}$
        Solve Problem 6.3 for the set of scenarios Ω with Algorithm 4 and store the solutions in δ_{bs}^* $\hat{\delta}_{bs}^{(\omega)}$, $\forall b \in \mathcal{B}^*$, $\forall s \in \mathcal{S}^*$, $\forall \omega \in \Omega$
        EXIT
    else
        $\mathcal{S}^* \leftarrow \mathcal{S}$
    end if
    Generate sets of i.i.d. scenarios $\mathcal{C} = \left\{\Omega^{(1)}, \Omega^{(1)}, \ldots, \Omega^{(C)}\right\}$ each of cardinality K' and estimate $\Pr_{\tilde{\mathcal{C}}}\left\{\tilde{\mathrm{RCP}}_s \geq \beta_s\right\}$, $\forall s \in \mathcal{S}^*$ with x_b^* and δ_{bs}^* $\forall b \in \mathcal{B}, \forall s \in \mathcal{S}^*$, from (6.45)
    Increase the cardinality K and K'
until $\Pr\left\{\tilde{\mathrm{RCP}}_s \geq \beta_s\right\} \geq \tau$, $\forall s \in \mathcal{S}^*$
Report x_b^* and δ_{bs}^*, $\forall b \in \mathcal{B}, \forall s \in \mathcal{S}^*$.

6.6.1 Evaluation Setup

We consider three RPs that make a total of 25 sub-6 GHz BSs available in an area of 2×2 km^2, as shown in Figure 6.2. It is part of a map of a real 4G network deployment [78]. All fourteen sub-6 GHz BSs of RP 1 transmit with a constant power of 23 dBm (e.g., femto-cell). All seven sub-6 GHz BSs of RP 2 transmit with a constant power of 30 dBm (e.g., pico-cell). All four sub-6 GHz BSs of RP 3 transmit with a constant power of 46 dBm (e.g., macro-cell). All 25 sub-6 GHz BSs operate over a bandwidth of 20 MHz. Noise variance (σ^2) is set to -174 dBm/Hz. Pathloss exponent (α) is set to 4. As an example, we picked the cost of leasing a sub-6 GHz BS to be 100 from RP 1, 200 from RP 2, and 300 from RP 3.

6.6.2 Evaluation of Algorithm 3

In this subsection, we benchmark the performance of Algorithm 3 against the brute-force-search (BFS) in terms of finding optimal solutions for Problem 6.1. To conduct this evaluation, we consider that there are two SPs who wish to provide wireless services within the geographical area shown in Figure 6.2. Both SPs have the same UE intensity of $20/\text{km}^2$. Each SP requires its UEs to have a minimum sub-6 GHz data rate of 1 Mbps with a minimum probability of β. We consider Ω containing 10^3 scenarios. We vary β and plot the costs of leasing sub-6 GHz BSs in Figure 6.3. As can be seen that the optimality gap between Algorithm 3 and the BFS is moderate. Furthermore, as the demands increase, the number of feasible solutions decreases. As a result, the optimality gap between Algorithm 3 and the BFS gradually reduces as β increases. Next, we plot the required CPU-time of Algorithm 3 and the BFS by varying the number of SPs in Figure 6.4. We ran the two algorithms in a 'i7-2.4 GHz' processor. Due to the limited capacity of the processor, it becomes challenging to run the BFS for large problem sizes. It can be seen from Figure 6.4 that Algorithm 3

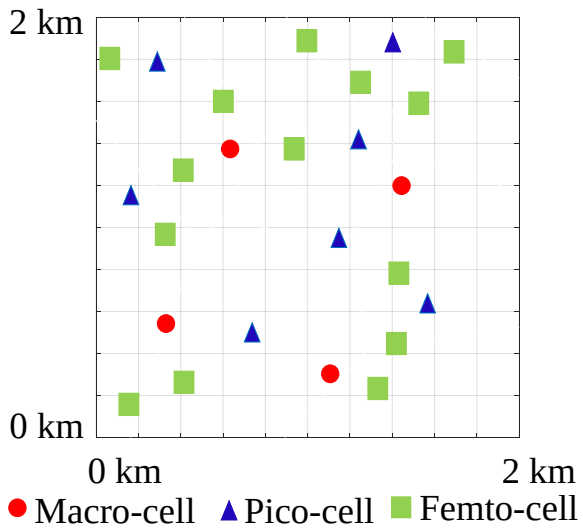

Figure 6.2: Locations of sub-6 GHz BSs.

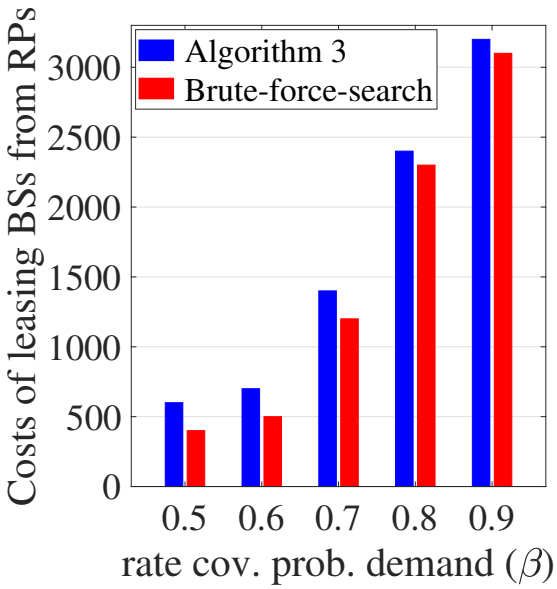

Figure 6.3: Costs of leasing sub-6 GHz BSs vs. sub-6 GHz RCP demands of the SPs.

has significantly lower complexity than the BFS. This shows the efficiency of Algorithm 3 in terms of finding good solutions of Problem 6.1 with affordable complexity.

6.6.3 Evaluation of Algorithm 4

In this subsection, we demonstrate the performance of our sequential virtual resource allocation scheme described in Algorithm 4. We consider four SPs who wish to provide wireless services within the considered geographical area shown in Figure 6.2. SP 1 requires its UEs to have a minimum sub-6 GHz data rate of 64 Kbps with a minimum probability of 0.95. SP 2 requires its UEs to have a minimum sub-6 GHz data rate of 256 Kbps with a minimum probability of 0.9. SP 3 requires its UEs to have a minimum sub-6 GHz data rate of 512 Kbps with a minimum probability of 0.85. SP 4 requires its UEs to have a minimum sub-6 GHz data rate of 1 Mbps with a minimum probability of 0.8. All SPs have same UE intensity. The SPs are ranked as follows. SP 1 is ranked as first. SP 2 is ranked as second. SP 3 is ranked as third and SP 4 is ranked as fourth. We consider Ω containing 10^3 scenarios.

In this set up, we evaluate Algorithm 4 by varying the UE intensity of the SPs. Table 6.1, shows the satisfied SPs. As can be seen that the SP demands are satisfied based on their ranks. This validates our proposed sequential virtual resource allocation scheme.

6.6.4 Evaluation of Algorithm 5

In this subsection, we benchmark the performance of Algorithm 5 with the optimal solutions obtained from CPLEX. To conduct this experiment, we consider the same four SPs from the previous evaluation except their priorities. All four SPs have the same UE intensity of $30/\text{km}^2$. Then, we consider a sub-6 GHz BS from the solutions obtained in the previous evaluation which is serving all of the four SPs (say, BS b^*). Now, we generate a set of 100 scenarios and solve the online statistical multiplexing problem formulated in Problem 6.4 for each of them using CPLEX and Algorithm 5. Table 6.2 shows the SPs satisfied with their minimum rate demands. As can be seen that the difference between the solutions of Algorithm 5 and the solutions obtained from CPLEX is moderately low.

6.6.5 Evaluation of Algorithm 6

In this subsection, we evaluate Algorithm 6 and compare its performance with the static virtual resource allocation scheme as described in [71] in terms of SP demands satisfaction and costs minimization. In the static virtual resource allocation scheme, the VNB aggregates the cheapest subset of sub-6 GHz BSs and slices them among the SPs to meet their minimum sub-6 GHz RCP demands, without performing the statistical multiplexing. To conduct this evaluation, we consider that there are three SPs who wish to provide wireless services within the geographical area shown in Figure 6.2. All three SPs have the same UE intensity λ. Each SP requires its UEs to have a minimum sub-6 GHz data rate of 1 Mbps. SP 1 requires a minimum RCP of 0.85. SP 2 requires a minimum sub-6 GHz RCP of 0.9 and SP 3 requires a minimum RCP of 0.95. In this set up, we execute Algorithm 6 with τ set to 0.99 and

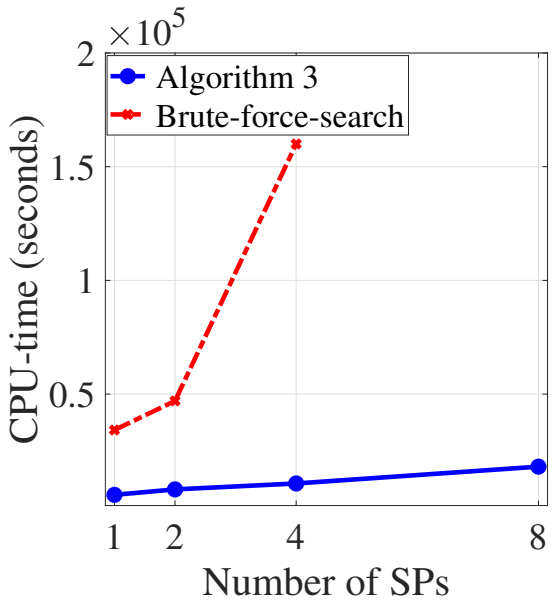

Figure 6.4: Required computation time vs. the number of SPs.

Table 6.1: Satisfaction of the minimum sub-6 GHz RCP demands of the SPs according to their ranks.

UE intensity of the SPs	Satisfied SPs
$30/\text{km}^2$	SP1, SP2, SP3, SP4
$40/\text{km}^2$	SP1, SP2, SP3
$60/\text{km}^2$	SP1, SP2
$100/\text{km}^2$	SP1

the static virtual resource allocation scheme. After we obtain the solutions, we generate a new set of 1000 scenarios (let us call it evaluation set Ω'). Then, with the static solutions of Algorithm 6, we perform statistical multiplexing in the evaluation set Ω' with Algorithm 5 and compute the sub-6 GHz RCP achieved by tne SPs in the evaluation set Ω'. On the other hand, we compute the sub-6 GHz RCP achieved by the SPs in the evaluation set Ω' from the solutions of the static virtual resource allocation scheme.

Now, we vary the UE intensity λ and plot the sub-6 GHz RCP achieved by the SPs in Figure 6.5 and the costs of leasing sub-6 GHz BSs in Figure 6.6. Furthermore, we perform another evaluation where all the three SPs ask for the same sub-6 GHz data rate of κ Mbps. The UE intensity of the SPs is set to 20/ km^2. Then, we vary the sub-6 GHz rate demand κ and plot the sub-6 GHz RCP achieved by the SPs in Figure 6.7 and the costs of leasing sub-6 GHz BSs in Figure 6.8.

As can be seen that both of the proposed scheme and the static virtual resource allocation

Table 6.2: Satisfaction of the minimum rate demands of the SPs.

Scenario index	Satisfied SPs	
	CPLEX	Algorithm 5
1st	SP1, SP2, SP4	SP1, SP2, SP4
40th	SP1, SP2, SP3, SP4	SP1, SP2, SP3, SP4
70th	SP4	SP4
100th	SP1, SP2, SP3	SP1, SP3, SP4

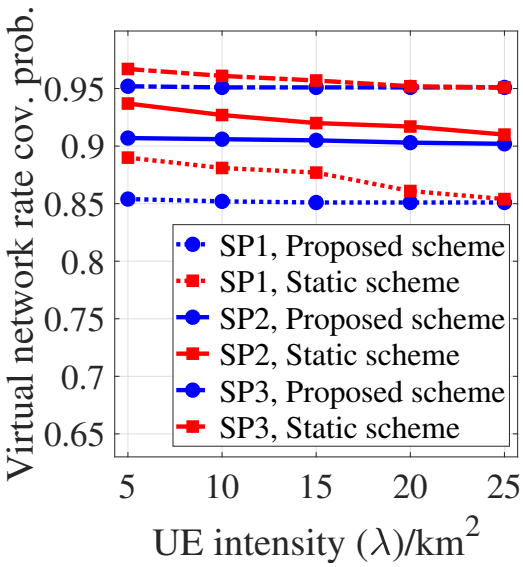

Figure 6.5: Sub-6 GHz RCP achieved by the SPs vs. UE intensity of the SPs.

scheme ensure satisfaction of the sub-6 GHz rate coverage demands of the SPs as well as isolation among the virtual networks in the presence of uncertainty in UE locations and channel conditions. However, the cost of leasing sub-6 GHz BSs obtained from Algorithm 6 is much less compared to the static scheme. This shows the efficiency of the proposed scheme in terms of minimizing the resource over-provisioning while meeting the SP demands through statistical multiplexing.

6.6.6 Studying Other Sub-6 GHz BS Cost Models

In our proposed virtualization framework, we considered a fixed-pricing model where RPs lease entire sub-6 GHz BSs to the VNB, i.e., charge full price of a sub-6 GHz BS to the VNB, regardless of the fraction of the sub-6 GHz BS that is needed to satisfy the minimum sub-6 GHz RCP demands of the SPs. In this subsection, we show that other pricing models such as usage-based pricing model, where RPs lease the required slices of sub-6 GHz BSs to the VNB, (i.e., charge the VNB based on the sizes of the slices of sub-6 GHz BSs it uses),

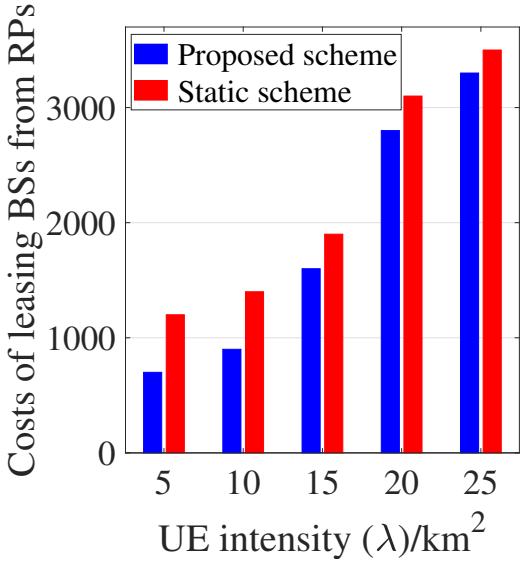

Figure 6.6: Costs of leasing sub-6 GHz BSs vs. UE intensity of the SPs.

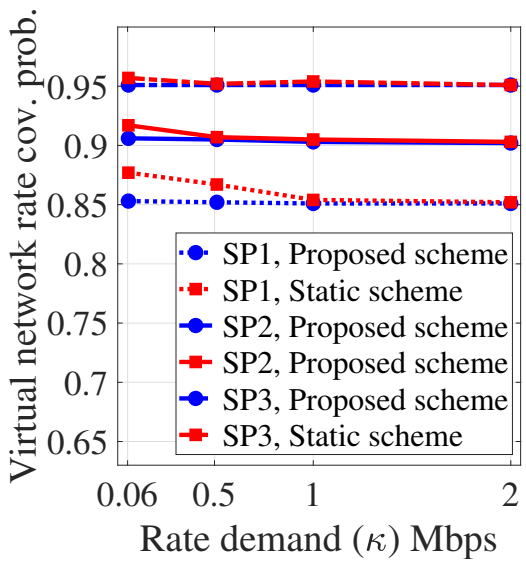

Figure 6.7: Sub-6 GHz RCP achieved by the SPs vs. sub-6 GHz rate demands of the SPs.

can also be studied using our proposed framework. With the usage-based pricing model, the VNB can perform either of the following two schemes. The VNB executes the static scheme as described in [71] to lease and slice the sub-6 GHz BSs. Then, according to the realized UE locations and channel conditions, returns the excess resources back to the RPs instead of performing the statistical multiplexing. In the second scheme, the VNB executes Algorithm 6 to lease and slice the sub-6 GHz BSs. Then, executes Algorithm 5 to perform statistical multiplexing in the realized UE locations and channel conditions. After executing Algorithm 5, if there remains excess resources, the VNB returns those excess resources to the RPs. We compare these two schemes in our evaluation set up by considering two SPs with the same demand parameters, i.e., $\kappa = 1$ Mbps and $\beta = 0.95$ and varying λ. In Algorithm 6, we set τ to 0.99. We compute the cost of leasing sub-6 GHz BSs in the evaluation set Ω'. As can be seen in Figure 6.9, the static scheme is able to reduce the costs up to a certain level by returning the excess resources. However, there exists a moderate performance gap between the two schemes. This is expected since the proposed scheme jointly optimizes the

virtual network deployment and the statistical multiplexing decisions.

6.6.7 Comparison with Existing Virtual Resource Allocation Schemes

In this subsection, we illustrate the gains brought by our recourse-action-based stochastic virtual resource allocation, as compared to the deterministic-optimization-based virtual resource allocation that is commonly adopted in the exiting works (e.g., [10, 11, 32, 33, 34, 35]). Specifically, we design a deterministic version of Problem 6.1 by replacing the sub-6 GHz RCP demands of the SPs with the sum-rate demands of the SPs. Furthermore, we replace the objective function of Problem 6.4 with the sum-rate demands of the SPs. Then, we compare the combined performance of the sum-rate versions of Problem 6.1 and Problem 6.4 with our proposed scheme. To conduct this evaluation, we consider two SPs who wish to provide wireless services within the geographical area shown in Figure 6.2. Both SPs have the same UE intensity λ. Each SP requires its UEs to have a minimum sub-6 GHz data rate of 1 Mbps. SP 1 requires a minimum sub-6 GHz RCP of 0.95 and SP 2 requires a minimum sub-6 GHz RCP of 0.9.

In this set up, we execute Algorithm 6 with τ set to 0.99. Then, with the static solutions of Algorithm 6, we perform statistical multiplexing in the evaluation set Ω' with Algorithm 5 and compute the sub-6 GHz RCP achieved by the SPs in the evaluation set Ω'. At the same time, we solve the sum-rate version of Problem 6.1 for a set of 1000 scenarios. With the solutions of the sum-rate version of Problem 6.1, we solve the sum-rate version of Problem 6.4 for the evaluation set Ω' and compute the sub-6 GHz RCP achieved by the SPs. Now, we vary the UE intensity λ and plot the sub-6 GHz RCP achieved by the SPs in Figure 6.10. Furthermore, we perform another evaluation where both SPs ask for the same sub-6 GHz data rate κ Mbps. The UE intensity of the SPs are set to 20/ km^2. Then, we vary the rate demand κ and plot the sub-6 GHz RCP achieved by the SPs in Figure 6.11. As can

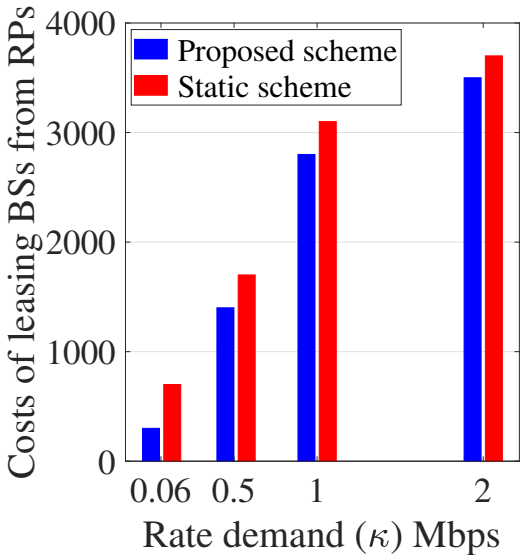

Figure 6.8: Costs of leasing sub-6 GHz BSs vs. sub-6 GHz rate demands of the SPs.

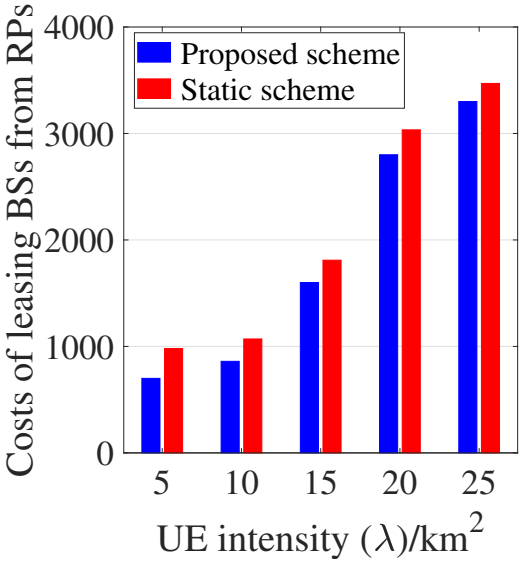

Figure 6.9: Costs of leasing sub-6 GHz BSs vs. UE intensity of the SPs in the usage-based cost model.

be seen that the sub-6 GHz RCP achieved from the sum-rate-based scheme is lower than that achieved by our proposed scheme. This is expected since the sum-rate model cannot efficiently capture the uncertainty in UE locations and channel conditions. As a result, our proposed recourse-action-based stochastic virtual resource allocation scheme significantly outperforms the existing sum-rate-based schemes in terms of ensuring probabilistic satisfaction of the sub-6 GHz rate coverage demands of the SPs in the presence of uncertainty in UE locations and channel conditions.

6.7 Summary

In this chapter, we provide an optimization framework for orchestrating sub-6 GHz virtualized cellular networks while enabling and exploiting statistical multiplexing. Our optimality criterion is to minimize resource over-provisioning while probabilistically satisfying SPs' sub-6 GHz rate coverage demands. Our proposed framework has two phases: virtual

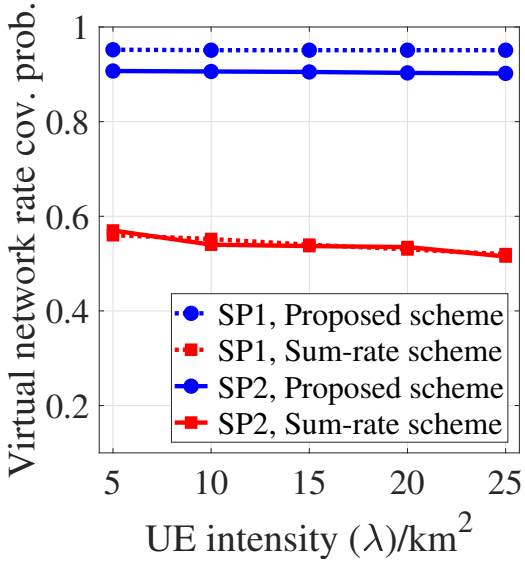

Figure 6.10: Sub-6 GHz RCP achieved by the SPs vs. UE intensity of the SPs.

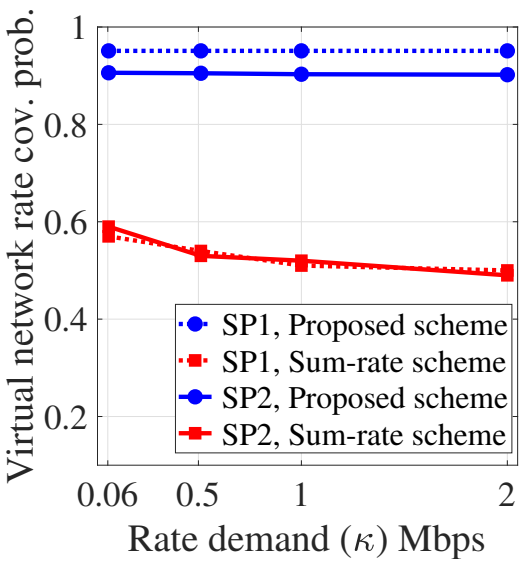

Figure 6.11: Sub-6 GHz RCP achieved by the SPs vs. sub-6 GHz rate demands of the SPs.

network deployment (static) and statistical multiplexing (adaptive). In the virtual network deployment phase, sub-6 GHz BSs are aggregated, sliced, and allocated to the SPs considering the presence of uncertainty in UE locations and channel conditions, without knowing which realization of UE locations and channel conditions will occur. Once the virtual networks are deployed, each of the aggregated BSs performs statistical multiplexing, i.e., allocates excess resources from the over-satisfied slices to the under-satisfied slices, according to the realized channel conditions of associated UEs. Our numerical results demonstrate that the proposed framework outperforms existing virtualization frameworks in terms of probabilistically satisfying SPs' sub-6 GHz rate and coverage demands while minimizing resource over-provisioning, in the presence of uncertainty in UE locations and channel conditions.

Chapter 7

MmW Virtual Network Deployment with Adaptive UE Assignment Framework [1]

7.1 Introduction

MmW systems typically use beamforming techniques to compensate for the high pathloss. However, directional communications in the presence of uncertainty in UE locations and channel conditions make maintaining coverage and connectivity challenging. In this context, we propose a joint stochastic optimization framework for mmW virtual network deployment and adaptive mmW UE assignment. The goal of our proposed framework is to determine the minimum number of required mmW BSs, their optimal locations, their optimal beam directions, and their optimal assignments to individual mmW UEs in order to meet SPs' mmW coverage demand and maximize the stability of mmW beams assigned to individual mmW UEs of SPs. The mmW virtual network deployment decisions (i.e., the required number of mmW BSs and their beam directions) are static and are taken before mmW UE locations and channel conditions are revealed. The mmW UE assignment decisions are taken under each realization of mmW UE locations and channel conditions considering the availability

[1] Part of the material in this chapter was published in [81] and additional material is submitted to [82].

and stability of the mmW beams. Towards developing this framework, first, using chance-constrained two-stage stochastic optimization, we develop a joint mmW BS placement (or aggregation), beam pointing, and *adaptive* mmW UE assignment framework. The goal of the first-stage is to optimally place the minimum number of mmW BSs and aim their beams optimally to meet SP's coverage demand. The first-stage decisions are static and they are taken before knowing the mmW UE locations and channel conditions. In the second-stage, we assign an optimal mmW link to each mmW UE according to the realized mmW UE locations and channel conditions considering the stability of the available links. Second, to optimally solve the first-stage of the problem, we obtain a closed-form expression for the coverage probability of a typical mmW network by considering the individual BS locations and their beam directions, unlike prior works (e.g., [83]) that typically assume uncertainty in the locations and beam directions of BSs. Third, to solve our two-stage chance-constrained stochastic optimization problem, we use the sample average approximation (SAA) framework, combined with various linearization techniques to derive an equivalent mixed integer linear formulation of the problem. The mixed integer linear formulation is then solved optimally using CPLEX. Furthermore, we statistically estimate the optimality gap of our proposed SAA framework for solving the two-stage chance-constrained problem. Fourth, given the computational complexity of solving our formulated problem for large networks, we develop a Benders decomposition-based suboptimal algorithm to solve our problem. The proposed algorithm can obtain a δ-optimal solution with reasonable computation complexity.

The rest of the chapter is organized as follows. In Section 7.2, we describe the mmW virtual network deployment with adaptive UE assignment model and problem statement. In Section 7.3, we present the optimal mmW BS deployment framework. The performance evaluation is presented and discussed in Section 7.4. Finally, the chapter is concluded in Section 7.5.

7.2 SP Demands Characterization, Framework Overview, and Problem Statement

7.2.1 SP Demands Characterization

SP $s, s \in \mathcal{S}$, characterizes its demand for mmW communications as follows: If we arbitrarily choose a mmW UE of SP s from the grid points in $\mathcal{K}$, the probability that this UE receives an SNR of at least T_s dB needs to be at least β_s. Let $\tilde{\gamma}_s$ be the SNR of an arbitrarily chosen mmW UE of SP s from grid points in $\mathcal{K}$. Then, the SNR demand of SP s can be expressed as: $\Pr\{\tilde{\gamma}_s \geq T_s\} \geq \eta_s$.

Let us call $\Pr\{\tilde{\gamma}_s \geq T_s\}$ the mmW virtual network downlink coverage probability.

7.2.2 Framework Overview

Our proposed framework has two stages, i.e., mmW virtual network deployment stage (static) and UE assignment stage (adaptive). In the virtual resource allocation stage, we place (or aggregate) the mmW BSs and point their beams towards the grids in $\mathcal{K}$ to meet the mmW downlink coverage probability demand of SP s. These decisions are taken based on the distribution of mmW UE locations and the distribution of the received SNR (i.e., u_j and $f^{(j)}_{\gamma_{nk}}(x), \forall n \in \mathcal{N}, \forall k, j \in \mathcal{K}$, described in Chapter 3). Hence, these decisions are static and they are taken before knowing which realization of mmW UE locations and channel conditions will occur.

When a UE of an SP wants to access the mmW BSs, it sends a request to the associated (i.e., nearest) sub-6 GHz BS. Upon receiving the request, the sub-6 GHz BS informs all of its associated mmW BSs that are assigned to the SP to switch on their beams according to the directions adjusted in the deployment stage. The UE starts to scan the availability of

the mmW beams.[2] A mmW beam is considered to be *available* to a UE if the SNR received from the beam is higher than the requested SNR τ. In each resource allocation cycle/time period, the UE sends its mmW beam availability information to the sub-6 GHz BS. If there is no mmW beam available for the UE, the sub-6 GHz BS is assigned to the UE. If more than one mmW beam is available for the UE, the legacy BS assigns the most stable beam to the UE.

7.2.3 Problem Statement

Our goal is to find (i) *the minimum number of required mmW BSs* and their placements in candidate locations $\mathcal{N}$, (or *the minimum number of mmW BSs to aggregate from* $\mathcal{N}$ *mmW BSs*) (ii) *their optimal beam directions*, and (iii) *the optimal assignment of these mmW beams to individual mmW UEs* in order to (i) ensure that the coverage probability is at least β and (ii) maximize the average stability of mmW beams assigned to UEs.

7.3 Optimization Framework

In this section, we propose a two-stage chance-constrained stochastic optimization framework that jointly optimizes the number of mmW BSs, their beam directions, and their assignment to individual mmW UEs of SPs. The goal of the first stage is to optimally place (or aggregate) the minimum number of mmW BSs and aim their beams towards the optimal directions knowing the distribution of mmW UE locations and received SNR, i.e., m_{sj} and $f^{(j)}_{\gamma_{nk}}(x), \forall n \in \mathcal{N}, \forall k, j \in \mathcal{K}$. In the second stage, the mmW beam assignment for individual mmW UEs of SPs is optimized under each realization of mmW UE locations and channel conditions knowing the distribution of the beams stability, $l_{nk}, n \in \mathcal{N}, k \in \mathcal{K}$.

[2]Note that in a traditional beam sweeping approach, mmW BSs sweep their beams in all possible directions which requires to apply several phase shifts over the antenna arrays. Here, the mmW BSs steer their beams in fixed directions, i.e., do not require any phase shift in real time. This reduces the overall hardware complexity and the delay and overhead of the initial access and cell discovery.

7.3.1 Problem Formulation

Let $x_n \in \{0,1\}$ $n \in \mathcal{N}$, be first-stage binary decision variables indicating whether to place a mmW BS at n or not. x_n equals one if a mmW BS is placed at location n and it equals zero otherwise. Let $y_{nsk} \in \{0,1\}$ $n \in \mathcal{N}, s \in \mathcal{S}, k \in \mathcal{K}$, be first-stage binary decision variables indicating whether to assign BS n to SP s and aim one of its beams towards grid k or not. y_{nsk} equals one if mmW BS s is assigned to SP s and one of its beams is pointed towards grid k, and it equals zero otherwise. Let $z_{nsj} \in \{0,1\}$ $n \in \mathcal{N}, s \in \mathcal{S}, j \in \mathcal{K}$ be second-stage binary decision variables representing the assignment of a beam of mmW BS n to a UE of SP s in grid j. z_{nsj} equals one if one of the beams ofmmW BS n is assigned to a UE of SP s in grid j, and it equals zero otherwise. Let $\tilde{H}_{nkj} \in \{0,1\}\, n \in \mathcal{N}, k, j \in \mathcal{K}$, denote the availability of the beam of BS n aimed towards grid k at grid j. $\tilde{H}_{nkj}$ equals one if the beam between BS n and grid k is available to grid j, and it equals zero otherwise. Let $\tilde{M}_{sk} \in \{0,1\}, s \in \mathcal{S}, k \in \mathcal{K}$, denote the UE occupancy in grid k. $\tilde{M}_{sk}$ equals one if there is a UE of SP s in grid k, and it equals zero otherwise. Let $\tilde{\boldsymbol{\zeta}} \triangleq \left(\tilde{\boldsymbol{H}}, \tilde{\boldsymbol{M}}\right)$, where $\tilde{\boldsymbol{H}}$ represents the vector of $\tilde{H}_{nkj}$, $\forall n \in \mathcal{N}$, $\forall k, j \in \mathcal{K}$, and $\tilde{\boldsymbol{M}}$ represents the vector of $\tilde{M}_{sk}$, $\forall s \in \mathcal{S}$, $\forall k \in \mathcal{K}$. Then, we can formulate the joint mmW virtual network deployment and adaptive UE assignment problem as follows:

Problem 7.1: MmW virtual network deployment and Adaptive UE Assignment

$$\underset{\substack{x_n, y_{nsk}, \\ \{n\in\mathcal{N}, s\in\mathcal{S}, k\in\mathcal{K}\}}}{\text{minimize}} \sum_{n\in\mathcal{N}} \sum_{n\in\mathcal{N}} x_n - q\, \mathbb{E}\left[h\left(\boldsymbol{y}, \tilde{\boldsymbol{\zeta}}\right)\right] \tag{7.1}$$

$$\text{subject to: } \Pr\left\{\tilde{\gamma}_s \geq T_s\right\} \geq \eta_s, \quad \forall s \in \mathcal{S} \tag{7.2}$$

$$\sum_{s\in\mathcal{S}} \sum_{k\in\mathcal{K}} y_{nsk} \leq B_n, \quad \forall n \in \mathcal{N} \tag{7.3}$$

$$x_n = \mathbb{1}_{\left\{\sum_{s\in\mathcal{S}} \sum_{k\in\mathcal{K}} y_{nsk} \geq 1\right\}}, \quad \forall n \in \mathcal{N} \tag{7.4}$$

$$y_{nsk} \in \{0, 1\}, \quad \forall n \in \mathcal{N}, \forall s \in \mathcal{S}, \forall k \in \mathcal{K} \tag{7.5}$$

where $h\left(\boldsymbol{y}, \tilde{\boldsymbol{\zeta}}\right)$ is the optimal value of the second-stage problem which is given by:

$$\underset{\substack{z_{nsj}, \\ \{n\in\mathcal{N}, s\in\mathcal{S}, j\in\mathcal{K}\}}}{\text{maximize}} \sum_{s\in\mathcal{S}} \left(\frac{\sum_{j\in\mathcal{K}} \sum_{n\in\mathcal{N}} \tilde{M}_{sj}\ z_{nsj}\ l_{nj}}{\sum_{j\in\mathcal{K}} \tilde{M}_{sj}} \right) \tag{7.6}$$

$$\text{subject to: } z_{nsj} \leq \tilde{M}_{sj}\ \tilde{H}_{nkj}\ y_{nk}, \quad \forall n \in \mathcal{N}, \forall s \in \mathcal{S}, \forall k, j \in \mathcal{K} \tag{7.7}$$

$$\sum_{n\in\mathcal{N}} z_{nsj} = \mathbb{1}_{\left\{\sum_{n\in\mathcal{N}} \sum_{k\in\mathcal{K}} y_{nsk}\ \tilde{M}_{sj}\ \tilde{H}_{nkj} \geq 1\right\}}, \quad \forall s \in \mathcal{S}, \forall j \in \mathcal{K} \tag{7.8}$$

$$z_{nsj} \in \{0, 1\}, \quad \forall n \in \mathcal{N}, \forall s \in \mathcal{S}, \forall j \in \mathcal{K} \tag{7.9}$$

where q is a design coefficient introduced to balance the tradeoff between minimizing the number of mmW BSs and the stability of mmW beams assigned to UEs.

In Problem 7.1, the first term of the first-stage objective function (7.1) represents the number of mmW BSs to deploy and the second term of the first-stage objective function (7.1) represents the expected optimal value of the second-stage objective function. Here, $\mathbb{1}_{\{.\}}$ is an indicator function which equals one if the condition inside the brackets $\{.\}$ is satisfied and it equals zero otherwise. Constraint (7.2) ensures the satisfaction of the mmW coverage probability demands of SPs in $\mathcal{S}$. Constraint (7.3) ensures that the number of

assigned beams of each BS does not exceed its total number of available beams. Constraint (7.4) relates between the two first-stage decisions. The second-stage objective function (7.6) represents the average stability of mmW beams assigned to UEs of SPs. Constraints (7.7) and (7.8) together ensure that if a UE of an SP has one or more available mmW beams, we need to assign that UE to one of the available mmW beams. Specifically, constraint (7.7) ensures that if a mmW beam is currently unavailable, we do not assign that beam. Constraint (7.8) ensures that if a UE of an SP has one or more available mmW beams, we need to assign a mmW beam to that UE.

7.3.2 Sample Average Approximation

A key challenge for solving Problem 7.1 is the evaluation of $\mathbb{E}\left[h\left(\boldsymbol{y}, \tilde{\boldsymbol{\zeta}}\right)\right]$. One standard technique for addressing this difficulty is to derive the sample average approximation (SAA) of Problem 7.1 [84]. The basic idea of SAA is to approximate the true distribution of stochastic variables with an empirical distribution by sampling. Then, approximate the expected value function by the corresponding sample average function. We generate a set of samples ("scenarios") Ω from the distributions of the UE occupancy and the received SNR, described in Chapter 3, by Monte Carlo sampling. A scenario $\omega, \omega \in \Omega$, represents a realization of the UEs distribution and the received SNR. After generating the set of scenarios, $\mathbb{E}\left[h\left(\boldsymbol{y}, \tilde{\boldsymbol{\zeta}}\right)\right]$ can be approximated by $\frac{1}{|\Omega|}\sum_{\omega\in\Omega} h\left(\boldsymbol{y}, \boldsymbol{\zeta}^{(\omega)}\right)$, where $h\left(\boldsymbol{y}, \boldsymbol{\zeta}^{(\omega)}\right)$ is the optimal value of the second-stage objective function for scenario ω. The SAA of Problem 7.1 can be written as follows:

SAA of Problem 7.1

$$\underset{\substack{x_n, y_{nsk}, z_{nsj}^{(\omega)}, \\ n\in\mathcal{N}, s\in\mathcal{S}, k,j\in\mathcal{K}, \omega\in\Omega}}{\text{minimize}} \left\{ \sum_{n\in\mathcal{N}} x_n - q\,\frac{1}{|\Omega|}\sum_{\omega\in\Omega}\sum_{s\in\mathcal{S}} \left(\frac{\sum_{j\in\mathcal{K}}\sum_{n\in\mathcal{N}} M_{sj}^{(\omega)}\; z_{nsj}^{(\omega)}\; l_{nj}}{\sum_{j\in\mathcal{K}} M_{sj}^{(\omega)}} \right) \right\} \tag{7.10}$$

$$\text{subject to: } \Pr\left\{\tilde{\gamma}_s \geq T_s\right\} \geq \eta_s, \;\; \forall s \in \mathcal{S} \tag{7.11}$$

$$\sum_{s\in\mathcal{S}}\sum_{k\in\mathcal{K}} y_{nsk} \leq B_n, \;\; \forall n \in \mathcal{N} \tag{7.12}$$

$$x_n = \mathbb{1}_{\left\{\sum_{s\in\mathcal{S}}\sum_{k\in\mathcal{K}} y_{nsk} \geq 1\right\}}, \;\; \forall n \in \mathcal{N} \tag{7.13}$$

$$z_{nsj}^{(\omega)} \leq M_{sj}^{(\omega)}\; H_{nkj}^{(\omega)}\; y_{nsk}, \;\; \forall n \in \mathcal{N}, \forall k,j \in \mathcal{K}, \forall s \in \mathcal{S}, \forall \omega \in \Omega \tag{7.14}$$

$$\sum_{n\in\mathcal{N}} z_{nsj}^{(\omega)} = \mathbb{1}_{\left\{\sum_{n\in\mathcal{N}}\sum_{k\in\mathcal{K}} y_{nsk}\; M_{sj}^{(\omega)}\; H_{nkj}^{(\omega)} \geq 1\right\}}, \;\; \forall k,j \in \mathcal{K}, \forall s \in \mathcal{S}, \forall \omega \in \Omega \tag{7.15}$$

$$y_{nsk} \in \{0,1\}, \;\; \forall n \in \mathcal{N}, \forall s \in \mathcal{S}, \forall k \in \mathcal{K} \tag{7.16}$$

$$z_{nsj}^{(\omega)} \in \{0,1\}, \;\; \forall n \in \mathcal{N}, \forall s \in \mathcal{S}, \forall j \in \mathcal{K}, \forall \omega \in \Omega. \tag{7.17}$$

Note that if o^* and $\hat{o}$ are the optimal objective function values of Problem 7.1 and its SAA, respectively, then, it follows from the strong law of large numbers that as $|\Omega| \to \infty$, $\hat{o}$ converges to o^* exponentially fast with probability 1 [84]. This means that we can obtain a good solution of Problem 7.1 by solving its SAA with a modest sample size.

In order to solve the SAA of Problem 7.1, we first need to find a closed-form expression of $\mathbb{P}_{\text{cov}}$.

7.3.3 Coverage Probability

Theorem 7.1. *In the mmW virtual network deployment model described in Section 7.2.2, the downlink coverage probability achieved by the virtual network of SP $s, s \in \mathcal{S}$, is given by*

$$\Pr\left\{\tilde{\gamma}_s \geq T_s\right\} = 1 - \frac{1}{K}\sum_{j\in\mathcal{K}} m_{sj} \prod_{n\in\mathcal{N}}\prod_{k\in\mathcal{K}}\left[1 - y_{nsk}\left(P_{L_{nj}}\int_{T_s}^{\infty} f^{(j)}_{\gamma_{nk},L}(x)\,\mathrm{d}x + \left(1 - P_{L_{nj}}\right)\int_{T_s}^{\infty} f^{(j)}_{\gamma_{nk},NL}(x)\,\mathrm{d}x\right)\right] \tag{7.18}$$

(7.18), *where* $f^{(j)}_{\gamma_{nk},L}(.)$ *and* $f^{(j)}_{\gamma_{nk},NL}(.)$ *are the PDFs of the SNR in* (3.6) *for the LOS and NLOS cases, respectively.*

Proof. Note that if we point a beam of BS $n, n \in \mathcal{N}$, towards grid $k, k \in \mathcal{K}$, then the probability that this beam covers grid $j, j \in \mathcal{K}$, can be expressed as:

$$p^{(j)}_{nk} = P_{L_{nj}}\int_{T_s}^{\infty} f^{(j)}_{\gamma_{nk},L}(x)\,\mathrm{d}x + P_{NL_{nj}}\int_{T_s}^{\infty} f^{(j)}_{\gamma_{nk},NL}(x)\,\mathrm{d}x. \tag{7.19}$$

Now, the coverage probability achieved at grid $j, j \in \mathcal{K}$, from the beams of the BSs in $\mathcal{N}$ aimed towards the grids in $\mathcal{K}$ can be expressed as:

$$\mathbb{P}^{(j)}_{\mathrm{cov}} = 1 - \prod_{n\in\mathcal{N}}\prod_{k\in\mathcal{K}}\left(1 - y_{nsk}\, p^{(j)}_{nk}\right). \tag{7.20}$$

Next, note that for K number of grids in $\mathcal{K}$, the probability of selecting a grid $j, j \in \mathcal{K}$, is $\frac{1}{K}$. Furthermore, the probability of grid j has a mmW UE of SP s is m_{sj}. Therefore, we compute the unconditioned coverage probability taking the probability of an arbitrarily chosen UE is at grid $j, j \in \mathcal{K}$, into consideration as follows:

$$\Pr\left\{\tilde{\gamma}_s \geq T_s\right\} = \sum_{j\in\mathcal{K}} \frac{1}{K}\, m_{sj}\, \mathbb{P}^{(j)}_{\mathrm{cov}}. \tag{7.21}$$

By substituting the expression of (7.20) in (7.21) we obtain (7.18). □

7.3.4 Mixed Integer Linear Programming Reformulation

In this subsection, we discuss how to efficiently solve the SAA of Problem 7.1. Our solution approach is based on deriving an equivalent mixed integer linear programing (MILP) formulation of the SAA of Problem 7.1.

As can be seen in the SAA of Problem 7.1, constraint (7.11), (7.13), and (7.15) are nonlinear expressions of the decision variables $y_{nsk},\ \forall n \in \mathcal{N}, \forall s \in \mathcal{S}, \forall k \in \mathcal{K}$. The coverage probability expression in (7.18) has the term $\mathbb{P}^{(j)} \triangleq \prod_{n\in\mathcal{N}} \prod_{k\in\mathcal{K}} (1 - y_{nk}\ p_{nk}^{(j)})$, which is a nonlinear expression of the decision variables $y_{nsk},\ \forall n \in \mathcal{N}, \forall s \in \mathcal{S}, \forall k \in \mathcal{K}$. Expanding $\mathbb{P}^{(j)}$, we can see that the nonlinear terms in $\mathbb{P}^{(j)}$ are in the form of products of binary decision variables. For example, if $N = 2$ and $K = 2$, $\mathbb{P}^{(j)}$ can be expressed as:

$$\begin{aligned}\mathbb{P}^{(j)} = 1 - \sum_{k=1}^{2}\sum_{n=1}^{2} p_{nk}^{(j)}\ y_{nsk} + p_{12}^{(j)}\ p_{21}^{(j)}\ y_{1s2}\ y_{2s1} + p_{11}^{(j)}\ p_{22}^{(j)}\ y_{1s1}\ y_{2s2} + \sum_{n=1}^{2}\prod_{k=1}^{2} p_{nk}^{(j)}\ y_{nsk} \\ + \sum_{k=1}^{2}\prod_{n=1}^{2} p_{nk}^{(j)}\ y_{nsk} + \prod_{n=1}^{2}\prod_{k=1}^{2} p_{nk}^{(j)}\ y_{nsk} - p_{11}^{(j)}\ p_{12}^{(j)}\ p_{21}^{(j)}\ y_{1s1}\ y_{1s2}\ y_{2s1} \\ - p_{11}^{(j)}\ p_{12}^{(j)}\ p_{22}^{(j)}\ y_{1s1}\ y_{1s2}\ y_{2s2} - p_{11}^{(j)}\ p_{21}^{(j)}\ p_{22}^{(j)}\ y_{1s1}\ y_{2s1}\ y_{2s2} \\ - p_{12}^{(j)}\ p_{21}^{(j)}\ p_{22}^{(j)}\ y_{1s2}\ y_{2s1}\ y_{2s2}. \qquad (7.22)\end{aligned}$$

A product of binary decision variables, say $\prod_{n=1}^{N} y_{nsk}$, can be equivalently expressed in a linear form by (i) introducing a new auxiliary non-negative decision variable, say y_k, (ii) replacing $\prod_{n=1}^{N} y_{nsk}$ by y_k, and (iii) adding the following constraints:

$$y_k \leq y_{nsk}, \forall n \in \{1, 2, \cdots, N\}, \quad y_k \geq \sum_{n=1}^{N} y_{nsk} - (N-1), \quad y_k \geq 0. \qquad (7.23)$$

In order to linearize constraint (7.13), we reformulate the indicator function as follows:

- If $\sum_{k\in\mathcal{K}} y_{nsk} \geq 1$ then $x_n = 1$ can be reformulated as:

$$\sum_{s\in\mathcal{S}}\sum_{k\in\mathcal{K}} y_{nsk} - (U+\epsilon)\, x_n \leq 1-\epsilon \tag{7.24}$$

  where U is an upper bound of $\sum_{k\in\mathcal{K}} y_{nsk} - 1$ and $\epsilon > 0$ is a small tolerance beyond which we regard the constraint as having been broken. Selecting U and ϵ to be $B_n - 1$ and 1, respectively, (7.24) reduces to $\sum_{s\in\mathcal{S}}\sum_{k\in\mathcal{K}} y_{nsk} \leq B_n\, x_n$.

- If $x_n = 1$ then $\sum_{k\in\mathcal{K}} y_{nsk} \geq 1$ can be reformulated as:

$$\sum_{s\in\mathcal{S}}\sum_{k\in\mathcal{K}} y_{nsk} + L\, x_n \geq L+1 \tag{7.25}$$

  where L is a lower bound of $\sum_{k\in\mathcal{K}} y_{nsk} - 1$. Selecting L to be -1, (7.25) reduces to $\sum_{k\in\mathcal{K}} y_{nsk} \geq x_n$. Note that this condition is equivalent to $\sum_{k\in\mathcal{K}} y_{nsk} = 0 \Rightarrow x_n = 0$, which is already enforced by the objective function, since it aims at minimizing the number of mmW BSs. Hence, (7.25) is redundant.

Therefore,

$$x_n = \mathbb{1}_{\left\{\sum_{s\in\mathcal{S}}\sum_{k\in\mathcal{K}} y_{nsk} \geq 1\right\}} \Leftrightarrow x_n \leq \sum_{s\in\mathcal{S}}\sum_{k\in\mathcal{K}} y_{nsk} \leq B_n\, x_n, \forall n \in \mathcal{N}. \tag{7.26}$$

Similarly, constraint (7.15) can be linearized as:

$$M_{sj}^{(\omega)} \geq \sum_{n\in\mathcal{N}} z_{nsj}^{(\omega)} \geq \frac{\sum_{n\in\mathcal{N}}\sum_{k\in\mathcal{K}} y_{nsk}\; M_{sj}^{(\omega)}\; H_{nkj}^{(\omega)}}{NK}, \forall j \in \mathcal{K}, \forall s \in \mathcal{S}, \forall \omega \in \Omega, \tag{7.27}$$

where N and K are the cardinality of sets $\mathcal{N}$ and $\mathcal{K}$, respectively.

In this way, we can express the coverage probability in (7.18) as a linear function of the decision variables. Thus, we reformulate the SAA of Problem 7.1 as an MILP. We solve the

MILP using CPLEX.

Thus far, we have discussed how to optimally solve the SAA of Problem 7.1. As we have stated earlier, the optimality gap between the objective function values of Problem 7.1 and the SAA of Problem 7.1 depends on the total number of scenarios considered in the SAA framework. In the following subsection, we statistically estimate the optimality gap of the solution of the SAA of Problem 7.1 obtained from a set of scenarios of size $|\Omega|$.

7.3.5 Statistical Estimation of the Optimality Gap of SAA Solutions

Lemma 7.2. *A set of solutions obtained from the SAA of Problem 7.1 is a subset of the feasible solutions of Problem 7.1.*

Proof. Note that while deriving the SAA of Problem 7.1, the chance constraint in (7.2) is formulated using the true probability distributions of the mmW UE occupancy of grids and the received SNR (i.e., considering all possible realizations of the mmW UE occupancy of grids and the received SNR). Therefore, the solutions of the first-stage decision variables x_n and $y_{nsk}, \forall n \in \mathcal{N}, \forall s \in \mathcal{S}, \forall k \in \mathcal{K}$, obtained from the SAA of Problem 7.1 (or the decomposed version of Problem 7.1) are feasible solutions of Problem 7.1.

Let $\hat{\boldsymbol{x}}$ and $\hat{\boldsymbol{y}}$ be feasible solutions of Problem 7.1 obtained by solving the SAA of Problem 7.1. For the first-stage decisions $\hat{\boldsymbol{y}}$, let $\mathcal{Z}$ be the set of feasible solutions of the second-stage decisions variables $z_{nsk}, \forall n \in \mathcal{N}, \forall s \in \mathcal{S}, \forall k \in \mathcal{K}$, of Problem 7.1. Now, for the first-stage decisions $\hat{\boldsymbol{y}}$, let $\hat{\boldsymbol{z}}^{(\Omega)}$ be the set of optimal solutions of the second-stage decision variables for a set of scenarios Ω obtained by solving the SAA of the second-stage of Problem 7.1 for the set of scenarios Ω. Since Ω contains a subset of all possible realizations of the mmW UE occupancy of grids and the received SNR, we have $\hat{\boldsymbol{z}}^{(\Omega)} \subseteq \mathcal{Z}$. Thus, a set

of solutions obtained from the SAA of Problem 7.1 is a subset of the feasible solutions of Problem 7.1. □

Statistical Upper Bound:

Note that in Problem 7.1, we aim to *minimize* the objective function value while satisfying constraints (7.2)-(7.9). Hence, for Problem 7.1, the objective function value evaluated at any feasible solution forms an upper bound to the optimal objective function value. Based on these observations, we can state the following lemma.

Lemma 7.3. *If o^* is the the optimal objective function value of Problem 7.1 and $\hat{o}$ is the optimal objective function value of the SAA of Problem 7.1 then, $\hat{o} \geq o^*$.*

From Lemma 7.3, we can obtain an upper bound of Problem 7.1 as follows. Consider we solve the SAA of Problem 7.1 with a scenario ω, $\omega \in \Omega$, and obtain the solutions of the first-stage decision variables $\hat{x}_n$ and $\hat{y}_{nsk}, \forall n \in \mathcal{N}, \forall s \in \mathcal{S}, \forall k \in \mathcal{K}$, and the second-stage decision variables $\hat{z}^{(\omega)}_{nsk}, \forall n \in \mathcal{N}, \forall s \in \mathcal{S}, \forall k \in \mathcal{K}$. Then, an upper bound of Problem 7.1 (say, $O^{(\omega)}$) can be expressed by evaluating the objective function value of its SAA for the scenario ω as:

$$O^{(\omega)} = \sum_{n \in \mathcal{N}} \hat{x}_n - q \left(\sum_{s \in \mathcal{S}} \frac{\sum_{j \in \mathcal{K}} \sum_{n \in \mathcal{N}} M^{(\omega)}_{js} \ \hat{z}^{(\omega)}_{nsj} \ l_{nj}}{\sum_{j \in \mathcal{K}} M^{(\omega)}_{js}} \right). \tag{7.28}$$

Now, we estimate the mean and the variance of the upper bound of Problem 7.1 as follows. Note that we can obtain the mean of the upper bound by solving the SAA for a set of scenarios Ω, and then evaluating the objective function value of the SAA. However, we usually consider a moderate number of scenarios to solve the SAA of Problem 7.1 in order to have an affordable computation complexity. This would result into a loose upper bound. To improve the tightness of the bound, we perform the following procedure. Consider we

solve the SAA of Problem 7.1 with a set of scenarios Ω and obtain the solutions of the first-stage decision variables $\hat{x}_n$ and $\hat{y}_{nsk}, \forall n \in \mathcal{N}, \forall s \in \mathcal{S}, \forall k \in \mathcal{K}$. Now, we generate a larger set of scenarios (say, Ω') where $|\Omega'| >> |\Omega|$. Then, with the first-stage solutions $\hat{x}_n$ and $\hat{y}_{nsk}, \forall n \in \mathcal{N}, \forall s \in \mathcal{S}, \forall k \in \mathcal{K}$, we solve the SAA of the second-stage of Problem 7.1 for the set of scenarios Ω'. Let the solutions of the second-stage decision variables be $\hat{z}^{(\omega)}_{nsj}, \forall n \in \mathcal{N}, \forall s \in \mathcal{S}, \forall j \in \mathcal{K}, \forall \omega \in \Omega'$. Then, we estimate the statistical upper bound of Problem 7.1 (say, $\bar{O}_{|\Omega|,\Omega'}$) by computing the objective function value of the SAA of Problem 7.1 for the set of scenarios Ω' with the solutions $\hat{y}_{nsk}, \hat{z}_{nsk}, \forall n \in \mathcal{N}, \forall j \in \mathcal{K}, \forall s \in \mathcal{S}, \forall \omega \in \Omega'$, as:

$$\bar{O}_{|\Omega|,\Omega'} = \frac{1}{|\Omega'|} \sum_{\omega \in \Omega'} O^{(\omega)} = \sum_{n \in \mathcal{N}} \hat{x}_n - q \, \frac{1}{|\Omega'|} \sum_{s \in \mathcal{S}} \sum_{\omega \in \Omega'} \left(\frac{\sum_{j \in \mathcal{K}} \sum_{n \in \mathcal{N}} M^{(\omega)}_{js} \; \hat{z}^{(\omega)}_{nsj} \; l_{nj}}{\sum_{j \in \mathcal{K}} M^{(\omega)}_{js}} \right). \quad (7.29)$$

The variance of the upper bound $\bar{O}_{\Omega,\Omega'}$ can be computed as:

$$\sigma^2_{|\Omega|,\Omega'} = \frac{1}{|\Omega'| \left(|\Omega'| - 1 \right)} \sum_{\omega \in \Omega'} \left(O^{(\omega)} - \bar{O}_{|\Omega|,\Omega'} \right)^2. \quad (7.30)$$

Statistical Lower Bound:

Note that the solutions obtained from the SAA of Problem 7.1 depends on the considered set of scenarios. Therefore, the optimal objective function value of the SAA of Problem 7.1 varies from one set of scenarios to another set of scenarios. Let $\mathbb{E}[\hat{o}]$ be the average of the optimal objective function values of the SAA of Problem 7.1 obtained from different sets of scenarios. Then, from [85], we know that $\mathbb{E}[\hat{o}] \leq o^*$, the optimal objective function value of Problem 7.1. Therefore, we can obtain a lower bound of Problem 7.1 as follows. Consider we solve the SAA of Problem 7.1 with a set of scenarios Ω and obtain the solutions of the first-stage decision variables $\hat{x}_n$ and $\hat{y}_{nsk}, \forall n \in \mathcal{N}, \forall s \in \mathcal{S}, \forall k \in \mathcal{K}$, and the second-stage decision variables $\hat{z}^{(\omega)}_{nk}, \forall n \in \mathcal{N}, \forall s \in \mathcal{S}, \forall k \in \mathcal{K}, \omega \in \Omega$. Then, a lower bound of Problem 7.1

(say, $o^{(\Omega)}$) can be expressed by evaluating the objective function value of its SAA for the set of scenarios Ω as:

$$o^{(\Omega)} = \sum_{n \in \mathcal{N}} \hat{x}_n - q \, \frac{1}{|\Omega|} \sum_{\omega \in \Omega} \sum_{s \in \mathcal{S}} \left(\frac{\sum_{j \in \mathcal{K}} \sum_{n \in \mathcal{N}} M_{js}^{(\omega)} \, \hat{z}_{nsj}^{(\omega)} \, l_{nj}}{\sum_{j \in \mathcal{K}} M_{js}^{(\omega)}} \right). \tag{7.31}$$

Then, we can obtain the mean and the variance of the lower bound of Problem 7.1 as follows. We generate a set $\mathcal{C} = \{\Omega_1, \Omega_2, \ldots, \Omega_C\}$ of independent sets of i.i.d. scenarios of the UE occupancy of grids and the received SNR from their distributions, described in Chapter 3, by Monte Carlo sampling. Each set of scenarios has the same cardinality $|\Omega|$. For each set of scenarios in $\mathcal{C}$, we solve the SAA of Problem 7.1. Let $\hat{o}_{|\Omega|}^{(c)}$, $c \in \mathcal{C}$, be the optimal objective function value of the SAA of Problem 7.1 for the set of scenarios Ω_c. Then, we estimate the statistical lower bound of Problem 7.1 (say, $\bar{o}_{|\Omega|,\mathcal{C}}$) and the variance of the lower bound $\bar{o}_{|\Omega|,\mathcal{C}}$ as:

$$\bar{o}_{|\Omega|,\mathcal{C}} = \frac{1}{C} \sum_{c \in \mathcal{C}} \hat{o}_{|\Omega|}^{(c)} \, , \quad \sigma^2_{|\Omega|,\mathcal{C}} = \frac{1}{C\,(C-1)} \sum_{c \in \mathcal{C}} \left(\hat{o}_{|\Omega|}^{(c)} - \bar{o}_{|\Omega|,\mathcal{C}} \right)^2 . \tag{7.32}$$

Optimality Gap:

After obtaining the mean and the variance of the upper and the lower bounds, we compute the upper bound of the optimality gap of the solution of the SAA of Problem 7.1 obtained from a set of scenarios of size $|\Omega|$ with a confidence of ρ (say, $\Delta_{|\Omega|,\rho}$) by applying the Central Limit Theorem as [85]:

$$\Delta_{|\Omega|,\rho} = \left(\bar{O}_{|\Omega|,\Omega'} - \bar{o}_{|\Omega|,\mathcal{C}} \right) + z_\rho \left(\sigma^2_{|\Omega|,\Omega'} + \sigma^2_{|\Omega|,\mathcal{C}} \right)^{\frac{1}{2}} , \tag{7.33}$$

where $z_\rho = \phi^{-1}\,(1-\rho)$, is the inverse cumulative distribution function of the standard normal distribution evaluated at $(1-\rho)$.

In this way, we can statistically estimate the quality of the solution of the SAA of Problem 7.1.

Now, note that the search space for the decision variables $y_{nsk}, n \in \mathcal{N}, s \in \mathcal{S}, k \in \mathcal{K}$, is 2^{NSK}, the search space for the auxiliary decision variables $x_n, n \in \mathcal{N}$, is 2^N, and the search space for the decision variables $z_{nsk}^{(\omega)}, n \in \mathcal{N}, s \in \mathcal{S}, k \in \mathcal{K}, \omega \in \Omega$, is $2^{NSK|\Omega|}$. This results a total search space of $2^{N+NSK(1+|\Omega|)}$ for the MILP of the SAA of Problem 7.1. Therefore, with a network of large number of candidate locations, N, large number of SPs S and grid points, K, it becomes computationally challenging to solve the MILP. This necessitates a suboptimal algorithm that can find good solutions with affordable computation complexity for large networks.

7.3.6 Benders Decomposition-based Sub-optimal Algorithm

One potential approach for solving large scale two-stage chance-constrained stochastic optimization problems with reasonable computation complexity is the Benders decomposition technique, also referred to as L-shaped method [86, 87]. The overall idea of the L-shaped method is to decompose a two-stage stochastic optimization problem into a master problem with only the first-stage decisions and sub-problems with only the second-stage decisions and solve the master and the sub-problems iteratively until the optimality gap is sufficiently reduced. Based on this idea, we design an iterative algorithm to solve the SAA of Problem 7.1 as follows. First, we decompose the two stages of Problem 7.1 into a master problem (the first-stage problem), and $|\Omega|$ sub-problems (the second-stage problems, one for each scenario), by introducing a new constraint (known as the Bender's cut constraint) in the first-stage problem. Now, in each iteration, first, the master problem is solved, and then based on the solutions of the master problem, the sub-problems are solved. With the solutions of the sub-problems, the cut constraint in the master problem is updated. After

that, we compute the optimality gap of the solutions obtained from the master problem and $|\Omega|$ sub-problems. In this way, the iterations are continued until the optimality gap is sufficiently reduced. Let us discuss these steps in details.

Problem Decomposition:

In iteration i, the master problem of Problem 7.1 can be written for a set of scenarios Ω as follows [86].

Master Problem of Problem 7.1

$$\underset{\substack{\{x_n, y_{nsk}, \psi_i^{(\omega)},\\ n\in\mathcal{N},\, k\in\mathcal{K},\, \omega\in\Omega\}}}{\text{minimize}} \left\{ \sum_{n\in\mathcal{N}} x_n - q\, \frac{1}{|\Omega|} \sum_{\omega\in\Omega} \psi_i^{(\omega)} \right\} \tag{7.34}$$

$$\text{subject to: } \Pr\left\{\tilde{\gamma}_s \geq T_s\right\} \geq \eta_s, \quad \forall s \in \mathcal{S} \tag{7.35}$$

$$\sum_{s\in\mathcal{S}} \sum_{k\in\mathcal{K}} y_{nsk} \leq B_n, \quad \forall n \in \mathcal{N} \tag{7.36}$$

$$x_n = \mathbb{1}_{\left\{\sum_{s\in\mathcal{S}} \sum_{k\in\mathcal{K}} y_{nsk} \geq 1\right\}}, \quad \forall n \in \mathcal{N} \tag{7.37}$$

$$\psi_i^{(\omega)} \leq \left(a_\iota^{(\omega)} \sum_{n\in\mathcal{N}} \sum_{k\in\mathcal{K}} y_{nsk} + b_\iota^{(\omega)} \right), \quad \forall \omega \in \Omega,\ \forall \iota \in \{1, 2, \ldots, i-1\}. \tag{7.38}$$

where (7.38) is the cut constraint and $a_\iota^{(\omega)}$ and $b_\iota^{(\omega)}$ are the cut coefficients in iteration ι. For the first iteration, the cut coefficients $a_0^{(\omega)}$ and $b_0^{(\omega)}$ are set to zero. From the next iterations, they are computed based on the solutions of the sub-problems. The cut constraint helps us to determine the first-stage decisions in the current iteration by considering all the solutions of the $|\Omega|$ sub-problems obtained in the previous iterations.

Let $\hat{x}_n^{(i)}$ and $\hat{y}_{nsk}^{(i)}, \forall n \in \mathcal{N}, \forall s \in \mathcal{S}, \forall k \in \mathcal{K}$, be the solutions obtained from the master problem in iteration i. Then, the sub-problem of Problem 7.1 can be written for scenario $\omega, \omega \in \Omega$, as follows.

Sub Problem of Problem 7.1

$$\underset{\substack{z_{nsj}^{(\omega)},\\ n\in\mathcal{N},j\in\mathcal{K}}}{\text{maximize}} \left\{ \sum_{s\in\mathcal{S}} \left(\frac{\sum_{j\in\mathcal{K}} \sum_{n\in\mathcal{N}} M_{js}^{(\omega)}\ z_{nsj}^{(\omega)}\ l_{nj}}{\sum_{j\in\mathcal{K}} M_{js}^{(\omega)}} \right) \right\} \tag{7.39}$$

$$\text{subject to: } z_{nsj}^{(\omega)} \leq M_{js}^{(\omega)}\ H_{nkj}^{(\omega)}\ \hat{y}_{nsk}^{(i)},\ \ \forall n \in \mathcal{N},\ \forall k,j \in \mathcal{K}, \forall s \in \mathcal{S},\ \forall \omega \in \Omega \tag{7.40}$$

$$\sum_{n\in\mathcal{N}} z_{nsj}^{(\omega)} \leq M_{js}^{(\omega)},\ \ \forall j \in \mathcal{K},\ \forall s \in \mathcal{S},\ \forall \omega \in \Omega \tag{7.41}$$

$$\sum_{n\in\mathcal{N}} z_{nsj}^{(\omega)} \geq \frac{\sum_{n\in\mathcal{N}} \sum_{k\in\mathcal{K}} \hat{y}_{nsk}^{(i)}\ M_{js}^{(\omega)}\ H_{nkj}^{(\omega)}}{NK},\ \ \forall j \in \mathcal{K},\ \forall \omega \in \Omega. \tag{7.42}$$

We linearize the objective function (7.34) and constraint (7.35) in the master problem by following the same procedure as described in Section 7.3.4, and then solve the linearized problems in CPLEX.

Cut Coefficients Computation:

Let us denote the optimal values of the dual variables corresponding to constraints (7.40), (7.41), and (7.42) of the sub-problem for scenario $\omega, \omega \in \Omega$, in iteration i by $\Lambda_{1_{nk}}^{(\omega)}, n \in \mathcal{N}, k \in \mathcal{K}$, $\Lambda_{2_j}^{(\omega)}, j \in \mathcal{K}$, and $\Lambda_{3_j}^{(\omega)}, j \in \mathcal{K}$, respectively. Then, the cut coefficients for scenario ω in iteration i, i.e., $a_i^{(\omega)}$ and $b_i^{(\omega)}$, can be expressed as [86]:

$$a_i^{(\omega)} = \sum_{s\in\mathcal{S}} \sum_{n\in\mathcal{N}} \sum_{k\in\mathcal{K}} \sum_{j\in\mathcal{K}} \Lambda_{1_{nk}}^{(\omega)}\ M_{js}^{(\omega)}\ H_{nkj}^{(\omega)} - \frac{1}{NK} \sum_{s\in\mathcal{S}} \sum_{k\in\mathcal{K}} \sum_{n\in\mathcal{N}} \sum_{j\in\mathcal{K}} \Lambda_{3_j}^{(\omega)}\ M_{js}^{(\omega)}\ H_{nkj}^{(\omega)} \tag{7.43}$$

$$b_i^{(\omega)} = \sum_{s\in\mathcal{S}} \sum_{j\in\mathcal{K}} \Lambda_{2_j}^{(\omega)}\ M_{js}^{(\omega)}. \tag{7.44}$$

Optimality Gap Computation:

Note that the cut constraint, i.e., constraint (7.38) in the master problem considers the optimal values of the dual variables of the sub-problems of the previous iterations. Hence, the objective function value of the master problem in the current iteration provides the lower bound of the SAA of Problem 7.1 [86, 87]. Therefore, the lower bound of the SAA of Problem 7.1 in iteration i, denoted by L_i, can be estimated from $\hat{x}_n^{(i)}, \forall n \in \mathcal{N}, \forall s \in \mathcal{S}, \forall k \in \mathcal{K}$, and $\hat{\psi}_i^{(\omega)}, \forall \omega \in \Omega$, the solution of the master problem in iteration i, as:

$$L_i = \sum_{n \in \mathcal{N}} \hat{x}_n^{(i)} - q \, \frac{1}{|\Omega|} \sum_{\omega \in \Omega} \hat{\psi}_i^{(\omega)}. \tag{7.45}$$

Next, note that the solution of the master problem $\hat{x}_n^{(i)}$ and $\hat{y}_{nsk}^{(i)}, \forall n \in \mathcal{N}, \forall s \in \mathcal{S}, \forall k \in \mathcal{K}$, is a feasible solution of the SAA of Problem 7.1. Furthermore, since we aim to minimize the objective function in the SAA of Problem 7.1, any of its feasible solutions can provide an upper bound. Hence, we compute the upper bound of the SAA of Problem 7.1 as follows. Let us denote the objective function value of the sub-problems in iteration i for scenario $\omega, \omega \in \Omega$, by $\hat{O}_i^{(\omega)}$. Then, the upper bound of the SAA of Problem 7.1 in iteration i, say U_i, can be estimated as [86]:

$$U_i = \sum_{n \in \mathcal{N}} \hat{x}_n^{(i)} - q \, \frac{1}{|\Omega|} \sum_{\omega \in \Omega} \hat{O}_i^{(\omega)}. \tag{7.46}$$

We summarize the steps of our Benders decomposition-based solution approach in Algorithm 7. As can be seen, in each iteration first, we solve the master problem and based on the solutions of the master problem, we solve the sub-problems for each scenarios in Ω. Based on the solutions of the master problem and the sub-problems, we compute the optimality gap. In this way, the iterations are continued until the optimality gap is reduced below the

desired threshold δ.

While implementing the algorithm in CPLEX, in iteration i, we add the following constraint to the master problem to prevent any oscillation between the lower and the upper bounds.

$$\left\{ \sum_{n \in \mathcal{N}} \hat{x}_n^{(i)} - q \, \frac{1}{|\Omega|} \, \sum_{\omega \in \Omega} \hat{\psi}_i^{(\omega)} \right\} \leq U_i \tag{7.47}$$

Algorithm 7 The Benders decomposition-based Approach for Solving Problem 7.1

Input: $\mathcal{N}$, $\mathcal{K}$, $l_{nk}, \forall n \in \mathcal{N}, \forall k \in \mathcal{K}$, $f_{\gamma_{nk}}^{(j)}(x), \forall n \in \mathcal{N}, \forall j, k \in \mathcal{K}$, $m_{sk}, \forall s \in \mathcal{S}, \forall k \in \mathcal{K}$, $P_{L_{nk}}, \forall n \in \mathcal{N}, \forall k \in \mathcal{K}$, Ω, δ.
Output: $\hat{x}_n, \hat{y}_{nsk}, \hat{z}_{nsk}^{(\omega)}, \forall n \in \mathcal{N}, \forall s \in \mathcal{S}, \forall k \in \mathcal{K}, \omega \in \Omega$.
Initialize: $L \leftarrow -\infty$, $U \leftarrow +\infty$, $a \leftarrow 0$, and $b \leftarrow 0$.
while $(U - L) > \delta$ Or $i \neq$ maximum limit **do**
    Solve the master problem and store the solutions in $\hat{x}_n$ and $\hat{y}_{nsk}, \forall n \in \mathcal{N}, \forall s \in \mathcal{S}, \forall k \in \mathcal{K}$.
    Solve the sub-problems with $\hat{y}_{nsk}, \forall n \in \mathcal{N}, \forall s \in \mathcal{S}, \forall k \in \mathcal{K}$ for each scenarios in Ω and store the solutions in $z_{nsk}^{(\omega)}, \forall n \in \mathcal{N}, \forall s \in \mathcal{S}, \forall k \in \mathcal{K}, \forall \omega \in \Omega$.
    Update the cut coefficients in constraint (7.38) of the master problem with (7.43) and (7.44).
    Store the objective function value of the master problem in O' and the objective function values of the sub-problems $\hat{O}^{(\omega)}, \forall \omega \in \Omega$.
    if $\left\{ \sum_{n \in \mathcal{N}} \hat{x}_n - q \, \frac{1}{|\Omega|} \sum_{\omega \in \Omega} \hat{O}^{(\omega)} \right\} < U$ **then**
        $U \leftarrow \left\{ \sum_{n \in \mathcal{N}} \hat{x}_n - q \, \frac{1}{|\Omega|} \sum_{\omega \in \Omega} \hat{O}^{(\omega)} \right\}$
    end if
    $L \leftarrow O'$
    $i \leftarrow i + 1$
end while

As can be seen in the master problem, the search space for the decision variables $y_{nsk}, n \in \mathcal{N}, s \in \mathcal{S}, k \in \mathcal{K}$, is 2^{NSK}, the search space for the auxiliary decision variables $x_n, n \in \mathcal{N}$, is 2^N, and the search space for the auxiliary decision variables $\psi_i^{(\omega)}, \omega \in \Omega$, is $2^{|\Omega|}$. This

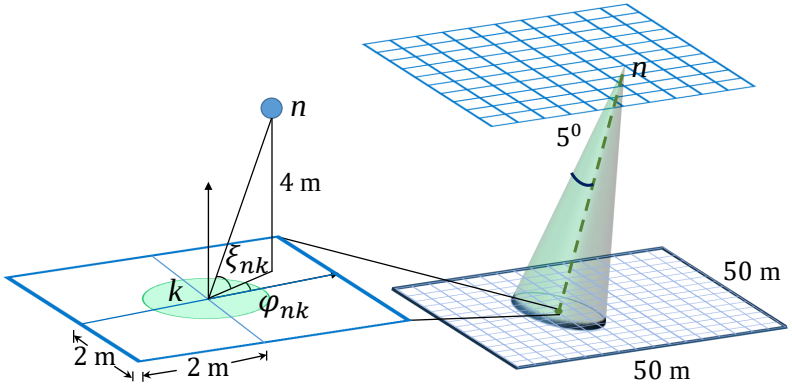

Figure 7.1: BS deployment architecture.

results in a total search space of $2^{N+NSK+|\Omega|}$ for the master problem. At the same time, the decision variables $z_{nsk}^{(\omega)}, n \in \mathcal{N}, s \in \mathcal{S}, k \in \mathcal{K}, \omega \in \Omega$, in the sub-problem for scenario ω have a search space of 2^{NSK}. Therefore, each iteration of Algorithm 7 has a search space of $(2^{N+NSK+|\Omega|}) + (|\Omega|\ 2^{NSK})$. Note that for large values of N and K, the search space of each iteration of Algorithm 7, $2^{NSK}\ \left(2^{N+|\Omega|} + |\Omega|\right) << 2^{NSK}\ (2^{N+NSK|\Omega|})$, i.e., the total search space of the monolithic (i.e., non-decomposed) MILP of the SAA of Problem 7.1. Therefore, by limiting the number of iterations in Algorithm 7, i.e., sacrificing the optimality, we can solve the SAA of Problem 7.1 for large networks with reasonable computation complexity.

7.4 Performance Evaluation

In this section, we evaluate the performance of our proposed indoor mmW network deployment and adaptive UE assignment scheme. We implement our proposed framework using Visual C++, CPLEX, and MATLAB.

7.4.1 Evaluation Setup

We consider an open indoor environment, such as a cafeteria space. The mmW BSs are to be mounted on the ceiling as shown in Figure 7.1. There are 100 potential access point

locations on the ceiling, arranged in a 10×10 square configuration. The height of the ceiling is assumed to be 4 m. The floor is 50×50 m^2. The floor is divided into 625 grid squares, each 2m $\times$ 2m. The number of beams that a mmW BS can have is set to 7. The channel parameters are set to the values described in [88]. Noise power spectral density is set to -114 dBm/Hz. The probability of LOS, $P_{L_{nj}}, n \in \mathcal{N}, j \in \mathcal{K}$, is given by $\exp(-0.01 d_{nj})$, where d_{nj} is the distance between BS n and grid j in meters [64]. We consider there is an SP who wish to provide mmW services in the considered geographical area. The SP wants a probabilistic guarantee β for an SNR threshold of -5 dB. The beam assignment time slot T is set to 100 milliseconds. The failure rates of the mmW beams, $\nu_{nk}, n \in \mathcal{N}, k \in \mathcal{K}$, are selected from a uniform distribution ranging from 0.05 to 0.1. The tradeoff factor (q) is set to 1 unless mentioned otherwise. Two different mmW UE distributions are considered: (i) uniform distribution [89] and (ii) log-normal distribution [90].

While linearizing $\mathbb{P}^{(j)}$, we assumed that, for each mmW UE, there are only four beams that can cover it. These four beams are taken to be the best (most available) mmW BS-UE beams (i.e., beams with the highest $p_{nk}^{(j)}$ values for a given j).

7.4.2 Evaluation of the SAA Framework

In this experiment, we evaluate the proposed SAA framework in terms of finding good solutions of Problem 7.1. Specifically, we study the optimality gap of the SAA of Problem 7.1 with respect to the number of scenarios considered to solve the SAA. We compute the optimality gap following the procedure described in Section 7.3.5. We set $|\mathcal{C}|$ to 50, $|\Omega'|$ to 10^5, and the confidence interval ρ to 0.9.

In Figures 7.2 and 7.3, we plot the number of required mmW BSs and the corresponding optimality gap with increasing number of scenarios considered to solve the SAA of Problem 7.1. In these figures, the mmW UEs are assumed to be distributed according to the

log-normal distribution. It can be seen, as the number of scenarios increases, the number of required mmW BSs increases and the optimality gap decreases. That is expected since a large set of scenarios includes the scenarios with bad channel conditions and dense mmW UE occupancy. This requires the optimizer to activate more mmW links to maximize the average stability of mmW beams assigned to mmW UEs in the large set of scenarios. Furthermore, note that as the number of scenarios increases, the sampling error (difference between the true distribution and the sampled distribution) decreases which reduces the optimality gap. However, when the considered set of scenarios is sufficient to closely represent the true distributions of the mmW UE occupancy of grids and the received SNR, increasing the number of scenarios does not significantly increase the number of required mmW BSs or reduce the optimality gap. In addition, note that ensuring high coverage probability β helps us to obtain good solutions with a smaller number of scenarios. This is due to the fact that we derived the chance constraint considering the true distributions of the mmW UE occupancy of grids and the received SNR. As a result, when β is sufficiently high, the set of mmW BSs required to satisfy the chance constraint makes sufficient mmW beams available to mmW UEs in any arbitrary set of scenarios, which gives us sufficient choices for assigning a mmW link to each mmW UE.

Figures 7.4 and 7.5 are similar to Figures 7.2 and 7.3, but assuming the MmW UEs to be uniformly distributed. Both figures show similar trends. However, the number of the required mmW BSs is higher and the optimality gap reduces slowly with increasing number of scenarios when the mmW UEs are distributed uniformly. In the case of log-normal distribution, mmW UEs are clustered geographically (in contrast to the case of uniform distribution). When the mmW UEs are clustered, we can cover almost all the mmW UEs by optimally pointing the fixed directional beams towards the clusters. As a result, we obtain good solutions with smaller number of mmW BSs.

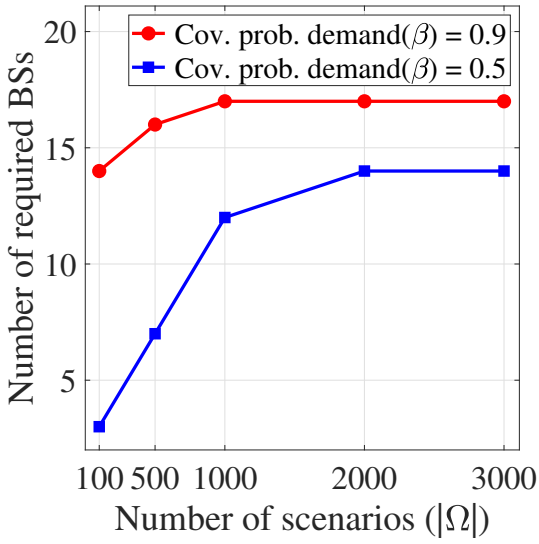

Figure 7.2: Number of required mmW BSs vs. number of scenarios considered to solve the SAA of Problem 7.1 for log-normally distributed mmW UEs.

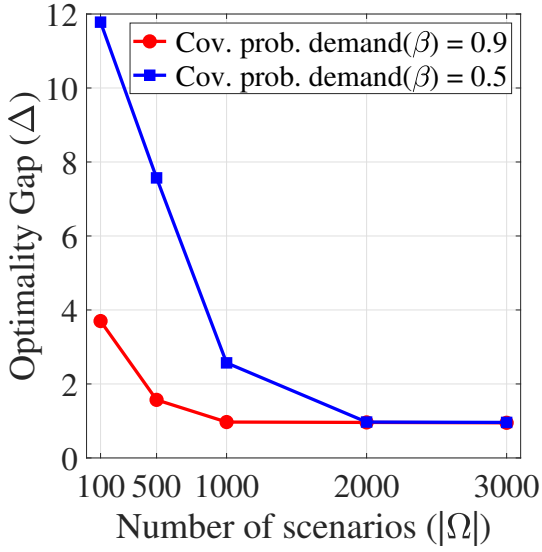

Figure 7.3: Optimality gap vs. number of scenarios considered to solve the SAA of Problem 7.1 for log-normally distributed mmW UEs.

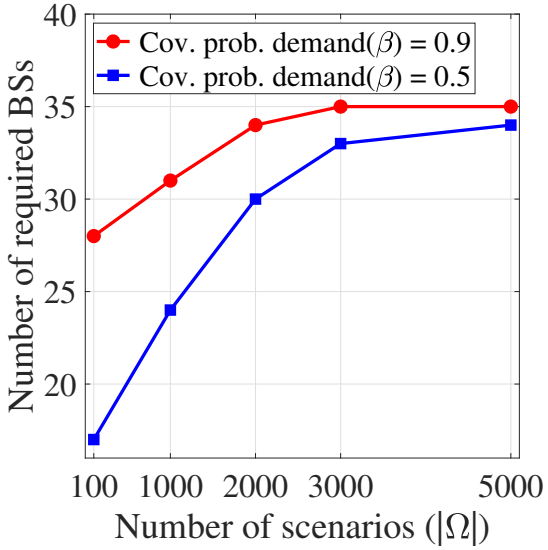

Figure 7.4: Number of required mmW BSs vs. number of scenarios considered to solve the SAA of Problem 7.1 for uniformly distributed mmW UEs.

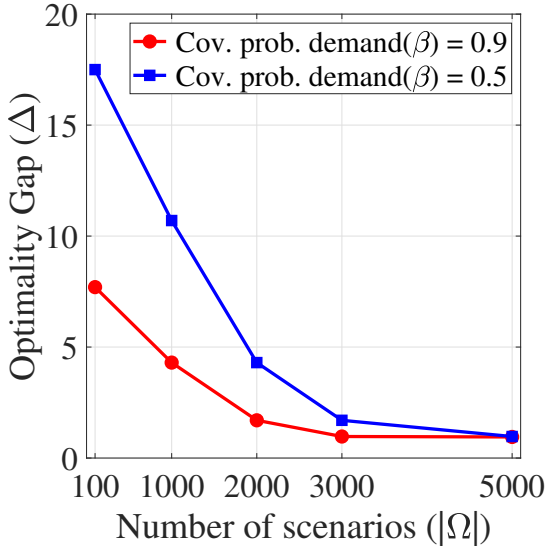

Figure 7.5: Optimality gap vs. number of scenarios considered to solve the SAA of Problem 7.1 for uniformly distributed mmW UEs.

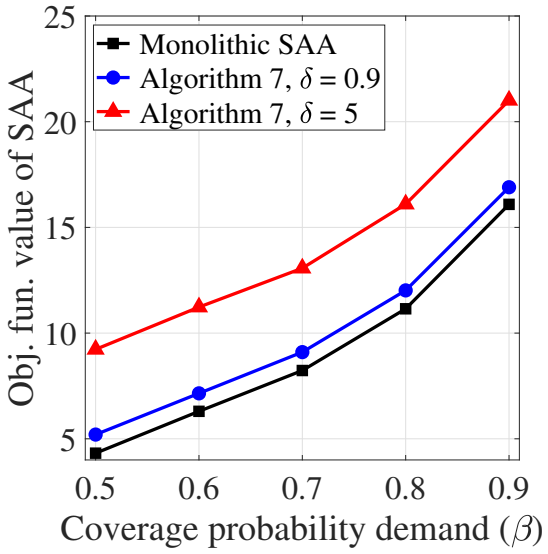

Figure 7.6: Objective function value of the SAA of Problem 7.1, i.e., (7.10) vs. minimum coverage probability for log-normally distributed mmW UEs and different values of tolerance (δ) in Algorithm 7.

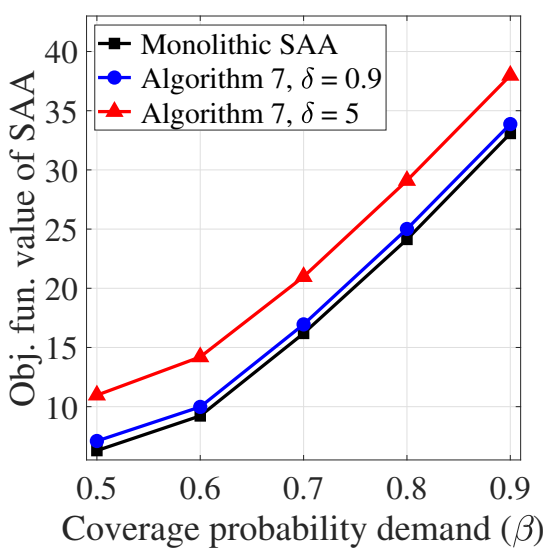

Figure 7.7: Objective function value of the SAA of Problem 7.1, i.e., (7.10) vs. minimum coverage probability for uniformly distributed mmW UEs and different values of tolerance (δ) in Algorithm 7.

From Figure 7.3, we can see that when mmW UEs are distributed following the log-normal distribution, the sufficient number of scenarios required to obtain good solutions is 2000. Similarly, from Figure 7.5, we can see that when mmW UEs are distributed uniformly, the sufficient number of scenarios required to obtain good solutions is 3000. Therefore, in the rest of the evaluations, we use these two sets of scenarios to solve the SAA of Problem 7.1 for the respective mmW UE distributions.

7.4.3 Evaluation of Algorithm 7

In this subsection, we evaluate the performance of Algorithm 7 for solving the SAA of Problem 7.1 compare to the monolithic solution approach.

In Figures 7.6 and 7.7, we plot the objective function value of the SAA of Problem 7.1, i.e., (7.10) with increasing coverage probability demand (β) for different values of the allowed

tolerance level (δ) in Algorithm 7. It can be seen, as the tolerance level δ decreases performance gap between Algorithm 7 and monolithic SAA decreases. This shows the efficiency of Algorithm 7 in terms of finding good solutions of the SAA of Problem 7.1.

In Figures 7.8 and 7.9, we plot the required CPU time to solve the SAA of Problem 7.1 with increasing problem sizes, i.e., number of candidate mmW BS locations, for different values of δ. As can be seen that by increasing δ, i.e., sacrificing the optimality in Algorithm 7, we can reduce the required CPU time for solving the SAA of Problem 7.1. However, note that for small problem sizes, the monolithic approach is more efficient, i.e., produces optimal solution with lesser CPU time than Algorithm 7. This is due to the fact that the monolithic approach has a moderately large search space for small problem sizes. On the other hand, to achieve a small optimality gap δ, Algorithm 7 needs to go through numerous iterations and each iteration has a moderate search space. As a result, when the problem size is small, the monolithic approach obtains the optimal solution with lesser CPU time than Algorithm 7. However, as the problem size increases, the search space of the monolithic approach increases significantly compare to the individual search spaces of the master problem and the subproblems in Algorithm 7. This results into higher CPU time for the monolithic approach.

Next, we study the effect of the second-stage of Problem 7.1 on the required number of mmW BSs. Specifically, we vary the trade-off factor (q) in the SAA of Problem 7.1 and plot the required number of mmW BSs in Figures 7.10 and 7.11. It can be seen that the required number of mmW BSs increases with q. As q increases, it becomes less important for the optimizer to minimize the number of mmW BSs compared to maximize the stability of mmW beams assigned to mmW UEs. On the other hand, as q decreases, the importance of the second-stage problem decreases which makes the two-stage chance-constrained problem similar to a single-stage chance-constrained problem. As a result, with small values of q, the monolithic approach and Algorithm 7 performs the same, i.e., minimizes the number of

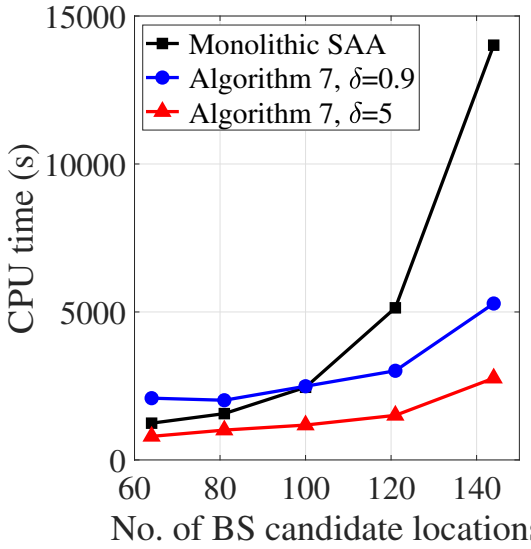

Figure 7.8: Required CPU time vs. number of candidate mmW BS locations for log-normally distributed mmW UEs and different values of the tolerance (δ) in Algorithm 7.

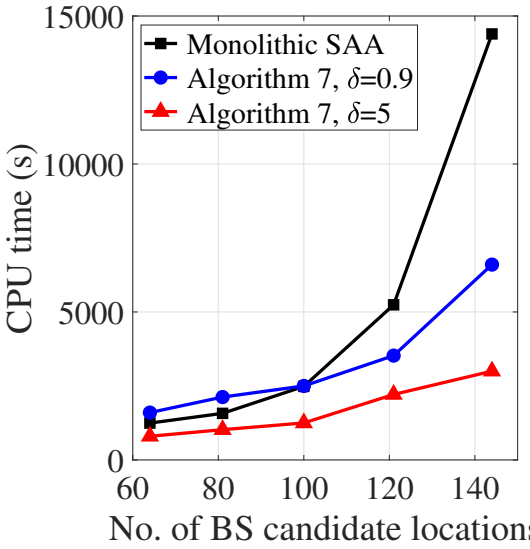

Figure 7.9: Required CPU time vs. number of candidate mmW BS locations for uniformly distributed mmW UEs and different values of the tolerance (δ) in Algorithm 7.

mmW BSs while satisfying the coverage probability demand β. Furthermore, note that the impact of q on the required number of mmW BSs reduces with β. When β is sufficiently high, the number of mmW BSs required to satisfy the chance constraint already brings the stability of mmW beams assigned to mmW UEs close to its maximum value. Hence, adding more mmW BSs does not improve the stability of mmW beams assigned to mmW UEs significantly.

7.4.4 Studying the Adaptive Beam Alignment Approach

In this subsection, we compare the network coverage obtained from the fixed directional beams to the network coverage that can be obtained from the adaptive beams in on our proposed framework. To conduct this evaluation, we consider a set of first-stage solutions, i.e., a set of mmW BSs and their fixed beam directions obtained from the monolithic approach in the previous evaluation with q set to 1. Let $\hat{x}_n, n \in \mathcal{N}$, denotes the set of mmW BSs and

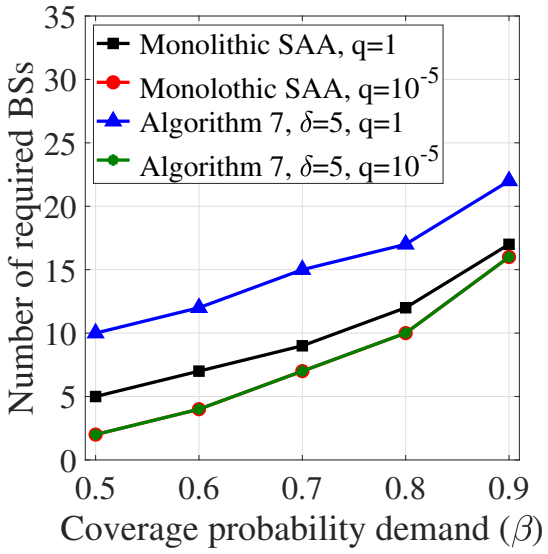

Figure 7.10: Number of required mmW BSs vs. minimum coverage probability for log-normally distributed mmW UEs and different values of q.

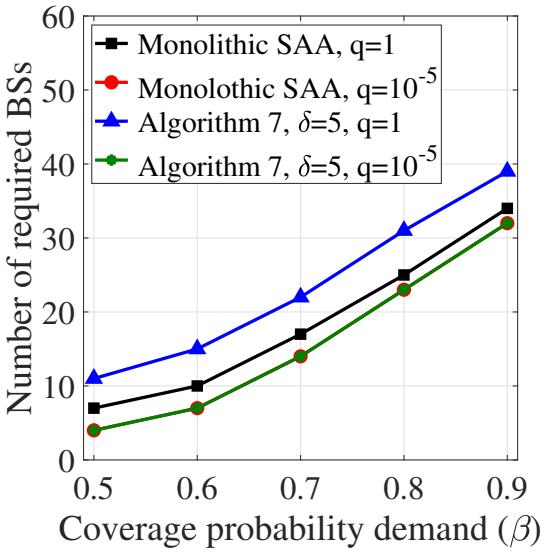

Figure 7.11: Number of required mmW BSs vs. minimum coverage probability for uniformly distributed mmW UEs and different values of q.

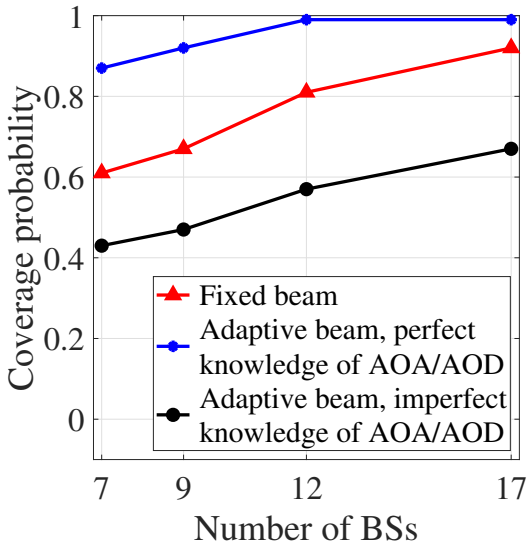

Figure 7.12: Coverage probability obtained vs. number of mmW BSs for log-normally distributed mmW UEs.

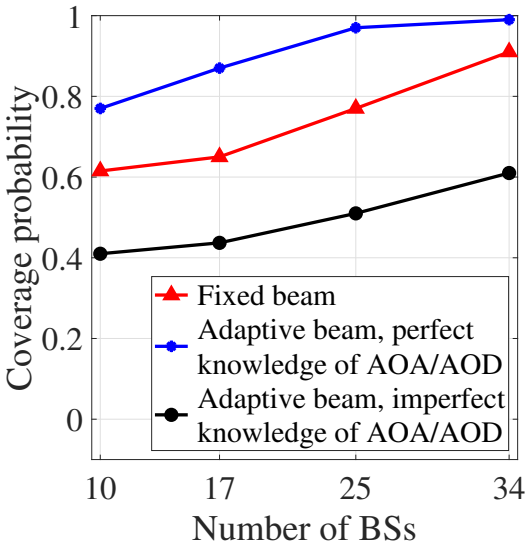

Figure 7.13: Coverage probability obtained vs. number of mmW BSs for uniformly distributed mmW UEs.

let $\hat{y}_{nk}, n \in \mathcal{N}, k \in \mathcal{K}$, be their fixed beam directions.

Now, we generate a new set of 1000 realizations of the mmW UE occupancy of grids

and the received SNR from their distributions, described in Section III, by Monte Carlo sampling. In this new set of scenarios (denoted by Ω'), we compute the coverage probability obtained from $\hat{x}_n, n \in \mathcal{N}$, and $\hat{y}_{nk}, n \in \mathcal{N}, k \in \mathcal{K}$. Specifically, in each scenario in Ω', we pick an mmW UE arbitrarily and compute the SNR obtained by the mmW UE based on $\hat{y}_{nk}, n \in \mathcal{N}, k \in \mathcal{K}$. Then, we estimate the coverage probability as the fraction of the scenarios where the arbitrarily selected mmW UEs obtain the SNR threshold τ.

Next, we perform the adaptive beam alignment in the set of scenarios Ω' with the set of mmW BSs in $\hat{x}_n, n \in \mathcal{N}$. Specifically, in each scenario in Ω', we sweep the beams of mmW BSs in $\hat{\boldsymbol{x}}$ over all the grid points in $\mathcal{K}$ to obtain the spatial directions (AoA/AoD) of UEs, and then determine the beam directions of mmW BSs. To perform this task, we introduce a new decision variable $y_{nk}^{(\omega)} \in \{0, 1\}, n \in \mathcal{N}, k \in \mathcal{K}, \omega \in \Omega'$, that indicates whether to steer a beam of mmW BS n to grid k in scenario ω or not. Then, in each scenario in Ω', we optimize $y_{nk}^{(\omega)}, \forall n \in \mathcal{N}, \forall k \in \mathcal{K}$, in order to maximize the number of mmW UEs covered with a minimum SNR of τ. After obtaining the beam alignment decisions $\hat{y}_{nk}^{(\omega)}, \forall n \in \mathcal{N}, \forall k \in \mathcal{K}, \forall \omega \in \Omega'$, we compute the coverage probability following the aforementioned procedure.

Now, note that in a real network, it is extremely challenging to know the AoA/AoD of mmW UEs. The imperfect knowledge of the AoA/AoD of mmW UEs introduces error (e.g., false positive cases) in adaptive beam alignment decisions. In that case, the adaptive beam alignment decisions can only ensure a probabilistic guarantee of coverage in a given scenario. For example, consider a beam of mmW BS n is steered towards grid k with an assumption of the presence of an mmW UE in grid k. The probability of grid k has an mmW UE is given by m_{sk}. Furthermore, the probability of the beam providing an SNR of at least τ at grid k is given by P_{nk}. In that case, the coverage probability obtained from $\hat{y}_{nk}^{(\omega)}, \forall n \in \mathcal{N}, \forall k \in \mathcal{K}$, the beam alignment decisions taken in scenario ω, in the presence of uncertainty in the knowledge of mmW UE occupancy of grids and SNR coverage can be computed from (7.18).

Now, to make a fair comparison, we compute the coverage probability obtained from the beam alignment decisions in each scenario in Ω', and then we compute the average coverage probability.

Figures 7.12 and 7.13 show the coverage probability obtained from the fixed-directional beams, the adaptive beams with perfect knowledge of the AoA/AoD of mmW UEs, and the adaptive beams with imperfect knowledge of the AoA/AoD of mmW UEs. As can be seen that the adaptive beams require the *perfect* knowledge of the AoA/AoD of mmW UEs to achieve a good coverage, whereas the fixed-directional beams can obtain a moderate coverage without any specific knowledge of the spatial directions of mmW UEs.

7.4.5 Comparison with Other MmW BS Deployment Schemes

In this subsection, we compare our proposed network deployment scheme with an existing mmW BS deployment scheme proposed in [40] where the mmW BSs are optimally placed to ensure a minimum RSS coverage at the grids without considering the mmW UE occupancy, channel conditions (e.g., LOS probability), and the potential beamforming gain at the grids. To conduct this evaluation, we use an RSS threshold (without beamforming gain) of -50 dB and the SNR threshold remains the same as -5 dB.

In Table 7.1-A, we compute the SNR coverage that can be obtained from the RSS-based mmW BS deployment scheme when the mmW BSs perform adaptive and fixed beam alignments. In this experiment, the mmW UEs are assumed to be distributed following the log-normal distribution. It can be seen, a large number of mmW BSs are deployed to achieve a RSS coverage without the potential beamforming gain. A large number of mmW BSs results a good SNR coverage when the beams are aligned adaptively based on the perfect knowledge of the AoA/AoD of mmW UEs (i.e., ideal case). However, the SNR coverage is significantly reduced when the mmW BSs do not have the perfect knowledge of the AoA/AoD

Table 7.1: Comparison between the RSS-based MmW BS deployment scheme and the proposed scheme with the log-normally distributed mmW UEs.

(A): RSS-based BS deployment

RSS coverage demand	Number of required BSs	SNR coverage obtained		
		Adaptive beams, perfect AoA/AoD	Adaptive beams, imperfect AoA/AoD	Fixed beams
85%	23	89.52%	44.67%	71.23%
90%	29	94.75%	51.11%	77.67%
95%	41	99.99%	77.5%	91.34%

(B): Proposed Scheme

SNR coverage demand	Number of required BSs
72%	10
78%	12
92%	18

of mmW UEs (i.e., realistic case). Furthermore, when the mmW BSs use fixed beams, they cannot achieve a good SNR coverage since the underlying channel conditions between mmW BSs and grids were not considered during the deployment. On the other hand, in Table 7.1-B, we present the number of mmW BSs required based on our proposed scheme to achieve a similar SNR coverage to that obtained in the RSS-based scheme with fixed beams. As can be seen that we are able to reduce the number of required mmW BSs up to 56% by optimally placing them and point their beams in optimal directions based on the distributions of the mmW UE occupancy of grids and the channel conditions.

In Table 7.2, we perform the similar experiment assuming that the mmW UEs are uniformly distributed. Both tables show similar trends. Note that the number of required mmW BSs remains the same in the RSS-based scheme since it does not consider the mmW UE occupancy of grids. However, in our proposed scheme, the number of required mmW BSs is lower when the mmW UEs are log-normally distributed compare to the case when they are uniformly distributed, due to the geographical clustering.

Table 7.2: Comparison between the RSS-based MmW BS deployment scheme and the proposed scheme with the uniformly distributed mmW UEs.

(A): RSS-based BS deployment

RSS coverage demand	Number of required BSs	SNR coverage obtained		
		Adaptive beams, perfect AoA/AoD	Adaptive beams, imperfect AoA/AoD	Fixed beams
85%	23	87.39%	38.34%	68.11%
90%	29	93.14%	49.67%	75.92%
95%	41	99.99%	71.28%	89.25%

(B): Proposed Scheme

SNR coverage demand	Number of required BSs
69%	16
76%	21
90%	34

7.5 Summary

In this chapter, we developed a two-stage chance-constrained stochastic optimization framework for mmW BS deployment, beam steering, and adaptive link assignment, considering the uncertainty in mmW UE locations and channel conditions. Our optimization criterion are: (i) minimizing the required number of mmW BSs and (ii) maximizing the stability of mmW links assigned to mmW UEs of SPs. Through simulations, we showed the gains brought by our proposed scheme in terms of minimizing resource over-provisioning in mmW virtual networks, e.g., our proposed scheme reduces the number of required mmW BSs up to 30% when the mmW UEs are uniformly distributed and up to 56% when the mmW UEs are log-normally distributed compare to the RSS-based scheme to achieve a similar downlink SNR coverage to that obtained in the RSS-based scheme with fixed beams. Furthermore, we showed the efficiency of Algorithm 7 in terms of finding good solutions of the optimization problem with reasonable computation complexity. In addition, our results indicate the followings. First, mmW BSs with the adaptive downlink beams require perfect knowledge of

the spatial directions of mmW UEs to provide a good coverage, whereas the same number of mmW BSs with the fixed-directional downlink beams can provide a moderate coverage without the knowledge of the spatial directions of mmW UEs. Second, ensuring high coverage probability in the network deployment stage helps us to assign stable mmW beams to mmW UEs in the link assignment stage. Finally, the number of mmW BSs required to achieve a certain coverage is lower when the mmW UEs are log-normally distributed compare to the case when they are uniformly distributed, due to the geographical clustering.

Chapter 8

Conclusion and Future Works

In this dissertation, we study research problems on enabling virtualization and mmW technologies in cellular networks. In the first chapter, we have provided the motivations and backgrounds of the two technologies and presented the potential deployment architecture for enabling them in cellular networks. Then, in Chapter 2, we have reviewed the existing literature and identified the key shortcomings of the existing schemes. We aimed to address these shortcomings and develop efficient frameworks to enable virtualization and mmW technologies in cellular networks. Specifically, in Chapter 3, we have presented our system model where we have described the UE distribution model, the sub-6 GHz and mmW channel models, and the UE association model that we have used to develop the frameworks. In Chapter 4, we have provided the first expression for the downlink RCP of a sub-6 GHz cellular network with known BS locations and stochastic UE locations and channel conditions. We have shown that by stochastically modeling the sub-6 GHz BS locations, we would underestimate the true achievable downlink RCP. In other words, if we would build the virtual networks by stochastically modeling the BS locations, we would over-provision significant amount of sub-6 GHz resources. Then, with the closed-form expression of the downlink RCP, in Chapter 5, we have provided a chance-constrained sub-6 GHz virtual resource allocation framework. The proposed framework allocates sub-6 GHz vritual resources to SPs in order to meet their sub-6 GHz downlink RCP demands while minimizing resource over-provisioning in the presence of uncertainty in UE locations and channel conditions with

reasonable computation complexity. Furthermore, considering the possibility of lack of sufficient sub-6 GHz network resources to satisfy the sub-6 GHz RCP demands of all SPs, we have designed a prioritized virtual resource allocation scheme where virtual networks are built sequentially based on their given priorities. Our results demonstrate that the proposed stochastic virtualization framework minimizes resource over-provisioning and outperforms existing deterministic virtualization frameworks in terms of probabilistically satisfying SPs' sub-6 GHz RCP demands. To further improve resource utilization, in Chapter 6, we have developed a joint stochastic optimization framework for sub-6 GHz virtual resource allocation and adaptive statistical multiplexing. The proposed framework has two phases: virtual network deployment (static) and statistical multiplexing (adaptive). In the virtual network deployment phase, sub-6 GHz BSs are aggregated, sliced, and allocated to the SPs considering the presence of uncertainty in UE locations and channel conditions, i.e., without knowing which realization of UE locations and channel conditions will occur. Once the virtual networks are deployed, each of the aggregated sub-6 GHz BSs performs statistical multiplexing, i.e., allocates excess resources from the over-satisfied slices to the under-satisfied slices, according to the realized channel conditions of associated UEs. Finally, in Chapter 7, we have developed an efficient framework for mmW virtual network deployment. The proposed framework jointly determines the optimal set of mmW BSs to deploy (or aggregate) and their beam directions to probabilistically satisfy SPs' mmW coverage demands in the presence of uncertainty in UE locations and channel conditions and adaptively assign the stable mmW beams to UEs according to the realized UE locations and channel conditions. The numerical results showed the gains brought by our proposed scheme in terms of minimizing resource over-provisioning while ensuring network-wide coverage in mmW virtual networks.

As an outcome of these contributions, this dissertation led us to the following publications.

8.1 List of Publications

8.1.1 Journal Articles

1. S. Chatterjee, M. J. Abdel-Rahman, and A. B. MacKenzie, "A Joint Optimization Framework for Enabling Virtualization with Statistical Multiplexing in Cellular Networks," *submitted to IEEE Transactions on Wireless Communication.*
2. S. Chatterjee, M. J. Abdel-Rahman, and A. B. MacKenzie, "A Joint Optimization Framework for Network Deployment and Adaptive User Assignment in Indoor Millimeter Wave Networks," *submitted to IEEE Transactions on Wireless Communication.*
3. S. Chatterjee, M. J. Abdel-Rahman, and A. B. MacKenzie, "On Optimal Orchestration of Virtualized Cellular Networks with Downlink Rate Coverage Probability Constraints," *IEEE Transactions on Wireless Communication*, vol. 19, no. 7, pp. 4378-4393, 2020.
4. M. M. Gomez, S. Chatterjee, M. J. Abdel-Rahman, A. B. MacKenzie, BH Martin, and Luiz DaSilva, "Market-Driven Stochastic Resource Allocation Framework for Wireless Network Virtualization," *IEEE Systems Journal*, vol. 14, no. 1, pp. 489-499, 2019.
5. S. Chatterjee, M. J. Abdel-Rahman, and A. B. MacKenzie, "Optimal Base Station Deployment with Downlink Rate Coverage Probability Constraint," *IEEE Wireless Communications Letters*, vol. 7, no. 3, pp. 340-343, 2018.

8.1.2 Conference Publications

1. S. Chatterjee, M. J. Abdel-Rahman, and A. B. MacKenzie, "Robust Access Point Deployment and User Assignment in Indoor Millimeter Wave Networks," *in Proceedings*

of the IEEE ICC Conference, pp. 1-6, 2020.

2. S. Chatterjee, M. J. Abdel-Rahman, and A. B. MacKenzie, "Virtualization Framework for Cellular Networks with Downlink Rate Coverage Probability Constraints", *in Proceedings of the IEEE GLOBECOM Conference*, pp. 1-6, 2018.

8.2 Future Works

The frameworks proposed in this dissertation can be extended in several directions.

8.2.1 Exploring Other QoS demands of SPs

In our proposed virtualization frameworks, we primarily focused on the rate and coverage demands of SPs. With advent of new 5G services, the importance of other QoS metrics such as, latency, jitter, and information age has been significantly increased. Taking this into consideration, one can extend our proposed frameworks with different types of QoS demands of SPs. In that case, the first challenge is to efficiently characterize the QoS demands of SPs. For example, latency demands of the SPs can be characterized based on Markov Queuing models. However, to the best of our knowledge, there is no such off-the-self statistical model available for characterizing jitter and information age demands of SPs. Therefore, an open problem is to efficiently characterize the different types of QoS demands of SPs. After that, the QoS demands need to be included in the optimization frameworks as constraints. Then, efficient algorithms need to be designed to solve the optimization problems.

8.2.2 End-to-End Slice

In this dissertation, we primarily focused on aggregating and slicing the Radio Access Network (RAN) components. The next step is to design efficient frameworks for aggregating and slicing core components (e.g., gateways) and combine them with our proposed frameworks to create end-to-end slices. An end-to-end slice can be viewed as a pipeline connecting

UEs to the services (e.g., data, PSTN) through RAN and core. The prospect and challenges of this joint framework is an interesting topic to explore.

8.2.3 Beam Tracking in MmW Virtual Networks

In Chapter 7, we developed a joint optimization framework for mmW virtual network deployment and adaptive UE assignment assuming that the mmW beams cannot be steered in real time. Consequently, UEs need to perform handovers to move from a footprint of a mmW BS to a footprint of another mmW BS. Due to the narrow beamwidth of mmW beams, UEs need to perform several handovers to move from one place to another place. In this context, a potential solution is to use adaptive mmW beams which can be steered in real time according to the instantaneous AoA/AoD of UEs. However, there are several technical challenges in designing adaptive mmW beams and developing the corresponding deployment frameworks. For example, to adaptively align transmit and receive beams, we need to adaptively adjust the transmit precoders and the receiver combiners [50]. This adjustment procedure is challenging by its very nature since it requires to solve a non-convex combinatorial optimization problem with NP-hard complexity. Besides, phase-shifters introduce calibration issues due to their limited adaptability (angle is quantized) [49]. Apart from the required hardware complexity, BSs need to efficiently estimate the spatial directions of individual UEs to adaptively steer the beams. These challenges need to be investigated thoroughly.

8.2.4 Hybrid Beamforming

Note that we developed the mmW virtual resource allocation framework assuming that the mmW BSs uses fixed-directional beams. A straightforward extension of the proposed framework is to study the similar problem assuming that the mmW BSs use hybrid (analog and digital) beams. In that case, we need to determine the optimal digital and analog precoding and combining metrics according to the realized UE locations and channel con-

ditions. Therefore, the two-stage optimization framework needs to be reformulated and efficient algorithms need to be designed to solve the problem.

8.2.5 Bringing WiFi into the Virtualization Architecture

In WNV, WiFi can play an important role to improve the performance of virtual networks by offloading the cellular traffics. However, when cellular networks and WiFi networks share spectrum, unfairness arises due to their different channel access mechanisms. For channel access, WiFi follows a carrier sense multiple access with collision avoidance (CSMA/CA) protocol where each WiFi transmitter senses the channel energy for a transmission opportunity, i.e. listen before talk (LBT) with a random backoff time. For cellular networks, each BS allocates frequencies and time slots to UE in a centralized fashion. Due to these different channel access mechanisms of cellular and WiFi (i.e. centralized and decentralized), it is likely that cellular would dominate WiFi when they share the same spectrum [91, 92, 93, 94, 95]. Therefore, an efficient coexistence protocol is needed to enable fair and harmonious spectrum sharing between these two technologies.

In search of harmonious coexistence, research has taken two approaches: LBT-based solutions (where cellular BS also performs LBT before accessing the channels [93, 94, 96]) and channel sensing (CS)-based solutions (where cellular BS senses the channel periodically and based on the sensed information about channel activity, takes action in the power domain [97, 98, 99] or in the frequency domain [98, 99, 100, 101, 102] or in the time domain [95, 100, 101, 103, 104, 105, 106, 107]). Such coexistence mechanisms need to be incorporated in cellular network virtualization frameworks. In addition, note that the slicing mechanism for WiFi network would be significantly different than the cellular network due to the LBT protocol. This necessitates a thorough investigation of the WiFi slicing mechanism and its fusion with the cellular network virualization frameworks.

Bibliography

[1] D. López-Pérez, M. Ding, H. Claussen, and A. H. Jafari, "Towards 1 Gbps/UE in Cellular Systems: Understanding Ultra-Dense Small Cell Deployments," *IEEE Communications Surveys & Tutorials*, vol. 17, no. 4, pp. 2078–2101, 2015.

[2] S. M. Greenstein and P. T. Spiller, "Modern Telecommunications Infrastructure and Economic Activity: An Empirical Investigation," *Industrial and Corporate Change*, vol. 4, no. 4, pp. 647–665, 1995.

[3] J. P. Doh, H. Teegen, and R. Mudambi, "Balancing Private and State Ownership in Emerging Markets' Telecommunications Infrastructure: Country, Industry, and Firm Influences," *Journal of International Business Studies*, vol. 35, no. 3, pp. 233–250, 2004.

[4] F. Fu and U. C. Kozat, "Stochastic Game for Wireless Network Virtualization," *IEEE Transactions on Networking*, vol. 21, no. 1, pp. 84–97, 2013.

[5] Q. Zhu and X. Zhang, "Bayesian-Game Based Power and Spectrum Virtualization for Maximizing Spectrum Efficiency Over Mobile Cloud-Computing Wireless Networks," in *Proceedings of the IEEE INFOCOM Workshops*, 2015, pp. 378–383.

[6] X. Chen, Z. Han, H. Zhang, G. Xue, Y. Xiao, and M. Bennis, "Wireless Resource Scheduling in Virtualized Radio Access Networks Using Stochastic Learning," *IEEE Transactions on Mobile Computing*, vol. 17, no. 4, pp. 961–974, 2018.

[7] S. A. Kazmi, N. H. Tran, T. M. Ho, and C. S. Hong, "Hierarchical Matching Game for

Service Selection and Resource Purchasing in Wireless Network Virtualization," *IEEE Communications Letters*, vol. 22, no. 1, pp. 121–124, 2018.

[8] T. M. Ho, N. H. Tran, L. B. Le, Z. Han, S. A. Kazmi, and C. S. Hong, "Network Virtualization With Energy Efficiency Optimization for Wireless Heterogeneous Networks," *IEEE Transactions on Mobile Computing*, vol. 18, no. 10, pp. 2386–2400, 2018.

[9] Z. Miao, Y. Wang, and Z. Han, "A Supplier-Firm-Buyer Framework for Computation and Content Resource Assignment in Wireless Virtual Networks," *IEEE Transactions on Wireless Communications*, vol. 18, no. 8, pp. 4116–4128, 2019.

[10] T. LeAnh, N. H. Tran, D. T. Ngo, and C. S. Hong, "Resource Allocation for Virtualized Wireless Networks with Backhaul Constraints," *IEEE Communications Letters*, vol. 21, no. 1, pp. 148–151, 2017.

[11] Z. Chang, Z. Han, and T. Ristaniemi, "Energy Efficient Optimization for Wireless Virtualized Small Cell Networks With Large-Scale Multiple Antenna," *IEEE Transactions on Communications*, vol. 65, no. 4, pp. 1696–1707, 2017.

[12] L. Doyle, J. Kibiłda, T. K. Forde, and L. DaSilva, "Spectrum Without Bounds, Networks Without Borders," *in Proceedings of the IEEE*, vol. 102, no. 3, pp. 351–365, 2014.

[13] T. S. Rappaport, S. Sun, R. Mayzus, H. Zhao, Y. Azar, K. Wang, G. N. Wong, J. K. Schulz, M. Samimi, and F. Gutierrez, "Millimeter Wave Mobile Communications for 5G Cellular: It Will Work!" *IEEE access*, vol. 1, pp. 335–349, 2013.

[14] "TS 38.101-2: NR; User Equipment (UE) Radio Transmission and Reception; Part 2: Range 2 Standalone," *3GPP*, 2020.

[15] P. Kall and S. W. Wallace, *Stochastic Programming*. Springer, 1994.

[16] D. P. Heyman and M. J. Sobel, *Stochastic Models in Operations Research: Stochastic Optimization*. Courier Corporation, 2004, vol. 2.

[17] K. Teague, M. J. Abdel-Rahman, and A. B. MacKenzie, "Joint Base Station Selection and Adaptive Slicing in Virtualized Wireless Networks: A Stochastic Optimization Framework," in *Proceedings of the IEEE ICNC Conference*, 1-6, 2019.

[18] A. Nabil, M. J. Abdel-Rahman, and A. B. MacKenzie, "Adaptive Channel Bonding in Wireless LANs Under Demand Uncertainty," in *Proceedings of the IEEE PIMRC Conference*, pp. 1–7, 2017.

[19] M. J. Abdel-Rahman, E. A. Mazied, K. Teague, A. B. MacKenzie, and S. F. Midkiff, "Robust Controller Placement and Assignment in Software-Defined Cellular Networks," in *Proceedings of the IEEE ICCCN Conference*, pp. 1–9, 2017.

[20] M. N. Soorki, M. J. Abdel-Rahman, A. MacKenzie, and W. Saad, "Joint Access Point Deployment and Assignment in mmWave Networks with Stochastic User Orientation," in *Proceedings of WiOpt International Workshop on Resource Allocation, Cooperation and Competition in Wireless Networks (RAWNET)*, pp. 1–6, 2017.

[21] M. J. Abdel-Rahman, E. A. Mazied, A. MacKenzie, S. Midkiff, M. R. Rizk, and M. El-Nainay, "On Stochastic Controller Placement in Software-Defined Wireless Networks," in *Proceedings of the IEEE WCNC Conference*, pp. 1–6, 2017.

[22] M. J. Abdel-Rahman, F. Lan, and M. Krunz, "Spectrum-efficient Stochastic Channel Assignment for Opportunistic Networks," in *Proceedings of the IEEE GLOBECOM Conference*, pp. 1272–1277, 2013.

[23] M. J. Abdel-Rahman and M. Krunz, "Stochastic Guard-Band-Aware Channel As-

signment with Bonding and Aggregation for DSA Networks," *IEEE Transactions on Wireless Communications*, vol. 14, no. 7, pp. 3888–3898, July 2015.

[24] N. Y. Soltani, S. J. Kim, and G. B. Giannakis, "Chance-Constrained Optimization of OFDMA Cognitive Radio Uplinks," *IEEE Transactions on Wireless Communications*, vol. 12, no. 3, pp. 1098–1107, March 2013.

[25] K. V. Cardoso, M. J. Abdel-Rahman, A. B. MacKenzie, and L. A. DaSilva, "Virtualization and Programmability in Mobile Wireless Networks: Architecture and Resource Management," in *Proceedings of the ACM SIGCOMM Workshop on Mobile Edge Communications (MECOMM)*, pp. 1–6, 2017.

[26] M. J. Abdel-Rahman, K. Cardoso, A. B. MacKenzie, and L. A. DaSilva, "Dimensioning Virtualized Wireless Access Networks from a Common Pool of Resources," in *Proceedings of the IEEE CCNC Conference*, pp. 1049–1054, 2016.

[27] M. J. Abdel-Rahman, M. AbdelRaheem, A. B. MacKenzie, K. Cardoso, and M. Krunz, "On the Orchestration of Robust Vrtual LTE-U Networks from Hybrid Half/Full-Duplex Wi-Fi APs," in *Proceedings of the IEEE WCNC Conference*, pp. 1–6, 2016.

[28] M. J. Abdel-Rahman, M. AbdelRaheem, and A. B. MacKenzie, "Stochastic Resource Allocation in Opportunistic LTE-A Networks with Heterogeneous Self-interference Cancellation Capabilities," in *Proceedings of the IEEE DySPAN Conference*, pp. 200–208, 2015.

[29] M. J. Abdel-Rahman, F. Al-Ogaili, M. A. Kishk, A. B. Mackenzie, P. C. Sofotasios, S. Muhaidat, and A. Nabil, "DBmmWave: Chance-constrained joint AP deployment and beam steering in mmWave networks with coverage probability constraints," *IEEE Networking Letters*, vol. 1, no. 4, pp. 151–155, 2019.

[30] A. Nabil, M. J. Abdel-Rahman, A. B. MacKenzie, and F. Hassan, "A Stochastic Optimization Framework for Channel Bonding in Wireless LANs Under Demand Uncertainty," *IEEE Transactions on Wireless Communications*, 2020.

[31] M. M. Gomez, S. Chatterjee, M. J. Abdel-Rahman, A. B. MacKenzie, M. B. H. Weiss, and L. DaSilva, "Market-Driven Stochastic Resource Allocation Framework for Wireless Network Virtualization," *IEEE Systems Journal*, vol. 14, no. 1, pp. 489–499, 2019.

[32] Q. Ye, W. Zhuang, S. Zhang, A.-L. Jin, X. Shen, and X. Li, "Dynamic Radio Resource Slicing for a Two-Tier Heterogeneous Wireless Network," *IEEE Transactions on Vehicular Technology*, vol. 67, no. 10, pp. 9896–9910, 2018.

[33] S. Parsaeefard, R. Dawadi, M. Derakhshani, and T. Le-Ngoc, "Joint User-Association and Resource-Allocation in Virtualized Wireless Networks," *IEEE Access*, vol. 4, pp. 2738–2750, 2016.

[34] S. Parsaeefard, R. Dawadi, M. Derakhshani, T. Le-Ngoc, and M. Baghani, "Dynamic Resource Allocation for Virtualized Wireless Networks in Massive-MIMO-Aided and Fronthaul-Limited C-RAN," *IEEE Transactions on Vehicular Technology*, vol. 66, no. 10, pp. 9512–9520, 2017.

[35] K. Wang, H. Li, F. R. Yu, W. Wei, and L. Suo, "Interference Alignment in Virtualized Heterogeneous Cellular Networks With Imperfect Channel State Information," *IEEE Transactions on Vehicular Technology*, vol. 66, no. 2, pp. 1519–1532, 2017.

[36] J. He, A. A. Verstak, L. T. Watson, C. A. Stinson, N. Ramakrishnan, C. A. Shaffer, T. S. Rappaport, C. R. Anderson, K. K. Bae, J. Jiang *et al.*, "Globally Optimal Transmitter Placement for Indoor Wireless Communication Systems," *IEEE Transactions on Wireless Communications*, vol. 3, no. 6, pp. 1906–1911, 2004.

[37] H. D. Sherali, C. M. Pendyala, and T. S. Rappaport, "Optimal Location of Transmitters for Micro-Cellular Radio Communication System Design," *IEEE Journal on Selected Areas in Communications*, vol. 14, no. 4, pp. 662–673, 1996.

[38] S. Chatterjee, M. J. Abdel-Rahman, and A. B. MacKenzie, "Optimal Base Station Deployment with Downlink Rate Coverage Probability Constraint," *IEEE Wireless Communications Letters*, vol. 7, no. 3, pp. 340–343, 2018.

[39] N. Palizban, S. Szyszkowicz, and H. Yanikomeroglu, "Automation of Millimeter Wave Network Planning for Outdoor Coverage in Dense Urban Areas Using Wall-Mounted Base Stations," *IEEE Wireless Communications Letters*, vol. 6, no. 2, pp. 206–209, 2017.

[40] I. Mavromatis, A. Tassi, R. J. Piechocki, and A. Nix, "Efficient Millimeter-Wave Infrastructure Placement for City-Scale ITS," in *Proceedings of the IEEE VTC Conference*, pp. 1–5, 2019.

[41] X. Wang, L. Kong, F. Kong, F. Qiu, M. Xia, S. Arnon, and G. Chen, "Millimeter Wave Communication: A Comprehensive Survey," *IEEE Communications Surveys & Tutorials*, vol. 20, no. 3, pp. 1–6, 2018.

[42] C. Jeong, J. Park, and H. Yu, "Random Access in Millimeter-Wave Beamforming Cellular Networks: Issues and Approaches," *IEEE Communications Magazine*, vol. 53, no. 1, pp. 180–185, 2015.

[43] Y. Li, J. G. Andrews, F. Baccelli, T. D. Novlan, and J. C. Zhang, "Performance Analysis of Millimeter-Wave Cellular Networks with Two-Stage Beamforming Initial Access Protocols," in *Proceedings of the Asilomar Conference on Signals, Systems and Computers*, pp. 1171–1175, 2016.

[44] A. Ali, N. González-Prelcic, and R. W. Heath, "Millimeter Wave Beam-Selection Using Out-of-Band Spatial Information," *IEEE Transactions on Wireless Communications*, vol. 17, no. 2, pp. 1038–1052, 2018.

[45] A. Klautau, N. González-Prelcic, and R. W. Heath, "LIDAR Data for Deep Learning-Based mmWave Beam-Selection," *IEEE Wireless Communications Letters*, vol. 8, no. 3, pp. 909–912, 2019.

[46] Y. Wang, M. Narasimha, and R. W. Heath, "MmWave Beam Prediction with Situational Awareness: A Machine Learning Approach," in *Proceedings of the IEEE International Workshop on Signal Processing Advances in Wireless Communications (SPAWC)Conference*, pp. 1–5, 2018.

[47] A. Klautau, P. Batista, N. González-Prelcic, Y. Wang, and R. W. Heath, "5G MIMO Data for Machine Learning: Application to Beam-Selection Using Deep Learning," in *Proceedings of the Information Theory and Applications Workshop (ITA)*, pp. 1–9, 2018.

[48] H. Hassanieh, O. Abari, M. Rodriguez, M. Abdelghany, D. Katabi, and P. Indyk, "Fast Millimeter Wave Beam Alignment," in *Proceedings of the ACM SIGCOMM Conference*, pp. 432–445, 2018.

[49] X. Yang, M. Matthaiou, J. Yang, C.-K. Wen, F. Gao, and S. Jin, "Hardware-Constrained Millimeter-Wave Systems for 5G: Challenges, Opportunities, and Solutions," *IEEE Communications Magazine*, vol. 57, no. 1, pp. 44–50, 2019.

[50] A. F. Molisch, V. V. Ratnam, S. Han, Z. Li, S. L. H. Nguyen, L. Li, and K. Haneda, "Hybrid Beamforming for Massive MIMO: A Survey," *IEEE Communications Magazine*, vol. 55, no. 9, pp. 134–141, 2017.

[51] Y. Li, F. Baccelli, J. G. Andrews, and J. C. Zhang, "Directional Cell Search Delay Analysis for Cellular Networks with Static Users," *IEEE Transactions on Communications*, vol. 66, no. 9, pp. 4318–4332, 2018.

[52] Z. Peng, L. Li, M. Wang, Z. Zhang, Q. Liu, Y. Liu, and R. Liu, "An Effective Coverage Scheme with Passive-Reflectors for Urban Millimeter-Wave Communication," *IEEE Antennas and Wireless Propagation Letters*, vol. 15, pp. 398–401, 2015.

[53] W. Khawaja, O. Ozdemir, Y. Yapici, I. Guvenc, and Y. Kakishima, "Coverage Enhancement for MmWave Communications using Passive Reflectors," in *Proceedings of the Global Symposium on Millimeter Waves (GSMM)*, pp. 1–6, 2018.

[54] S. Hiranandani, S. Mohadikar, W. Khawaja, O. Ozdemir, I. Guvenc, and D. Matolak, "Effect of Passive Reflectors on the Coverage of IEEE 802.11 ad MmWave Systems," in *Proceedings of the IEEE VTC Conference*, pp. 1–6, 2018.

[55] Y. Xu, H. S. Ghadikolaei, and C. Fischione, "Adaptive Distributed Association in Time-Variant Millimeter Wave Networks," *IEEE Transactions on Wireless Communications*, vol. 18, no. 1, pp. 459–472, 2018.

[56] A. Alizadeh and M. Vu, "Load Balancing User Association in Millimeter Wave MIMO Networks," *IEEE Transactions on Wireless Communications*, vol. 18, no. 6, pp. 2932 – 2945, 2019.

[57] Y. Liu, X. Fang, M. Xiao, and S. Mumtaz, "Decentralized Beam Pair Selection in Multibeam Millimeter-Wave Networks," *IEEE Transactions on Communications*, vol. 66, no. 6, pp. 2722–2737, 2018.

[58] H. Zhang, S. Huang, C. Jiang, K. Long, V. C. Leung, and H. V. Poor, "Energy Efficient User Association and Power Allocation in Millimeter-Wave-Based Ultra Dense

Networks with Energy Harvesting Base Stations," *IEEE Journal on Selected Areas in Communications*, vol. 35, no. 9, pp. 1936–1947, 2017.

[59] A. Mesodiakaki, F. Adelantado, L. Alonso, M. Di Renzo, and C. Verikoukis, "Energy- and Spectrum-Efficient User Association in Millimeter-Wave Backhaul Small-Cell Networks," *IEEE Transactions on Vehicular Technology*, vol. 66, no. 2, pp. 1810–1821, 2016.

[60] M. Polese, M. Giordani, M. Mezzavilla, S. Rangan, and M. Zorzi, "Improved Handover Through Dual Connectivity in 5G MmWave Mobile Networks," *IEEE Journal on Selected Areas in Communications*, vol. 35, no. 9, pp. 2069–2084, 2017.

[61] C. Skouroumounis, C. Psomas, and I. Krikidis, "Low-Complexity Base Station Selection Scheme in MmWave Cellular Networks," *IEEE Transactions on Communications*, vol. 65, no. 9, pp. 4049–4064, 2017.

[62] V. K. Gupta and G. S. Kasbekar, "Stability Analysis of Simple and Online User Association Policies for Millimeter Wave Networks," *arXiv preprint:1905.00237*, 2019.

[63] J. G. Andrews, F. Baccelli, and R. K. Ganti, "A Tractable Approach to Coverage and Rate in Cellular Networks," *IEEE Transactions on Communications*, vol. 59, no. 11, pp. 3122–3134, 2011.

[64] T. Bai, R. Vaze, and R. W. Heath, "Analysis of Blockage Effects on Urban Cellular Networks," *IEEE Transactions on Wireless Communications*, vol. 13, no. 9, pp. 5070–5083, 2014.

[65] S. K. Yoo, L. Zhang, S. L. Cotton, H. Q. Ngo, and W. G. Scanlon, "Ceiling-or Wall-Mounted Access Points: An Experimental Evaluation for Indoor Millimeter Wave

Communications," in *Proceedings of the European Conference on Antennas and Propagation (EuCAP)*, pp. 1–5, 2019.

[66] R. Ford, S. Rangan, E. Mellios, D. Kong, and A. Nix, "Markov Channel-based Performance Analysis for Millimeter Wave Mobile Networks," in *Proceedings of the IEEE WCNC Conference*, pp. 1–6, 2017.

[67] V. Pratt, "Factoring Heron," *The College Mathematics Journal*, vol. 40, no. 1, pp. 15–16, 2009.

[68] R. Pure and S. Durrani, "Computing Exact Closed-form Distance Distributions in Arbitrarily-shaped Polygons with Arbitrary Reference Point," *The Mathematica Journal*, vol. 17, pp. 1–27, 2015.

[69] A. Leon-Garcia, *Probability, Statistics, and Random Processes for Electrical Engineering*. Pearson/Prentice Hall 3rd ed. Upper Saddle River, NJ, 2008.

[70] S. Chatterjee, M. J. Abdel-Rahman, and A. B. MacKenzie, "Virtualization Framework for Cellular Networks with Downlink Rate Coverage Probability Constraints," in *Proceedings of the IEEE GLOBECOM Conference*, pp. 1–6, 2018.

[71] S. Chatterjee, M. J. Abdel-Rahman, and A. B. MacKenzie, "On Optimal Orchestration of Virtualized Cellular Networks with Downlink Rate Coverage Probability Constraints," *IEEE Transactions on Wireless Communication*, vol. 19, no. 7, pp. 4378–4393, 2020.

[72] J. van de Belt, H. Ahmadi, and L. E. Doyle, "Defining and Surveying Wireless Link Virtualization and Wireless Network Virtualization," *IEEE Communications Surveys & Tutorials*, vol. 19, no. 3, pp. 1603–1627, 2017.

[73] S. Melkote and M. S. Daskin, "Capacitated Facility Location/Network Design Problems," *European Journal of Operational Research*, vol. 129, no. 3, pp. 481–495, 2001.

[74] S. Boyd and L. Vandenberghe, *Convex Optimization*. Cambridge University Press, 2004.

[75] H. Amin, K. M. Curtis, and B. R. Hayes-Gill, "Piecewise Linear Approximation Applied to Nonlinear Function of a Neural Network," *IEE Proceedings-Circuits, Devices and Systems*, vol. 144, no. 6, pp. 313–317, 1997.

[76] P. M. Vaidya, "Speeding-up Linear Programming using Fast Matrix Multiplication," in *Proceedings of the IEEE Annual Symposium on Foundations of Computer Science*, pp. 332–337, 1989.

[77] O. Kramer, D. E. Ciaurri, and S. Koziel, "Derivative-free Optimization," *Computational optimization, Methods and Algorithms*, pp. 61–83, 2011.

[78] H. S. Dhillon, R. K. Ganti, F. Baccelli, and J. G. Andrews, "Modeling and Analysis of K-Tier Downlink Heterogeneous Cellular Networks," *IEEE Journal on Selected Areas in Communications*, vol. 30, no. 3, pp. 550–560, 2012.

[79] S. Chatterjee, M. J. Abdel-Rahman, and A. B. MacKenzie, "On Optimal Orchestration of Virtualized Cellular Networks with Statistical Multiplexing," *submitted to IEEE Transactions on Wireless Communication*.

[80] J. L. Hodges and L. Le Cam, "The Poisson Approximation to the Poisson Binomial Distribution," *The Annals of Mathematical Statistics*, vol. 31, no. 3, pp. 737–740, 1960.

[81] S. Chatterjee, M. J. Abdel-Rahman, and A. B. MacKenzie, "Robust Access Point Deployment and Adaptive User Assignment for Indoor Millimeter Wave Networks," in *Proceedings of the IEEE ICC Conference*, pp. 1–6, 2020.

[82] S. Chatterjee, M. J. Abdel-Rahman, and A. B. MacKenzie, "A Joint Optimization Framework for Network Deployment and Adaptive User Assignment in Indoor Millimeter Wave Networks," *submitted to IEEE Transactions on Wireless Communication*.

[83] J. G. Andrews, T. Bai, M. N. Kulkarni, A. Alkhateeb, A. K. Gupta, and R. W. Heath, "Modeling and Analyzing Millimeter Wave Cellular Systems," *IEEE Transactions on Communications*, vol. 65, no. 1, pp. 403–430, 2016.

[84] B. K. Pagnoncelli, S. Ahmed, and A. Shapiro, "Sample Average Approximation Method for Chance Constrained Programming: Theory and Applications," *Journal of Optimization Theory and Applications*, vol. 142, no. 2, pp. 399–416, 2009.

[85] A. J. Kleywegt, A. Shapiro, and T. Homem-de Mello, "The Sample Average Approximation Method for Stochastic Discrete Optimization," *SIAM Journal on Optimization*, vol. 12, no. 2, pp. 479–502, 2002.

[86] R. M. Van Slyke and R. Wets, "L-Shaped Linear Programs with Applications to Optimal Control and Stochastic Programming," *SIAM Journal on Applied Mathematics*, vol. 17, no. 4, pp. 638–663, 1969.

[87] T. Santoso, S. Ahmed, M. Goetschalckx, and A. Shapiro, "A Stochastic Programming Approach for Supply Chain Network Design under Uncertainty," *European Journal of Operational Research*, vol. 167, no. 1, pp. 96–115, 2005.

[88] S. K. Yoo, S. L. Cotton, R. W. Heath, and Y. J. Chun, "Measurements of The 60 GHz UE to eNB Channel for Small Cell Deployments," *IEEE Wireless Communications Letters*, vol. 6, no. 2, pp. 178–181, 2017.

[89] D. Lee, S. Zhou, and Z. Niu, "Spatial Modeling of Scalable Spatially-Correlated Log-

Normal Distributed Traffic Inhomogeneity and Energy-Efficient Network Planning," in *Proceedings of the IEEE WCNC*, pp. 1285–1290, 2013.

[90] D. Lee, S. Zhou, X. Zhong, Z. Niu, X. Zhou, and H. Zhang, "Spatial Modeling of the Traffic Density in Cellular Networks," *IEEE Wireless Communications*, vol. 21, no. 1, pp. 80–88, 2014.

[91] A. T. Saeed, A. Esmailpour, and N. Nasser, "Performance Analysis for the QoS Support in LTE and WiFi," in *Proceedings of the IEEE WCNC Workshops*, pp. 289–295, 2016.

[92] Z. Zhou, F. Teng, J. Liu, and W. Xiao, "Performance Evaluation for Coexistence of LTE and WiFi," in *Proceedings of the IEEE ICNC Conference*, pp. 1–6, 2016.

[93] Y. Song, K. W. Sung, and Y. Han, "Coexistence of Wi-Fi and Cellular with Listen-Before-Talk in Unlicensed Spectrum," *IEEE Communications Letters*, vol. 20, no. 1, pp. 161–164, 2016.

[94] J. Wang, L. Liu, L. Wang, H. Harada, and H. Jiang, "Downlink HARQ Enhancement for Listen-Before-Talk based LTE in Unlicensed Spectrum," in *Proceedings of the IEEE WCNC Conference*, pp. 1–6, 2016.

[95] S. Chatterjee, M. J. Abdel-Rahman, and A. B. MacKenzie, "Optimal distributed allocation of almost blank subframes for lte/wifi coexistence," in *Proceedings of WiOpt International Workshop on Resource Allocation, Cooperation and Competition in Wireless Networks (RAWNET)*, pp. 1–6, 2017.

[96] H. Wang, M. Kuusela, C. Rosa, and A. Sorri, "Enabling Frequency Reuse for Licensed-Assisted Access with Listen-Before-Talk in Unlicensed Bands," in *Proceedings of the IEEE Vehicular Technology Conference (VTC Spring)*, pp. 1–5, 2016.

[97] F. S. Chaves, E. P. Almeida, R. D. Vieira, A. M. Cavalcante, F. M. Abinader, S. Choudhury, and K. Doppler, "LTE UL Power Control for the Improvement of LTE/Wi-Fi Coexistence," in *Proceedings of the IEEE Vehicular Technology Conference (VTC Fall)*, pp. 201–207, 2013.

[98] A. Galanopoulos, F. Foukalas, and T. A. Tsiftsis, "Efficient Coexistence of LTE with WiFi in the Licensed and Unlicensed Spectrum Aggregation," *IEEE Transactions on Cognitive Communications and Networking*, vol. 2, no. 2, pp. 129–140, 2016.

[99] Q. Chen, G. Yu, and Z. Ding, "Optimizing Unlicensed Spectrum Sharing for LTE-U and WiFi Network Coexistence," *IEEE Journal on Selected Areas in Communications*, vol. 55, no. 3, pp. 20–33, 2016.

[100] J. Xiao and J. Zheng, "An Adaptive Channel Access Mechanism for LTE-U and WiFi Coexistence in an Unlicensed Spectrum," in *Proceedings of the IEEE ICC Conference*, pp. 1–6, 2016.

[101] "Extending LTE advanced to unlicensed spectrum." Qualcomm, 2013.

[102] O. Sallent, J. Pérez-Romero, R. Ferrús, and R. Agustí, "Learning-based Coexistence for LTE Operation in Unlicensed Bands," in *Proceedings of the IEEE ICC Workshop*, pp. 2307–2313, 2015.

[103] M. J. Abdel-Rahman, M. AbdelRaheem, A. MacKenzie, K. Cardoso, and M. Krunz, "On the Orchestration of Robust Virtual LTE-U Networks from Hybrid Half/Full-duplex Wi-Fi APs," in *Proceedings of the IEEE WCNC Conference*, pp. 44–50, 2016.

[104] E. Almeida, A. M. Cavalcante, R. C. Paiva, F. S. Chaves, F. M. Abinader, R. D. Vieira, S. Choudhury, E. Tuomaala, and K. Doppler, "Enabling LTE/WiFi Coexistence by

LTE Blank Subframe Allocation," in *Proceedings of the IEEE ICC Conference*, pp. 5083–5088, 2013.

[105] M. Sriyananda, I. Parvez, I. Güvene, M. Bennis, and A. I. Sarwat, "Multi-Armed Bandit for LTE-U and WiFi Coexistence in Unlicensed Bands," in *Proceedings of the IEEE WCNC Conference*, pp. 1–6, 2016.

[106] N. Rupasinghe and İ. Güvenç, "Reinforcement Learning for Licensed-Assisted Access of LTE in the Unlicensed Spectrum," in *Proceedings of the IEEE WCNC Conference*, pp. 1279–1284, 2015.

[107] S. Han, Y.-C. Liang, Q. Chen, and B.-H. Soong, "Licensed-Assisted Access for LTE in Unlicensed Spectrum: A MAC Protocol Design," in *Proceedings of the IEEE ICC Conference*, pp. 21–27, 2016.